1992

Bioreductive Alkylating Agents As Probes For Tissue Hypoxia

Paul A. Culbert

Bioreductive Alkylating Agents as Probes for Tissue Hypoxia

by
Paul A. Culbert
Department of Chemistry

Submitted in partial fulfilment
of the requirements for the degree of
Doctor of Philosophy

Faculty of Graduate Studies
The University of Western Ontario
London, Ontario
February, 1992

ISBN 0-315-71966-4

Canada

Abstract

The research discussed in the following thesis falls under the general categories of organic chemistry and radiochemistry and the application of these disciplines to the development of imaging agents and labelling techniques for the branch of Nuclear Medicine involving single photon emitting radionuclides. The thesis is made up of three sections; one dealing with the synthesis, labelling and biological testing of a series of radioiodinated 2-nitrobenzyl alcohol derivatives as potential probes for tissue hypoxia; a second chapter dealing with the synthesis, labelling and biological testing of 1-(4-[^{123}I]-iodophenyl-2,6,7-trioxabicyclo-[2.2.2]octane as a potential imaging agent for the $GABA_A$ receptor and a third chapter which deals with a novel radiolabelling procedure based on an organotin polymer.

The radioiodinated 2-nitrobenzyl alcohol derivatives were tested in the EMT-6 tumour model in Balb/c mice to determine whether specific uptake was occurring in the tumours. The first compound in the series, O-(N-methyl carbamoyl),3-iodo-6-nitrobenzyl alcohol did not show specific tumour uptake and appeared to be metabolically deiodinated *in vivo*. The second compound tested, O-(N-methyl carbamoyl),4-iodo-6-nitrobenzyl alcohol did not show specific tumour uptake but showed a decrease in metabolic deiodination. A third compound, O-(N-methyl carbamoyl), 4-iodo-2,6-dinitrobenzyl alcohol, did appear to exhibit specific uptake in the tumour.

Unfortunately, high levels of blood activity preclude the use of this compound as an hypoxia imaging agent.

1-(4-[^{123}I]-iodophenyl-2,6,7-trioxabicyclo-[2.2.2]octane was synthesized, labelled and was then tested in male CD1 mice for specific uptake in the brain. The compound underwent rapid metabolic elimination via the kidneys resulting in a short plasma half-life. The compound was found to be unacceptably lipophilic. The lipophilicity of the molecule coupled with its rapid metabolic elimination rendered it unsuitable as a receptor imaging agent.

A new polymer with aryltrialkyltin functions coupled to a polystyrene backbone was prepared. The specific aryl group used was N-isopropyl amphetamine. The new polymer was successfully employed in the synthesis of N-isopropyl-p-[^{131}I] iodoamphetamine. The method should have general applicability and may eliminate the need for chromatographic purification of some iodine radiopharmaceuticals.

For Mom, and Dad, and Brenda.

Acknowledgements

Many times throughout the course of this interdisciplinary research I have found myself mired in problems which lay far outside my area of expertise. I would like to take this opportunity to thank all those who have patiently fielded my questions. In particular, I would like to thank Andrew Wearring for his expertise and enthusiasm throughout our work with the EMT-6 tumour model. Thanks to Richard Mycroft for many useful discussions and his assistance with the organic electrochemistry. I am indebted to Renate Foerch for performing the XPS experiments, to Doug Hairsine for obtaining the mass spectra and to Susan England for running innumerable magnetic resonance spectra.

I will be forever grateful to Michael Chamberlain and Pam Zabel for administering to the Radiopharmaceutical Development Group and for their continued interest in the research. Thanks, and the very best of luck in the future! We are indebted to Merck Frosst and NSERC for their financial support.

I owe a special note of thanks to Peter Pityn for his enthusiasm and to Martin King for his expertise in a number of areas.

I will hold a special place in my heart for the post-docs and graduate students of the RDG, both past and present, for making my days in the group so enjoyable. My special thanks to Lou Anne Strickland for blazing a trail and to Vince and

Mahejabeen, for, amongst many other things--their tolerance!

My debt to Duncan Hunter can never be repaid, nor adequately acknowledged. Nevertheless, I thank him for his tutelage, his enthusiasm, and for his various and sundry leaps of faith.

I am grateful to my family for their unflagging (if somewhat bewildered!) support and to Brenda, without whom none of this was possible, nor worthwhile.

Table of Contents

	Page
Certificate of Examination	ii
Abstract	iii
Dedication	iv
Acknowledgements	vi
Table of Contents	viii
List of Figures	xi
List of Schemes	xiii
List of Tables	xv
List of Appendices	xvii
Chapter 1: A Brief Overview of Modern Nuclear Medicine and Radiochemistry	1
1.1) Introduction	1
1.2) Some Historical Aspects of Nuclear Medicine	1
1.3) Nuclear Medicine: The Classical Period 1913-1934	4
1.4) Artificial Radioactivity: The Modern Era of Nuclear Medicine	5
1.5) Radioactivity: Basic Principles	7
1.6) Radioactive Decay	8
1.7) Radionuclides for Nuclear Medicine	10
1.8) Positron Emission Computed Tomography (PET)	10
1.9) γ-Emitting Radionuclides	11
1.10) ^{99m}Tc Radiopharmaceuticals	15
1.11) Iodine Radiopharmaceuticals	19
1.12) γ-Ray Detection	23
1.13) The Geiger-Muller Detector	24
1.14) NaI(Tl) Scintillation Detector	25
1.15) Applications of the NaI(Tl) Scintillation Detector	27
1.16) γ-Ray Images	29
1.17) References	31
Chapter 2: Radioiodinated 2-Nitrobenzyl Alcohols as potential Probes for Tissue Hypoxia	35
2.1) Hypoxia and Cancer	35
2.2) The Reducing Properties of Hypoxic Cells	37
2.3) Quinone Bioreductive Alkylating Agents	38
2.4) Nitroheterocyclic Radiosensitizers	41
2.5) Radioactive Markers for Identification of Hypoxic Cells	44
2.6) Approaches to an Hypoxia Marker for Nuclear Medicine	45
2.7) Nitrobenzyl Carbamates: Potential Bioreductive Alkylating Agents Labelled with Iodine	50

2.8) Activation of the p-Nitrobenzyl System: $S_{RN}1$? 50
2.8.1) The $S_{RN}1$ Mechanism 51
2.9) Chemistry 57
2.10) Target Molecule 2.7: Iodine *Para* to the Nitro Group 57
2.11) Target Molecule 2.15: Iodine *Meta* to the Nitro Group 60
2.12) Target Molecule 2.23: The Dinitro Analogue . 62
2.13) Partition Coefficients of the Target Molecules 67
2.14) Electrochemical Studies 71
2.15) Biological Studies 73
2.16) Discussion 79
2.17) Experimental 82
2.18) Radiolabelling 102
2.19) Recrystallization to Constant Specific Activity 103
2.20) Partition Coefficients 103
2.21) Biological Studies 105
2.22) References 110

Chapter 3. 1-(4-[^{123}I]-iodophenyl-2,6,7-trioxabicyclo [2.2.2] Octane as a Potential Imaging Agent for the $GABA_A$ Receptor 115

3.1) Introduction 115
3.2) Receptor Pharmacology 116
3.2.1) Receptor Binding Molecules 117
3.3) The Theoretical Model of Receptor Binding . . 119
3.4) The Kinetics of Receptor Binding 122
3.5) Practical Aspects of Receptor Pharmacology . 123
3.6) Assays for Receptor Binding 125
3.7) Equilibrium Dialysis 126
3.8) Filter Assays 126
3.9) Competitive Binding 127
3.10) The Pharmacology of GABA Receptors 130
3.11) Muscimol 132
3.12) Bicuculline 133
3.13) Baclofen 135
3.14) Picrotoxin 137
3.15) Cage Convulsants 139
3.16) Why Image the $GABA_A$ Receptor? 144
3.17) Chemistry 147
3.18) Results and Discussion 150
3.19) Specific Activity Determination 156
3.20) Plasma Binding 158
3.21) Partition Coefficient Determination 159
3.22) Summary 164
3.23) Experimental 165
3.24) Radiolabelling 173
3.25) Determination of Partition Coefficient . . . 174

3.26) Biological Studies 176
3.27) References 177

Chapter 4. Radiopharmaceuticals via an Organotin Polymer 181

4.1) Introduction 181
4.2) A Kit Based on a Polymeric Organotin? 184

4.3) X-Ray Photoelectron Spectroscopy as an Analytical Tool in Polymer Chemistry 198
4.4) Discussion 205
4.5) Experimental 208
4.6) References 226

Appendix I. The Calculation of Log P's 228

Appendix II. Equipment 231

Curriculum Vitae 232

List of Figures

Figure 1.1 The Positron Annihilation Event 11
Figure 1.2 The ^{99m}Tc Generator 15
Figure 1.3 The Geiger-Muller Tube 24
Figure 1.4 The Sodium Iodide Scintillation Detector . . 26
Figure 1.5 Schematic of the Gamma Well Counter 27
Figure 1.6 Schematic of the Gamma Camera 28
Figure 1.7 Basic Collimator Function 29

Figure 2.1 Diagrammatic Representation of a Solid, Slow-Growing Mammalian Tumour 36
Figure 2.2 Survival of EMT-6 Cells Irradiated In Vitro 36
Figure 2.3 Mitomycin C treated DNA undergoes reversible Denaturation 39
Figure 2.4 Survival of V79-379 Cells Irradiated In Vitro 42
Figure 2.4a Plot for Log P Determination 69
Figure 2.5 Micro-Cell for Polarography Experiments . . 72
Figure 2.6 Healthy Biodistribution of [I-125]-**2.7** . . . 73
Figure 2.7 Healthy Biodistribution of [I-125]-**2.15** . . 75
Figure 2.8 Healthy Biodistribution of [I-125]-**2.23** . . 76
Figure 2.9 Biodistribution of [I-125]-**2.15** in Balb/c Mice Bearing EMT-6 Tumours 77
Figure 2.10 Biodistribution of [I-125]-**2.23** in Balb/c Mice Bearing EMT-6 Tumours 78

Figure 3.1 Schematic Representation of the Receptor-Receptor Agonist Interaction 117
Figure 3.2 Schematic Representation of the Receptor-Partial Agonist Interaction 117
Figure 3.3 Schematic Representation of the Receptor-Competitive Antagonist Interaction 118
Figure 3.4 Schematic Representation of the Receptor-Non-competitive Agonist Interaction 118
Figure 3.5 Schematic Representation of the Receptor-Non-competitive Antagonist Interaction . . . 119
Figure 3.6 Plot of Bound Receptor versus ligand concentration 121
Figure 3.7 Determination of K_D from a plot of B versus [L] 121
Figure 3.8 The Scatchard Plot 122
Figure 3.9 Receptor labelling with a high specific activity Ligand 124
Figure 3.10 Receptor labelling with a low specific activity Ligand 125
Figure 3.11 Competitive Inhibition Plot 128
Figure 3.12 The Hill Plot 129
Figure 3.13 Classification of GABA Receptors 136
Figure 3.14 Biodistribution of [^{131}I] **3.11** in male CD-1

mice 150
Figure 3.15 HPLC Radiochromatogram of 4'[^{123}I] TBOB after four hours incubation in human plasma 152
Figure 3.16 HPLC Radiochromatogram of 4'[^{123}I] TBOB isolated from mouse urine at one hour post-injection 154
Figure 3.17 Standard Curve for 4'[^{123}I] TBOB 157
Figure 3.18 Plots for Log P Determination 161
Figure 4.1 HPLC Analysis of [^{131}I] N-isopropyl-p-iodoamphetamine 197
Figure 4.2 Schematic of the XPS Experiment 198
Figure 4.3 XPS Data for Polymer **4.1** 200
Figure 4.4 XPS Data for Polymer **4.8** 202
Figure 4.5 XPS Data for Polymer **4.19** 203

List of Schemes

Scheme	Page
Scheme 1.1	12
Scheme 1.2	13
Scheme 1.3	13
Scheme 1.4	16
Scheme 1.5	17
Scheme 1.6	17
Scheme 2.1	40
Scheme 2.2	42
Scheme 2.3	43
Scheme 2.4	45
Scheme 2.5	47
Scheme 2.6	48
Scheme 2.7	48
Scheme 2.8	51
Scheme 2.9	52
Scheme 2.10	53
Scheme 2.11	53
Scheme 2.12	54
Scheme 2.13	55
Scheme 2.14	55
Scheme 2.15	56
Scheme 2.16	57
Scheme 2.17	58
Scheme 2.18	59
Scheme 2.19	59
Scheme 2.20	59
Scheme 2.21	60
Scheme 2.22.	60
Scheme 2.23	61
Scheme 2.24	62
Scheme 2.25	62
Scheme 2.26	63
Scheme 2.27	64
Scheme 2.28	64
Scheme 2.29	65
Scheme 2.30	65
Scheme 2.31	66
Scheme 3.1	147
Scheme 3.2	147
Scheme 3.3	148
Scheme 3.3	148
Scheme 3.5	148
Scheme 3.6	149
Scheme 3.7	149
Scheme 4.1	182
Scheme 4.2	183

Scheme 4.3 184
Scheme 4.4 185
Scheme 4.5 187
Scheme 4.6 188
Scheme 4.7 189
Scheme 4.8 189
Scheme 4.9 190
Scheme 4.10 191
Scheme 4.11 193
Scheme 4.12 193
Scheme 4.13 194

List of Tables

Table		Page
Table 1.1	Positron emitting isotopes suitable for PET	11
Table 1.2	γ-Emitting radionuclides suitable for SPECT	14
Table 2.1	Yields and rates for the alkylation of the lithium salt of 2-nitropropane with 4-nitrobenzyl halides	52
Table 2.2	Partition Coefficients of the test compounds	68
Table 2.3	Retention data for figure 2.4a	70
Table 2.4	Linear Regression values for figure 2.4a	70
Table 2.5	Comparison of Experimental and calculated log P values	71
Table 2.6	Polarography Results for the test compounds	72
Table 2.7	Biodistribution data for Potential Hypoxia Imaging Agents at one hour post-injection	79
Table 2.8	Healthy Biodistribution data for [I-125]-**2.7** in male CD1 mice	106
Table 2.9	Healthy Biodistribution data for [I-125]-**2.15** in male CD1 mice	106
Table 2.10	Healthy Biodistribution data for [I-125]-2.23 in male CD1 mice	107
Table 2.11	Biodistribution data for [I-125]-**2.15** in Balb/c mice bearing EMT-6 tumours	108
Table 2.12	Biodistribution data for [I-125]-**2.23** in Balb/c mice bearing EMT-6 tumours	109
Table 2.13	Biodistribution data for [I-125]-**2.23** in Balb/c mice bearing EMT-6 tumours-later time points	109
Table 3.1	Percent of injected dose excreted in urine--as parent compound--at up to 48 hours post injection	141
Table 3.2	LD_{50} and Receptor IC_{50} vs. ^{35}S TBPS values for a series of 4'-substituted 4-*t*-butyl ortho-benzoates	142
Table 3.3	Protein binding data for 4'-[^{123}I]-TBOB	159
Table 3.4	Retention data for plot one of figure 3.17	161
Table 3.5	Retention data for plot two of figure 3.17	162
Table 3.6	Linear Regression values for plot one and two in figure 3.17	162
Table 3.7	Uptake of [^{131}I]-labelled **3.8** in female CD1 mice	176
Table 4.1	Photoelectric Cross-Sections for Various Elements	200
Table 4.2	Calculated and Observed Elemental Compositions in Polymer **4.1**	201
Table 4.3	Calculated and Observed Elemental Compositions in Polymer **4.8**	203

Table 4.4 Calculated and Observed Elemental Compositions in Polymer 4.19 204

Table A1 The substituent constant π for a number of functional groups 228

List of Appendices

Appendix Page

Appendix I The Calculation of Partition Coefficients . 228
Appendix II Equipment 231

Chapter 1. A Brief Overview of Modern Nuclear Medicine and Radicchemistry

1.1 Introduction

Each year, one in thirty-five North Americans can expect to undergo a diagnostic or therapeutic Nuclear Medicine procedure[1]. Despite the advent of computer assisted tomography (CAT, x-ray) and magnetic resonance imaging (MRI) techniques, Nuclear Medicine continues to enjoy modest growth and remains an important non-invasive diagnostic tool. The continued success of this discipline lies in the fact that of all the medical imaging techniques, Nuclear Medicine alone furnishes images which reflect physiological function[2].

1.2 Some Historical Aspects of Nuclear Medicine

Nuclear Medicine has been described as the discipline resulting from the convergence of the separate disciplines of nuclear physics, chemistry, electronics, engineering, physiology, and medicine[3]. Perhaps it is not surprising that the birth of Nuclear Medicine followed closely on the heels of the discovery of radioactivity by Becquerel in 1895.

Becquerel was studying the natural phosphorescence of materials, believing that Roentgen's recently discovered "X-rays" were also responsible. Becquerel demonstrated that a phosphorescent uranium salt, if placed on a light-tight envelope containing an unexposed photographic plate and placed in the sun, gave rise to black spots on the developed photo-

graphic plate. Becquerel reasoned that the dark spots were due to X-rays emitted after excitation of the material by the sun. It was not until the same spots were observed for material left in the dark that Becquerel realized that the uranium salt emitted these penetrating "X-rays" even in its natural, unexcited state. Becquerel had discovered natural radioactivity.

Becquerel suggested to his graduate student Marie Sklodowska (Curie) that she investigate what it was about uranium that gave rise to the observed radiation. She began by carefully measuring the "radioactivity" by means of the piezoelectric phenomena discovered by her husband. Soon it was discovered that the same radioactivity was also found in Thorium and that this radioactivity was not X-rays but something much more energetic and much more penetrating.

The Curies set about the investigation of a number of different Pitchblendes, the ores from which uranium was extracted, and were surprised to discover ores that were more radioactive that the equivalent weight of uranium itself. As a result of this discovery, the Curies set about the isolation of individual radioactive elements from the Pitchblendes. They were able to isolate an element 400 times more radioactive than Uranium and called this new element Polonium. A second element Radium was soon discovered which was 1,000,000 times more radioactive than Uranium. Starting with 2 tons of pitchblende, Marie Curie was able to isolate 100 milligrams of

$RaCl_2$ (25% of the theoretical yield!) and was able to determine its atomic mass to be 226.5 amu correct to within ±0.2% of the best modern value.

Ernest Rutherford, working at McGill University, was able to show that the radiations consisted of two components[4]. The first component, which he termed α-radiation was easily absorbed in the first few μm of an aluminum foil shield, while a second component which he called β-radiation was about 100 times more penetrating in the same material.

In 1900, Becquerel was able to show that the β-ray was actually an electron travelling at nearly the speed of light[5]. A third component of radiation was identified that same year by Villard[6] which was much more penetrating than the α or β-rays and was electromagnetic in nature. Villard named this radiation the γ-ray.

Rutherford was able to show through very careful study that α-rays were charged particles travelling at approximately one-tenth the speed of light and having one-half the charge-to-mass ratio of hydrogen. It was long suspected that the α-particle was in fact a helium nucleus since helium was always found in uranium ores but it would be some time later that the definitive experiments to prove that the α-particle was indeed the helium nucleus were performed. Rutherford, with the aid of Thomas Royd, a spectroscopist, and Otto Baumbach, a talented glassblower, was able to show that α-rays that were allowed to pass through a thin glass membrane into an evacuated vessel

gave rise to a gas which, when collected and subjected to an electrical discharge, clearly furnished the spectrum of Helium[7].

The next two decades, produced great strides in the understanding of natural radioactivity. Almost all the natural radioelements had been discovered and their decay series were understood. The disintegration theory of radioactivity, the group displacement laws, and isotopy were established to such an extent that the discipline of radiochemistry nearly ceased to exist having enjoyed an almost "suicidal" success[8]. The resurrection of the science awaited the discovery of artificial radioactivity in 1934.

1.3 Nuclear Medicine: The Classical Period 1913-1934

The "Classical" period[9] of Nuclear Medicine was marked by the first use of radioactive "tracers" by the great Hungarian chemist G. von Hevesy in 1913*. In 1914, Seil studied the appearance of emanation (^{222}Rn) in the breath and Radium in the urine of humans after the intravenous injection of Radium.

Hevesy[10] continued his research into radioactive tracers by using a natural isotope of lead to investigate the metabolism of lead in plants. He found that the detection of radioactivity was one thousand times more sensitive than

---

*The use of Radium and its emanation (^{222}Rn) for medical purposes was already widespread at this time. Alexander Graham Bell suggested its use for the treatment of cancer as early as 1903.

existing chemical assays. So little lead was used that no toxic effect was observed.

The first medical use of a radiotracer is generally attributed to Blumgart[11] a Boston physician working in the late 1920's. Blumgart injected Radium C (^{214}Bi) in one arm and determined the "velocity of circulation" by detecting the appearance of radioactivity in the other arm. He was able to show that the mean "velocity" was 18 seconds in healthy subjects but was prolonged in patients with heart disease.

The early medical use of radioactivity was frustrated by the availability of only naturally occurring radionuclides. It would take the discovery of artificial radioactivity by Irene Curie and Frederic Joliot in 1934[12] to usher in the modern era of Nuclear Medicine.

1.4 Artificial Radioactivity: The Modern Era of Nuclear Medicine.

A study[13] of the "natural scintillations" produced when α-particles from Radium C (^{214}Bi) were allowed to impinge on a variety of gases was published by Ernest Rutherford in June 1919. Rutherford noted that the action of α-particles on nitrogen gas was anomalous in that it appeared to increase the number of scintillations at the end of the apparatus rather than decreasing the number as most other gases did.

Rutherford drew the important conclusion that the structure of matter could be altered by bombarding elements

with α-particles.

The next important discovery on the route to artificial radioactivity was the invention of the cyclotron by Ernest O. Lawrence in 1931[14]. The cyclotron was used to accelerate particles to high speeds in order to bombard metal targets. Though Lawrence did not realize it until some time later, the cyclotron was inducing radioactivity in the targets from the beginning. It was Irene Curie (daughter of Marie) and her husband Frederic Joliot who first reported[15] the transmutation of elements. Their chemical analyses showed that boron targets bombarded with α-particles from polonium had been transmuted to radioactive nitrogen-13 and aluminum targets were transmuted to radiophosphorous-30. The "classical" period of Nuclear Medicine had ended[16].

The bombarding of elements with charged particles was plagued with an inherent difficulty. In order for the particle to enter the nucleus of the target atoms it was necessary to overcome the large electrostatic repulsion. This difficulty was overcome when the neutron was discovered by Chadwick in 1932[17]. By the summer of 1934, Enrico Fermi had used this chargeless particle to penetrate many targets producing a number of new elements.

Lawrence bombarded sodium with deuterons and reported the production of radiosodium in the fall of 1934[18]. He immediately recognized the interesting biological implications of a radioactive form of sodium. The seminal study of the use of

a radioactive tracer in a physiological system was published by Hevesy and Chiewitz[19] in 1935. They fed rats $Na_3{}^{32}PO_4$ at a known specific activity and studied its distribution throughout the organs, tissues and excreta of the animal. They were able to show that the radiophosphorus was resident in the bones of the rat for about two months, proving that the process of bone formation was a dynamic one. The radiotracer work of Hevesy won him the Nobel prize of 1943.

The production of artificial isotopes was the subject of intense research in the years following the initial discovery by Curie and Joliot. Two hundred new isotopes were discovered in the three years immediately following their initial discovery and continued such that by 1975 over 2500 isotopes had been reported[20].

1.5 Radioactivity: Basic Principles.

A study of the isotopes, stable or radioactive, for any element immediately leads to the following question: Can one predict which isotopes will be stable and which isotopes will be radioactive?

The stability of the nucleus depends on the excess or deficiency of positive charge in the nucleus. This excess or deficiency can be expressed by the ratio of the number of neutrons to the number of protons (N/P) in the nucleus. Stability is achieved for the lighter nuclei (atomic number ≤ 20) when N/P=1. For heavier nuclei (atomic number >20)

stability is achieved only when the ratio N/P is greater than one.

1.6 Radioactive Decay.

An unstable nucleus can decay by one or more of the following routes:

1. α-Decay

α-Decay occurs when a helium nucleus (2 protons and 2 neutrons) gains sufficient energy to overcome its nuclear binding energy and is ejected from the nucleus. α-Decay only occurs in heavy nuclei.

$$^{226}_{88}Ra \rightarrow {}^{222}_{86}Rn + {}^{4}_{2}\alpha$$

2. β-Decay (3-types)

i) positron decay: The excess positive nuclear charge is reduced by ejecting a positively charged electron and a neutrino.

$$^{22}_{11}Na \rightarrow {}^{22}_{10}Ne + {}^{0}_{1}\beta + \upsilon$$

ii) negatron decay: The amount of positive charge in the nucleus is increased by ejection of a negatively charged electron and an anti-neutrino.

$$^{14}_{6}C \rightarrow {}^{14}_{7}N + {}^{0}_{-1}\beta + \upsilon^{-}$$

iii) electron capture: An electron (usually from the k-shell) is spontaneously incorporated into the nucleus accompanied by the release of a γ-ray. In this way the amount of

positive nuclear charge is decreased.

$$^{123}_{53}I + ^{0}_{-1}e^- \rightarrow ^{123}_{52}Te + h\nu$$

3. Spontaneous Fission

$$^{252}_{98}Cf \rightarrow ^{140}_{54}Xe + ^{108}_{44}Ru + 4^{1}_{0}n$$

Very heavy nuclei may decay by splitting into two atoms of approximately equal atomic number. Spontaneous fission is accompanied by the release of neutrons.

4. Isomeric Transition

$$^{99}_{42}Mo \rightarrow ^{99m}_{43}TcO_4^- + ^{0}_{-1}e \qquad t_{1/2} = 66 \text{ hrs}$$

$$^{99m}_{43}TcO_4^- \rightarrow ^{99}_{43}TcO_4^- + h\nu \qquad t_{1/2} = 6.01 \text{ hrs}$$

The daughter nuclide produced in a radioactive decay process is often formed in an excited (isomeric) nuclear state. In the majority of cases, the excited nuclear state decays to the ground nuclear state instantaneously accompanied by a photon but in some cases the decay from the excited state is delayed and the collapse to the ground nuclear state has a half-life on the order of minutes or hours. $^{99}_{42}Mo$ undergoes β-decay to *metastable* $^{99m}_{43}TcO_4^-$ which subsequently decays by isomeric transition to $^{99}_{43}TcO_4^-$ accompanied by the emission of a single γ-photon with an energy of 140 KeV.

1.7 Radionuclides for Nuclear Medicine

Particulate radiation (α and β rays) undergoes very strong interactions with matter resulting in a high absorption of the radiation by tissues and significant tissue damage. This high absorption of radiation makes α and β-emitters unsuitable for use in Nuclear Medicine since neither particle can be detected through more than a few millimetres of biological tissue. Particulate radiation, especially α particles, causes dense ionization in living tissue giving rise to unacceptable radiation damage. In practice, the radionuclides of primary importance to diagnostic Nuclear Medicine are those which give rise to electromagnetic radiation only. These radionuclide fall into two categories: positron emitters and gamma-ray emitters.

1.8 Positron Emission Computed Tomography (PET)

$$^{11}_{6}C \rightarrow {}^{11}_{5}B + {}^{0}_{1}e$$

When a neutron-deficient nucleus undergoes positron decay, the net nuclear charge is made more negative through the ejection of a positron. A positron is the anti-particle to an electron and the two are annihilated when they collide. The annihilation event gives rise to two 512 keV photons which leave the annihilation site in essentially opposite directions (Figure 1.1[21]).

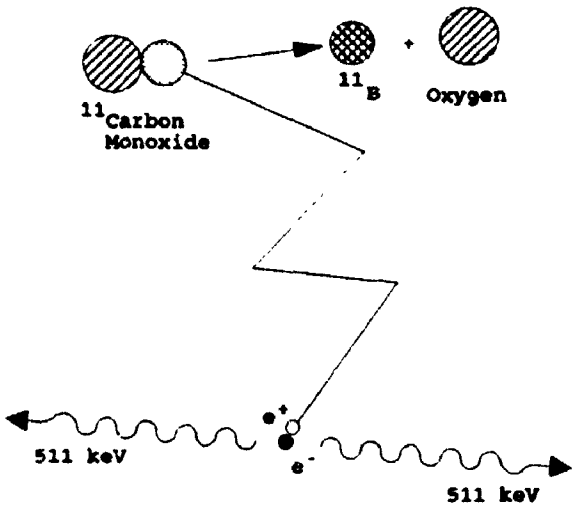

Figure 1.1. The Positron Annihilation Event.

One of the primary advantages to PET is the availability of suitable isotopes of carbon, nitrogen and oxygen. Table 1.1 lists the isotopes commonly used in PET[22].

Table 1.1. Positron emitting isotopes suitable for PET.

Isotope	Half-life	Method of Production
^{11}C	20.3 min	Cyclotron
^{13}N	10.0 min	Cyclotron
^{15}O	124.0 sec	Cyclotron
^{18}F	110.0 sec	Cyclotron
^{82}Rb	75.0 sec	^{82}Sr Generator
^{68}Ga	68.3 min	^{68}Ge Generator
^{75}Br	1.6 hrs	Cyclotron

The primary advantage of PET lies in the labelling of biologically important molecules with isotopes of carbon nitrogen and oxygen without altering their biochemical properties. The disadvantages of PET are also apparent. The half-lives of positron emitting isotopes are extremely short

and the important radionuclides must be produced in an on-site cyclotron. The extremely short half-lives of the positron emitting radionuclides places severe restrictions on the radiochemistry which can be used to label potential radiopharmaceuticals. The following examples of positron-emitting radiopharmaceuticals have recently appeared and are representative of some approaches used to deal with the short half-lives of the positron emitters. [^{15}O]-n-Butanol is considered the "platinum standard" for measuring regional cerebral blood flow using PET. Kabalka[23] has successfully used a boron functionalized polystyrene polymer for the production of ^{15}O-n-butanol (Scheme 1.1).

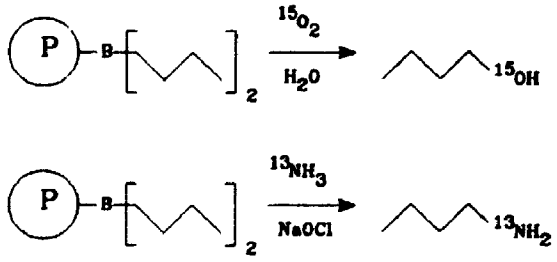

Scheme 1.1

The same polymer can be used to synthesize ^{13}N-labelled n-butyl amine. The extremely short half-lives of ^{15}O and ^{13}N restricts the radiochemistry to these types of relatively simple, high yield reactions. The short half-lives also make the isotopes highly desirable as radiopharmaceuticals since the radiation dose per unit activity is extremely low.

MK 801 (Scheme 1.2) is an anticonvulsant that binds to the N-methyl-D-aspartate sub-class of glutamate receptors. It

was labelled with ^{18}F by Wieland and co-workers in the following manner (Scheme 1.2):

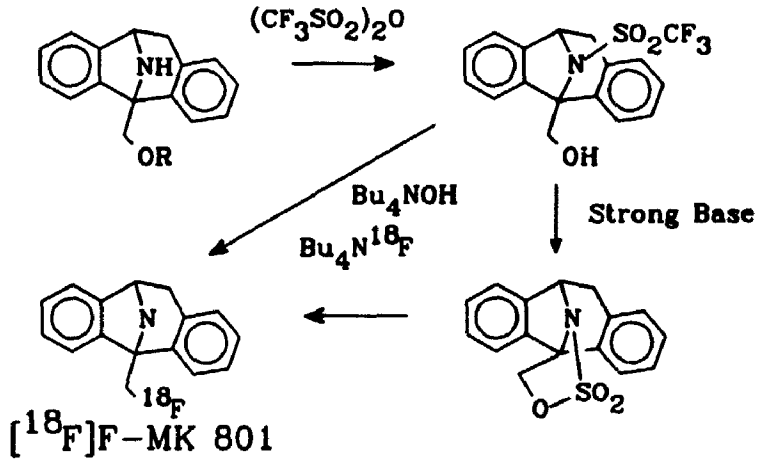

Scheme 1.2

The chemistry of ^{11}C-labelled compounds poses some of the most daunting challenges to the PET radiochemist, but also carries with it the most potential for success. Atenolol is an antagonist (see chapter 3) for the β-adrenergic receptor and has been labelled with ^{11}C by the following route (Scheme 1.3):

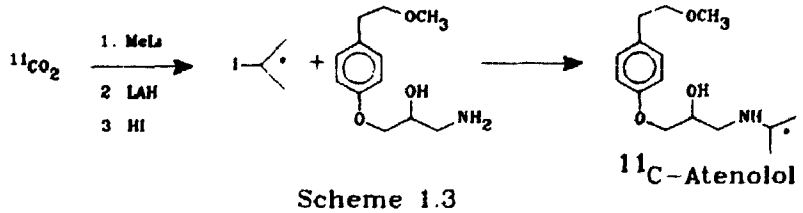

Scheme 1.3

1.9 γ-Emitting Radionuclides

Single photon emission computed tomography (SPECT) is the branch of Nuclear Medicine concerned with the external imaging of radionuclides which decay by the emission of a single photon in the γ-energy range. Table 1.2 lists some of the isotopes commonly used in SPECT[24].

Table 1.2. γ-Emitting radionuclides suitable for SPECT.

Isotope	Half-life	Method of Production
^{99m}Tc	6.01 hours	^{99}Mo Generator
^{123}I	13.1 hours	Cyclotron
^{131}I	8.04 days	Reactor
^{111}In	2.81 days	Cyclotron
^{67}Ga	78.3 hours	Cyclotron

Technetium-99m has emerged as the most important radionuclide in SPECT. The half-life and the γ-photon energy of ^{99m}Tc are ideal at 6.01 hours and 140 keV respectively. Perhaps the most important advantage of ^{99m}Tc is its availability and low cost. A generator system has been devised[25] which furnishes a constant supply of ^{99m}Tc in the Nuclear Medicine clinic. ^{99m}Tc is produced from the fission product ^{99}Mo according to the following decay scheme[26]:

$$^{99}_{42}Mo \rightarrow {}^{99m}_{43}TcO_4^- + {}^{0}_{-1}e \qquad t_{1/2} = 66 \text{ hrs}$$

$$^{99m}_{43}TcO_4^- \rightarrow {}^{99}_{43}TcO_4^- + h\nu \qquad t_{1/2} = 6.01 \text{ hrs}$$

$$^{99}_{43}TcO_4^- \rightarrow {}^{99}_{44}Ru + {}^{0}_{-1}e \qquad t_{1/2} = 2.1 \text{ e } 05 \text{ yrs}$$

Reactor produced ^{99}Mo is adsorbed on an alumina column and the

product 99m-pertechnetate ($^{99m}TcO_4^-$) can be eluted with sterile saline (Figure 1.2).

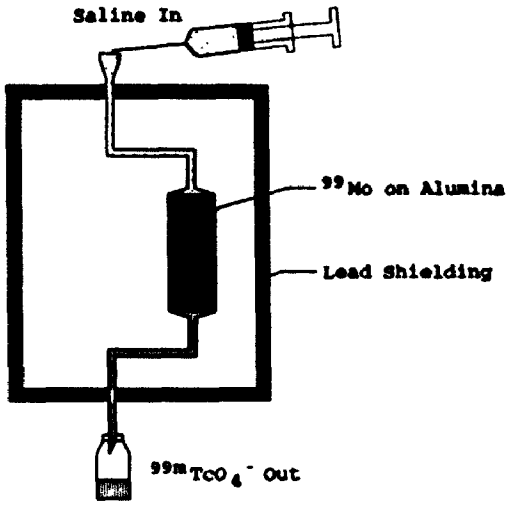

Figure 1.2. The ^{99m}Tc Generator

A drawback in the use of ^{99m}Tc as a radionuclide is the difficulty involved in incorporating the isotope in molecules of biological interest. The chemistry of ^{99m}Tc is limited to that which can occur with transition metals. In order to label a molecule with ^{99m}Tc the radionuclide must first be chelated and the resulting complex can then be attached to the molecule to be labelled. Despite the limitations imposed by the chemistry of ^{99m}Tc an ever-increasing battery of radiopharmaceuticals based on this isotope is available to the SPECT clinician.

1.10 ^{99m}Tc Radiopharmaceuticals

^{201}Tl has been the radioisotope of choice for cardiac imaging for some time[27] despite its less-than-ideal physical

characteristics. The search for a ^{99m}Tc-labelled cardiac imaging agent has been extensive and has been plagued by innumerable failures. ^{99m}Tc-*hexakis*-methoxyisobutylisonitrile (^{99m}Tc MIBI) was reported in the early 1980's as an agent suitable for SPECT imaging of the heart.

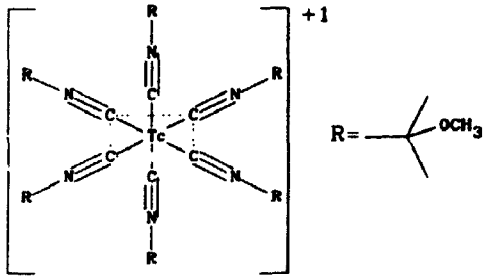

^{99m}Tc MIBI

The discovery of a ^{99m}Tc-labelled brain imaging agent for SPECT was reported in 1987[28]. ^{99m}Tc-d,l-HMPAO or hexamethyl propylene amine oxime is a neutral, lipophilic complex which accumulates in the brain to an extent of 3-4% of the injected dose at four hours post-injection. The ligand is synthesized according to Scheme 1.4:

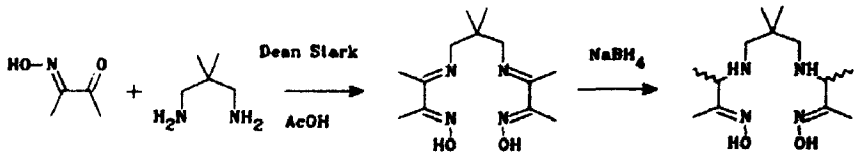

Racemic HMPAO

Scheme 1.4

The diastereomeric mixture can be separated by fractional crystallization from ethyl acetate. It has been shown[29] that the complex using the d,l isomer demonstrates consistently higher brain uptake than the meso isomer. The complex is formed by first reducing the $^{99m}TcO_4^-$ with stannous chloride

followed by complexation with the d,l HMPAO ligand (Scheme 1.5).

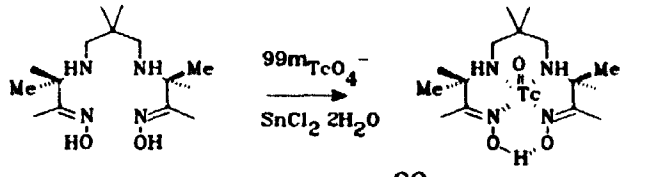

d,l-HMPAO ^{99m}Tc-d,l-HMPAO

Scheme 1.5

^{99m}Tc-HMPAO has recently come into competition with ^{99m}Tc-ECD[30] (ethyl cysteinate dimer, Scheme 1.6) as the complex of choice for the SPECT imaging of the brain.

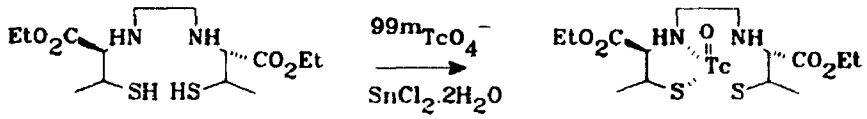

l,l-ECD ^{99m}Tc-l,l-ECD

Scheme 1.6

It was demonstrated that both the d,d and the l,l isomers were taken up by the brain. The l,l isomer however, had the unique property of undergoing selective hydrolysis of one ester unit in the brain. The result was that ^{99m}Tc-l,l ECD crossed easily into the brain but became ionized within the brain and was unable to escape. Human clinical trials of ECD have shown a truly remarkable result. At twenty-four hours post-injection approximately 2% of the injected dose remained in the brain while much of the rest of the original dose was excreted from the body.

One of the most important procedures in the Nuclear Medicine clinic is the bone scan. In 1971, a ^{99m}Tc phosphate

complex was introduced[31] which provided excellent SPECT images of the bone. Several structural refinements have appeared[32] and two complexes have emerged as the bone-imaging agents of choice; ^{99m}Tc-MDP, and ^{99m}Tc-HMDP (methylene diphosphonate and hydroxymethylene diphosphonate).

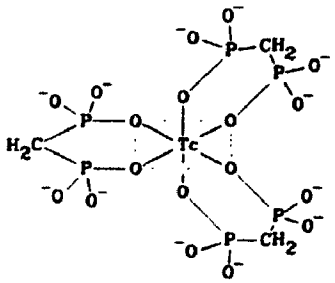

^{99m}Tc-MDP

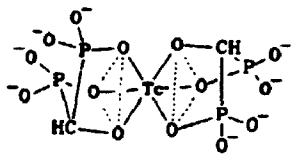

^{99m}Tc-HMDP

Autoradiographic studies[33] have shown that these agents are incorporated into the growing face of the apatite crystal in bone.

1.11 Iodine Radiopharmaceuticals

Iodine has played an important role in Nuclear Medicine for over 50 years. Non-radioactive iodine is a trace nutrient that is taken up in the thyroid gland where it is covalently bound to the molecule *thyroxin*[34].

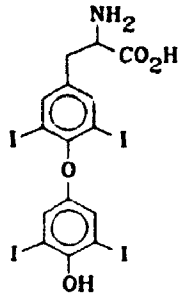

Thyroxin

Thyroxin is an important amino acid which exerts a stimulatory effect on metabolism. When radioactive iodide is injected into humans 10 to 40% of the injected dose accumulates in the thyroid at 24 hours[35]. The high uptake allows imaging of the thyroid gland and hence the remote assessment of thyroid function.

The first radioactive isotope of iodine was ^{131}I reported by Livingood and Seaborg in 1938[36]. The uptake of ^{131}I in the thyroid glands of rabbits[37] and humans[38] was demonstrated immediately following the discovery of the radionuclide. ^{131}I is readily obtained through the bombardment of tellurium targets with reactor-produced thermal neutrons[39] making it an extremely economical radionuclide. Unfortunately, ^{131}I has a number of drawbacks which limit its use in the Nuclear Medicine clinic. ^{131}I is a neutron-rich isotope which decays according to the following equation:

$$^{131}_{53}I \rightarrow ^{131}_{54}Xe + ^{0}_{-1}\beta + h\nu \quad t_{1/2}=8.04 \text{ days}$$

The presence of a β-particle component to ^{131}I decay results in a very high radiation dose to surrounding tissues. The γ-ray emitted when ^{131}I undergoes decay has an energy of 364 keV. This photon has an energy far above the optimal range of conventional γ-cameras (100-200 keV)[40]. The result is that a large fraction of the high-energy photons pass through the detector rendering the detection process very inefficient. Despite these limitations ^{131}I remains an important *therapeutic* radionuclide. ^{131}I is used routirely in a therapeutic procedure call *thyroid ablation*[41]. A patient suffering from hyperthyroidism is given sufficient ^{131}I to kill a portion of his/her thyroid. The β-emissions are a benefit in this instance since they are responsible for most of the radiation damage and hence most of the therapeutic response.

Another radioactive isotope of iodine ^{123}I was discovered in 1959[42] which is much better suited for use in diagnostic radiopharmaceuticals. ^{123}I is a neutron deficient radionuclide which must be cyclotron produced. ^{123}I decays by electron capture according to the following scheme:

$$^{123}_{53}I + ^{0}_{-1}e^- \rightarrow ^{123}_{52}Te + h\nu \quad t_{1/2}=13.3 \text{ hrs}$$

^{123}I decays without particulate emission and the energy of the γ-photon is ideal for detecton at 159 keV. The radiation dose from ^{123}I is only 2% that of an equivalent activity of ^{131}I. The 13.3 hour half-life of ^{123}I is sufficiently long that the isotope can be produced at a central facility and shipped to

remote locations*.

The availability of large quantities of inexpensive ^{99m}Tc in the Nuclear Medicine clinic brings into question the role of the much more expensive ^{123}I ($1.62/MBq for ^{123}I versus $0.005/MBq for ^{99m}Tc**) in diagnostic Nuclear Medicine. The ability of the radiochemist to introduce radioactive isotopes of iodine into relatively simple organic molecules via covalent bonds may secure the future of ^{123}I in the Nuclear Medicine clinic.

A great deal of effort has been directed in recent years toward the development of novel imaging agents targeted at the various ligand-receptor systems in the human body. ^{123}I has proven to be the radionuclide of choice for the preparation of labelled ligands suitable for imaging using SPECT. The following ^{123}I-labelled compounds have recently appeared:

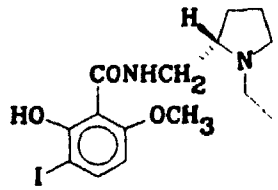

S(-)-IBZM

S(-)-IBZM is a Dopamine D_2 receptor antagonist which has been labelled with ^{123}I for use as a ligand for SPECT. The radio-

---

*The ^{123}I used at the University of Western Ontario is produced at the TRIUMF cyclotron in Victoria, British Columbia.

**Approximate cost to Department of Nuclear Medicine, University Hospital, London Ontario as of February, 7, 1992.

active ligand has been tested successfully in humans[43]. A related compound S(-)-IBF has recently been reported by the same authors[44]. The compound is nearly five times more selective for the dopamine D_2 receptor than S(-)-IBZM and preliminary results from primates have been encouraging.

The final analysis of the role of receptor specific imaging agents in the diagnosis of disease will come only after a great deal of data has been accumulated using these ligands. The imaging of receptors using PET has already begun to shed light on such diseases as schizophrenia and Parkinson's[45]. The production of newer, more specific SPECT ligands for a number of receptor systems promises to be the concern of iodine radiochemists for some time to come.

1.12 γ-Ray Detection

Central to the science of Nuclear Medicine is the ability to detect the extremely high energy γ-photons. There have been numerous approaches to the detection of γ-rays but for the purposes of this discussion we need consider only two: the Geiger-Muller tube and the thallium doped sodium iodide (NaI(Tl)) scintillation detector. When high energy photons interact with matter the following processes can occur.

Photoelectric Effect: An energetic photon disappears by giving up all its energy to an inner shell electron of the absorbing matter through a simple collision. The electron gains the photon energy in the form of kinetic energy and is ejected from its orbital. A hole is created in the orbital of the struck atom and is filled by an electron *falling in* from an outer orbital. An X-ray of a characteristic frequency is emitted as part of the *falling in* process.

Compton Scattering: The process called Compton Scattering is similar to the photoelectric effect except that it begins with the interaction of the high energy photon with an outer shell electron. The electron absorbs only a portion of the photon energy and is ejected from its orbital. The photon loses energy and changes direction in the process but does not disappear entirely.

The probability of a photoelectric interaction roughly

increases with the third power of the atomic number of the absorbing material while the probability of Compton Scattering does not depend to a great extent on the atomic number of the absorbing material. These factors explain why lead (Z=82) is an efficient absorber of γ-rays while these same rays pass through biological tissues quite efficiently.

A third process called *Pair Production* is possible with photons of very high energy (> 1.02 MeV). The process is not important in Nuclear medicine but involves the disappearance of the high-energy photon coupled with the production of a positron and an electron.

1.13 The Geiger-Muller Detector[46]

The Geiger-Muller consists of a metal tube which serves as the cathode surrounding a metal wire which serves as the anode. A potential difference of about 900 volts is held across the two electrodes and the tube is filled with argon or neon mixed with 0.1% chlorine gas (Figure 1.3).

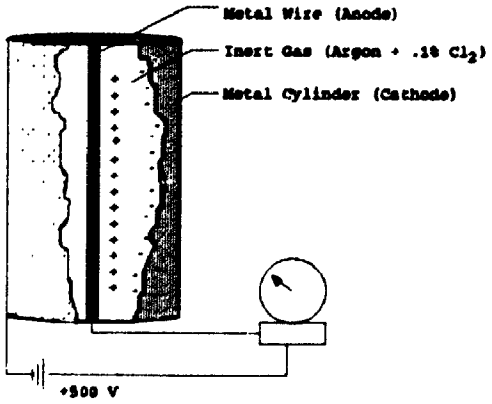

Figure 1.3. The Geiger-Muller Detector.

When a γ-photon enters the gas-filled container it may interact with an atom of the noble gas to produce an ion pair. The ions are accelerated toward the electrodes by the high potential difference and collide with other noble gas atoms to create secondary ion pairs. The chlorine gas serves to quench the secondary ions in order to prepare the tube for the next ionization event. The process is repeated and an "avalanche" of electrons are collected at the anode. Each "avalanche" is registered as a count or an audible "tick" and the count rate per second is registered by an electronic meter. Geiger-Muller detectors are relatively inexpensive, portable, and sufficiently sensitive for use as radioactivity survey meters.

1.14 NaI(Tl) Scintillation Detector[47]

Crystalline sodium iodide is an efficient absorber of high energy photons. The energy from the absorbed photon can be dissipated in two ways: by transferring its energy to other electrons thereby heating the crystal slightly or by the release of photons of visible light (scintillations). The first process predominates in pure sodium iodide but in the presence of a small amount of thallium (NaI(Tl)) the excited electrons travel to the thallium impurity and lose their excess energy by emitting photons having an energy of approximately 3 eV. Sodium iodide is transparent to the low energy photons allowing their detection at the faces of the crystal. The detection is accomplished by coupling each NaI(Tl) crystal

to a photomultiplier tube (Figure 1.4).

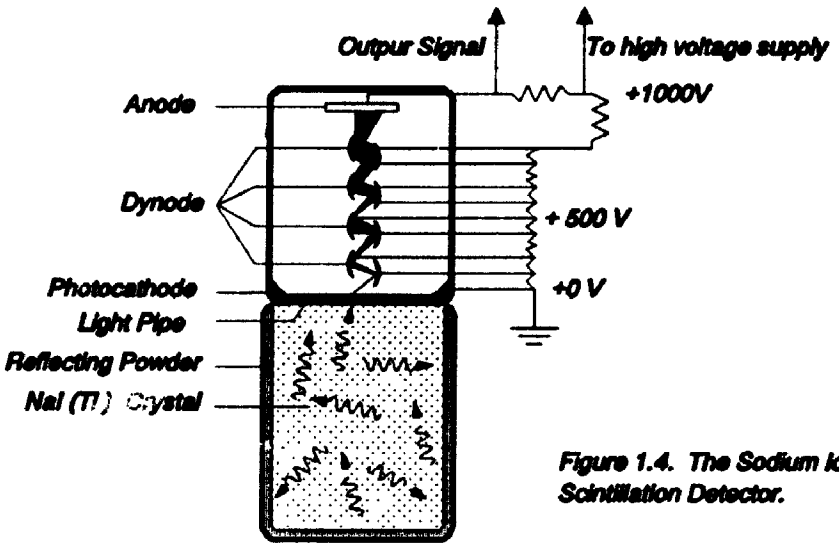

Figure 1.4. The Sodium Iodide Scintillation Detector.

The 3 eV photons are reflected out the end of the crystal and are conducted through a transparent light-pipe to the end of the photomultiplier tube. The photons then enter the photomultiplier tube and cause electrons to be released from the photocathodic material lining the end of the photomultiplier tube. The released electrons are accelerated to the first of a series of dynodes by the potential difference between the first dynode and the photocathode. When the accelerated electron strikes the first dynode a series of secondary electrons are released from the dynode and are accelerated toward a second dynode held at a higher potential relative to the first dynode. This process is repeated over a series of 8-10 dynodes and an overall gain of about 10^6 is achieved. The net result is the formation of a current pulse following the absorption of each γ-photon in the NaI(Tl)

crystal. The number of 3 eV photons emitted in the scintillation is proportional to the energy of the absorbed γ-photon. Pulse height analysis allows discrimination of scintillations due to the original decay event and those due to Compton scattered photons. Pulse height analysis also allows the detection of two or more radionuclides at one time.

1.15 Applications of the NaI(Tl) Scintillation Detector

γ-Well Counter

It is often necessary to assay small biological samples for radioactivity in both clinical and experimental Nuclear Medicine. This task is accomplished using a γ-well counter. The basic design is shown in Figure 1.5[48]:

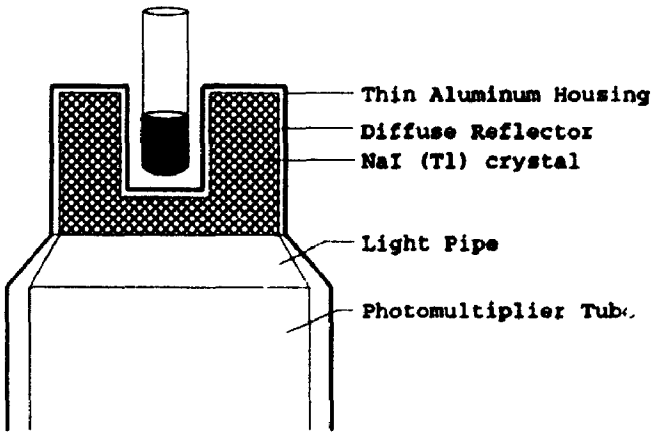

Figure 1.5. Schematic of the Gamma Well Counter

The central component of a γ-well counter is an NaI(Tl) scintillation detector which has been machined in such a manner that a test-tube containing a sample for assay can be lowered into a cavity in the sodium iodide crystal. The close

contact of the sample to the detector crystal allows for very accurate determinations of small amounts of radioactivity. Pulse height analysis once again allows the discriminations of primary and secondary scintillations and the simultaneous assay of several radionuclides.

The Anger Scintillation Camera[49]

Central to the field of Nuclear Medicine is the ability to obtain two and three-dimensional information on the distribution of radionuclides in the human body. The scintillation camera was invented by Anger in 1958[50] (Figure 1.6)

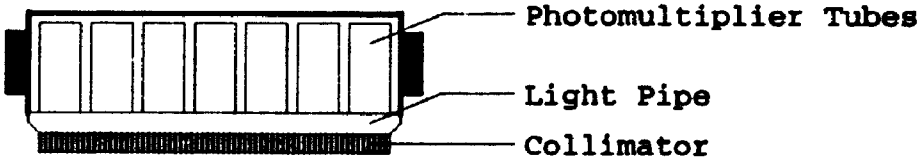

Figure 1.6. Schematic of the Gamma Camera

The scintillation camera consists of a two-dimensional array of NaI(Tl) scintillation detectors separated from the subject by a collimator. Since γ-rays are too energetic to be focused by conventional lenses a collimator is used instead. The simplest collimator design is a lead plate machined with a network of parallel holes (Figure 1.7).

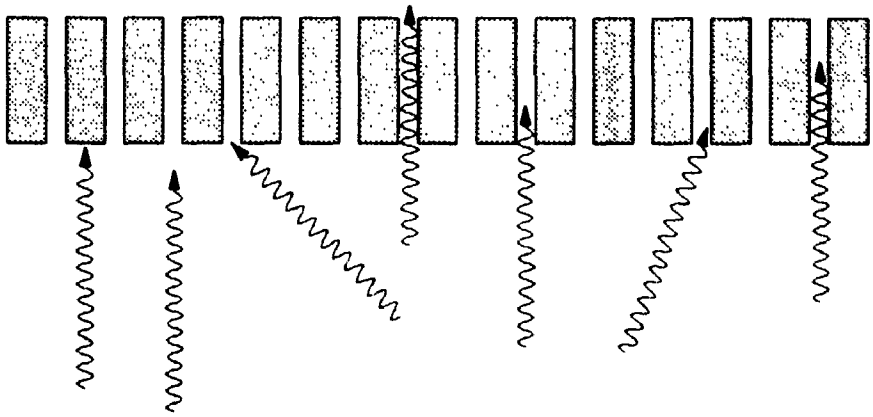

Figure 1.7. Basic Collimator Function.

The purpose of the collimator is to absorb all the γ-photons which are not perpendicular to the face of the detector crystal . The elimination of all but the perpendicular photons preserves the spatial information necessary to create an image of the radionuclide distribution.

An analogue or digital circuit is used to fix the position of the scintillation event by comparing the pulse height generated in each of the photomultiplier tubes. The resolution which can be achieved using modern scintillation cameras is in the range of 4-5 millimetres. The X and Y coordinates of each scintillation are converted to an electronic signal which can be stored in computer memory or displayed on a cathode ray screen in order to construct the γ-ray image.

1.16 γ-Ray Images

Two types of images can be acquired using the modern γ-

camera. The most common type is the projection image where both the subject and the camera remain stationary. The second type is called tomography and involves moving the camera over or around the stationary subject.

1.17 References.

1.Gottschalk, A.; Hoffer, P.B.; Potchen, E.J.; eds. *Diagnostic Nuclear Medicine,* 2nd edition; Williams and Wilkins, c. 1988 p. 11.

2.Sharp, P.F.; Gemmell, H.G.; Smith, F.W. eds.; *Practical Nuclear Medicine,* IRL Press at Oxford University Press. c. 1989 p.3.

3.Myers, W.G.; Wagner, H.N; in Wagner, H.N. (ed), *Nuclear Medicine,* H.P. Publishing Co. Inc. New York, N.Y. c. 1975. p. 11.

4.Rutherford, E.; *The Collected Papers of Lord Rutherford of Nelson,* George Allen and Unwin LTD., London c. 1962 vol 2. pp. 169-215.

5.Becquerel, H.; *Compt. Rend.* **1900,** *130,* **809-815.**

6.Villard, P.; *Compt. Rend.,* **1900,** *130,* **1010-1012.**

7.Rutherford, E.; *The Collected Papers of Lord Rutherford of Nelson,* George Allen and Unwin LTD., London c. 1962 vol 2. pp 134, 163-167.

8.Badash, L.; *Radioactivity in America: Growth and Decay of a Science,* The Johns Hopkins University Press, Baltimore ·1979, pp. 213.

9.Myers, W.G.; Wagner, H.N.; in *Nuclear Medicine,* Wagner, H.N. ed.; HP Publishing Co. Inc. New York, N.Y. c. 1975, page 5.

10.Hevesy, G.; *Biochem. J.,* **1923,***17,* **439.**

11.Blumgart, H.L., Yens, O.C., *Am. J. Physiol.,* **1925,** *72,* **216.**

12.Joliot, F., Curie, I., *Nature,* **1934,** *133,* **201-202.**

13.Rutherford, E.; *The Collected Papers of Lord Rutherford of Nelson,* George Allen and Unwin LTD., London c. 1962 vol 2. p. 585-590.

14.Lawrence, E.O., Edlefson, N.E., *Science,* **1930,** *72,* **376-377.**

15.Joliot, F., Curie, I., *Nature,* **1934,** *133,* **201-202.**

16.Myers, W.G.; Wagner, H.N.; in *Nuclear Medicine,* Wagner, H.N. ed.; HP Publishing Co. Inc. New York, N.Y. c. 1975, page 7.

17.Chadwick, J., *Proc. Soc. London, Ser. A.*, 1932, *136*, 692-708.

18.Lawrence, E.O.; *Physical Review*, 1934, *46*, 746.

19.Chiewitz, O., Hevesy, G., *Nature*, 1935, *136*, 754-755.

20.Friedlander, G.; Kennedy, J.W.; Macias, E.S.; Miller, J.M.; *Nuclear and Radiochemistry*, John Wiley and Sons, c. 1981 pp 12.

21.Gottschalk, A., Hoffer, P.B., Potchen, E.J., (eds) *Diagnostic Nuclear Medicine*, 1988, *Williams and Wilkens*, Baltimore.

22.Gottschalk, A., Hoffer, P.B., Potchen, E.J., (eds) *Diagnostic Nuclear Medicine*, 1988, *Williams and Wilkens, Baltimore*, page 130.

23.Kabalka, G.W., Green, J.F., McCollum, G., *Seventh Int. Symp. Radiopharm. Chem.*, 1988, Gronigen, The Netherlands, p. 76, 90.

24.Subramanian, G., Rhodes, B.A., Cooper, J.F., Sodd, V.J., *Radiopharmaceuticals*, 1975, The Society of Nuclear Medicine Inc., New York.

25.Maisey, M.N., Britton, K.E., Gilday, D.L. (eds); *Clinical Nuclear Medicine*, 1983, Chapman and Hall, London, p. 407.

26.Heindel, N.D., Burns, H.D., Honda, T., Brady, L.W. (eds), *The Chemistry of Radiopharmaceuticals*, 1978, Masson Publishers, U.S.A., p 270.

27.Berman, D.S., Garcia, E.V., in Berman, D.S., Mason, D.T., (eds); *Clinical Nuclear Cardiology*, 1981, New york, Grune and Stratton, pp 49-106.

28.Neirinckx, R.D., Canning, L.P., Piper, I.M., Nowotnik, D.P., Pickett, R.D., Holmes, R.A., Volkert, W.A., Forster, A.M., Weisner, P.S., Marriott, J.A., Chaplin, S.B., *J. Nucl. Med.*, 1987, *28*, 191-202.

29.Sharp, P.F., Smith, F.W., Gemmell, H.G., Lyall, D., Evans, N.T.S., Grosdanovic, D., Davidson, J., Tyrell, D.A., Pickett, R.D., Neurincks, R.D., *J. Nucl. Med.*, 1986, *27*, 171-177.

30.Vallabhajosula, S., Zimmerman, R.E., Picard, M., Stritzke, P., Mena, I., Hellman, R.S., Tikofsky, R.S., Stabin, M.G., Morgan, R.A., Goldsmith, S.J., *J. Nucl. Med.*, 1989, *30*, 599-604.

31.Subramanian, G., McAfee, J.G., *Radiology*, 1971, *99*, 192.

32.Bevan, J.A., Tofe, A.J., Benedict, J.J., Francis, M.D., Barnett, B.L., *J. Nucl. Med.*, 1980, *21*, 967.

33.Francis, M.D., Ferguson, D.L., Tofe, A.J., Bevan, J.A., Michaels, S.E., *J. Nucl. Med.*, 1980, *21*, 1185.

34.Windholz, M., (ed), *The Merck Index*, volume 9, 1976, Merck and Co., Rahway, New Jersey. p. 1215.

35.Braverman, L.E., Vagenakix, A.G., *in* Wagner, H.N. ed.; *Nuclear Medicine*, HP Publishing Co. Inc. New York, N.Y. c. 1975, Chapter 13.

36.Livingood, J.J., Seaborg, G.T., *Phys. Rev.*, 1938, *53*, 1015.

37.Hertz, S., Roberts, A., Evans, R.D., *Proc. Soc. Exp. Biol. Med.*, 1938, *38*, 510-513.

38.Hamilton, J.G., *Am. J. Physiol.*, 1938, *124*, 667-678,

39.Wellman, H.N., Anger, R.T.Jr., Sodd, V.J., Paras, P., *CRC Crit. Rev. Clin. Radiol. Nucl. Med.*, 1975, *6*, 81.

40.Hawkins, L.A., *in* Theobald, A.E., *Radiopharmacy and Radiopharmaceuticals*, 1985, *Taylor and Francis, London*, Chapter 6.

41.Hertz, S., Roberts, A., *J. Clin. Invest.*, 1942, *21*, 624.

42.Mitchell, A.C.G., Juliano, J.O., Creager, C.B., Kocher, C.W., *Phys. Rev.*, 1959, *113*, 628-633.

43.Kung, H.F., Alavi, A., Chang, W., Kung, M-P, Keyes, J.W., Velchik, M.G., Billings, J., Pan, S., Noto, R., Rausch, A., Reilley, J., *J. Nucl. Med.*, 1990, *31*, 573-579.

44.Kung, M-P, Kung, H.F., Billings, J., Yang, Y., Murphy, R.A., Alavi, A., *J. Nucl. Med.*, 1990, *31*, 648-654.

45.Muhr, C., Bergstrom, M., Lundberg, P.O., Bergstrom, K., Hertsig, P., Lundquist, H., Antoni, G., Langstom, B., *J. Comput. Assist. Tomogr.*, 1986, *10*, 175. Hagglund, J., Aquilonius, S.-M., Eckernas, S.-A., Hartzig, P., Lundquist, H., Gullberg, P., Langstom, B., *Acta. Neurol. Scand.*, 1987, *75*, 87. Smith, M., Wolf, A.P., Brodie, J.D., Arnett, C.D., Barouche, F., Shino, G.-Y., Fowler, J.S., Russell, J.A.G., MacGregor, R.R., Wolken, A., Amgrist, B., Rotrosen, J., Peselow, E., *Biol. Psychiatry*, 1988, *23*, 653.

46.Bushberg, J.T., Mettler, F.A., *in* Gottschalk, A.; Hoffer, P.B.; Potchen, E.J.; eds. *Diagnostic Nuclear Medicine,* 2nd edition; Williams and Wilkins, c. 1988, chapter 14, p 178.

47.Gottschalk, A.; Hoffer, P.B.; Potchen, E.J.; eds. *Diagnostic Nuclear Medicine,* 2nd edition; Williams and Wilkins, c. 1988 p. 56.

48.Gottschalk, A.; Hoffer, P.B.; Potchen, E.J.; eds. *Diagnostic Nuclear Medicine,* 2nd edition; Williams and Wilkins, c. 1988 p. 65.

49.Oppenheim, B.E., Beck, N.B., in Gottschalk, A.; Hoffer, P.B.; Potchen, E.J.; eds. *Diagnostic Nuclear Medicine,* 2nd edition; Williams and Wilkins, c. 1988, chapter 7, p. 55.

50.Anger, H.O., *Rev. Sci. Instrum.*, **1958**, *21*, 27.

Chapter 2: Radioiodinated 2-Nitrobensyl Alcohols as Potential Probes for Tissue Hypoxia

2.1 Hypoxia and Cancer

The most recent data[1] concerning cancer mortality indicates that solid slow-growing tumours continue to form the most lethal class of cancers. The high mortality rate associated with solid, slow-growing tumours is a result of their extreme resistance to standard treatment regimes. A large amount of evidence has accumulated suggesting that the resistance to treatment displayed by these cancers is a direct result of their heterogeneous nature. Typically a solid, slow growing tumour will consist of several distinct regions, each having a unique response to a given treatment modality. The rapid cell proliferation involved with tumour growth quickly outstrips the nutrient supply in the vascular bed. This process results in regions of necrosis, where nutrient deficiencies result in cell death along with regions where well-oxygenated cells undergo normal cycling.

Thomlinson and Gray[2] published the seminal paper on tumour hypoxia in 1955. By careful analysis of human tumours they were able to conclude that in solid slow-growing tumours there should exist a region of cells that are severely hypoxic (oxygen deficient) at the border between the necrotic region and the region of normally oxygenated cells (Figure 2.1).

The significance of this discovery was not realized until

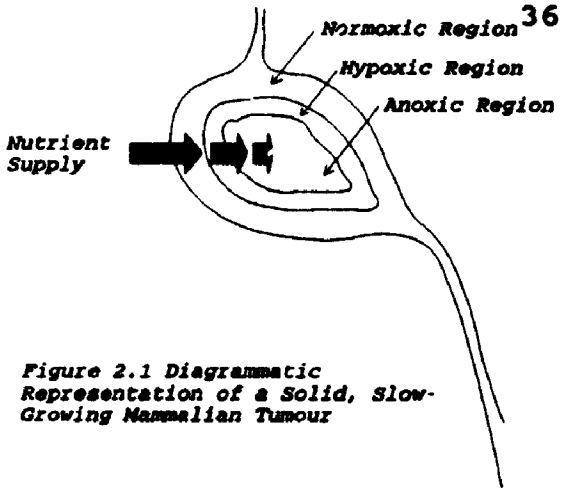

Figure 2.1 Diagrammatic Representation of a Solid, Slow-Growing Mammalian Tumour

some time later. Hewitt and Wilson[3] were able to show that tumours with a high hypoxic fraction were resistant to the effects of ionizing radiation. It was soon shown[4] that the hypoxic fraction of human tumours could survive large doses of ionizing radiation. This phenomenon can be demonstrated elegantly *in vitro* (Figure 2.2).

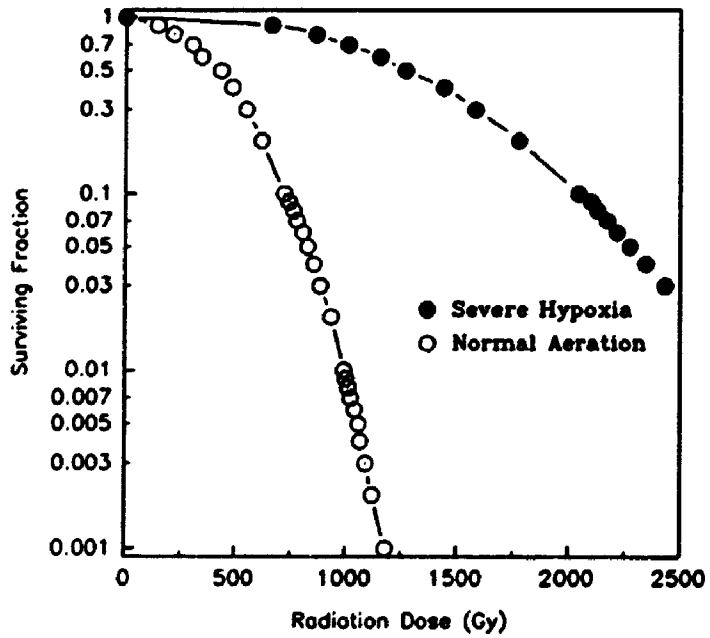

Fig. 2.2 Survival of EMT-6 Cells Irradiated *In Vitro*

Normally oxygenated cells show a very steep dose-response curve (fig. 2.2, open circles) when treated with ionizing radiation *in vitro*. In contrast, cells which have been made hypoxic by incubation in a nitrogen atmosphere prior to

irradiation show a much shallower dose-response curve (fig. 2.2, solid circles). The radiation dose required to kill hypoxic cels is often two to three times higher than that required to kill the same fraction of normally oxygenated cells. This observation has important implications with respect to the treatment of human cancers. Tumours with low hypoxic fractions are expected to be quite susceptible to radiation therapy while those with high hypoxic fractions shrink as the aerobic cells are killed but will be re-established when the oxygen supply is returned to the hypoxic cell. The radioresistance of hypoxic cells has stimulated a great deal of research directed toward specific treatments for these cells.

2.2 The Reducing Properties of Hypoxic Cells

Electrochemical studies of biological systems undertaken nearly fifty years ago[5] showed that amoeba cultures maintained in air had a reduction potential of -.07 volts (vs SCE) while the same amoeba cultures maintained in an atmosphere of nitrogen alone had a reduction potential of -.25 volts (vs SCE). The authors concluded that the more reducing environment under N_2 is the result of the exertion of reducing activities normally inhibited in the presence of oxygen rather than a release of specific reducing substances by the cells. It has become clear[6] that the reducing properties expressed by anaerobic amoeba are also expressed in hypoxic tumour cells.

There is growing evidence that the hypoxia associated with perfusion defects in such disease states as stroke[7] and myocardial infarct[8] also expresses these same reducing properties.

A number of chemotherapeutic agents have been discovered which have been shown to exploit the reducing properties of hypoxic cells in the expression of their cytotoxic properties. In general these agents fall into two categories: the quinone bioreductive alkylating agents and the nitroaromatic hypoxic cell sensitizers.

2.3 Quinone Bioreductive Alkylating Agents

Mitomycin C (MC) was first isolated from *Streptomyces Caesipitosus* in 1958[9].

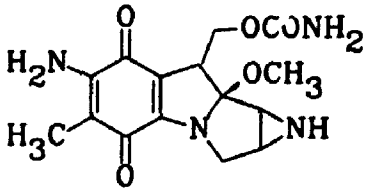

Mitomycin C (MC)

The molecule gained immediate attention due to its activity against several strains of bacteria and against tumours in animals.

It was observed[10] that Mitomycin C was relatively stable in aerobic tissue homogenates but was rapidly metabolized by anaerobic homogenates. The quinone structure of MC suggested to the authors that the selective toxicity of the molecule was

a result of its activation following its facile reduction in hypoxic tissues.

A study[11] of the DNA isolated from bacteria cultured in the presence of MC began to shed light on the nature of MC activity. The isolated DNA behaved in a curious way when the authors attempted to denature it (fig. 2.3).

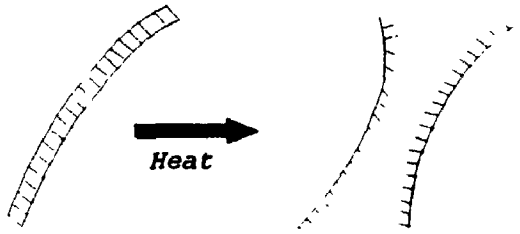

Normal DNA Denaturation

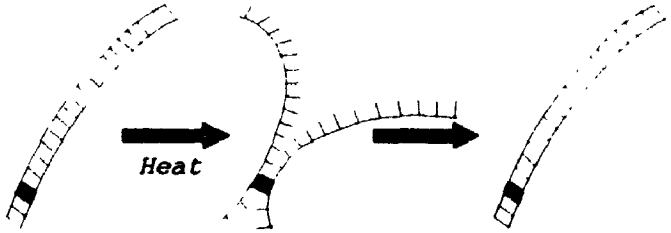

MC -Treated DNA undergoes reversible denaturation

Figure 2.3

In the normal heat-denaturation of DNA, the product appears as a band in the low-density region of a density centrifugation experiment. In the MC-treated sample the product appeared at a region consistent with the starting DNA. Experiments with formaldehyde showed that the DNA was being denatured but through some process was undergoing spontaneous renaturation. The authors concluded that the spontaneous renaturation was due to the cross-linking of DNA by MC and that the very rapid cell death caused by MC was a result of its action as a mitotic poison.

The mechanism of MC bioactivation has been studied by several investigators[12]. It is believed to be activated according to the following scheme: (Scheme 2.1)

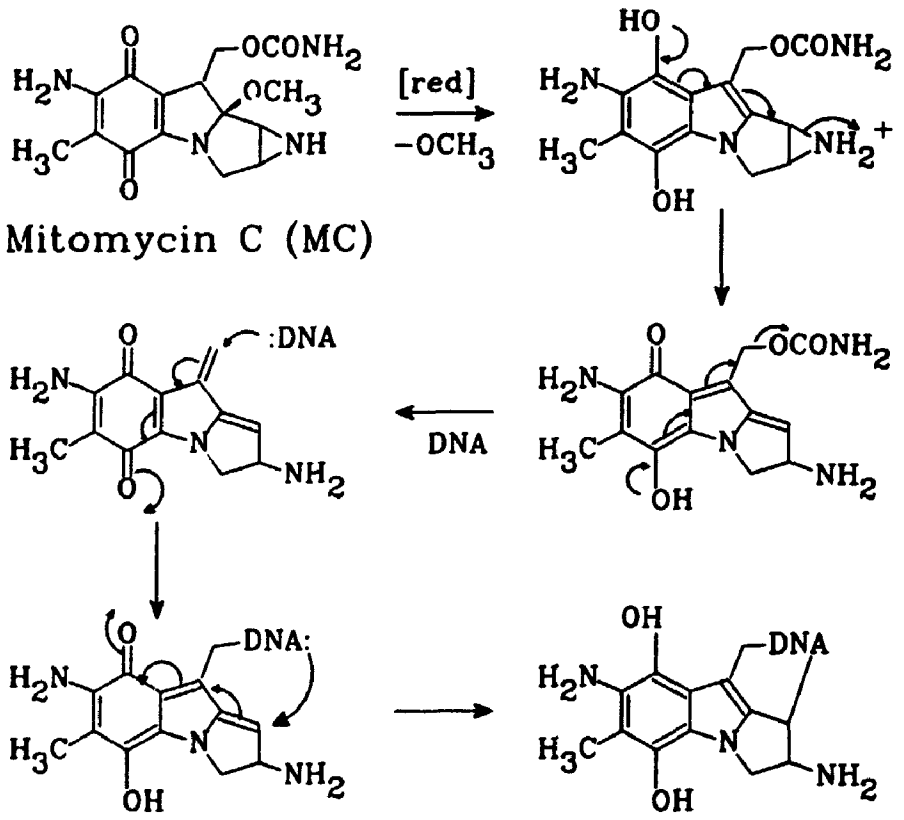

Scheme 2.1

The binding of MC to DNA was shown[13] to be sequence specific and required a high content of guanine or cytosine in the target DNA. A thorough search of the chemical literature has not revealed any studies with radioactive analogues of MC despite the fact that its total synthesis was reported some time ago[14]. Porfiromycin is an analogue of MC bearing a methyl group on the aziridinyl nitrogen. Since the binding of MC to hypoxic tissue is implied in its mode of action a study of the uptake of ^{11}C-porfiromycin at a positron facility might

prove fruitful. Unfortunately, there appears to be no simple route to the labelling of MC with a γ-emitting radionuclide such that the isotope would be stable *in vivo* and such that the biological properties of the molecule would not be significantly altered.

2.4 Nitroheterocyclic Radiosensitizers

The early 1970's saw the introduction of a new class of bioreductive alkylating agents called radiosensitizers. These agents were generally aromatic heterocycles functionalized with a nitro group. Misonidazole (MISO), and Metronidazole (METRO) are examples of this class of compounds.

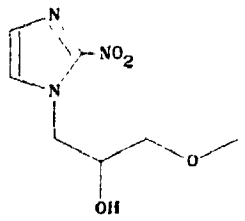

Misonidazole

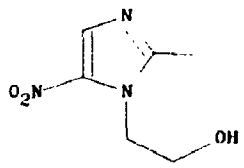

Metronidazole

These compounds are called "radiosensitizers" because the co-administration of these agents with ionizing radiation tends to potentiate the effects of the radiation. They are alternatively called "oxygen mimetics" since the administration of these agents to hypoxic tissue cultures followed by treatment with ionizing radiation results in kill levels comparable to normally oxgenated tissues (Figure 2.4).

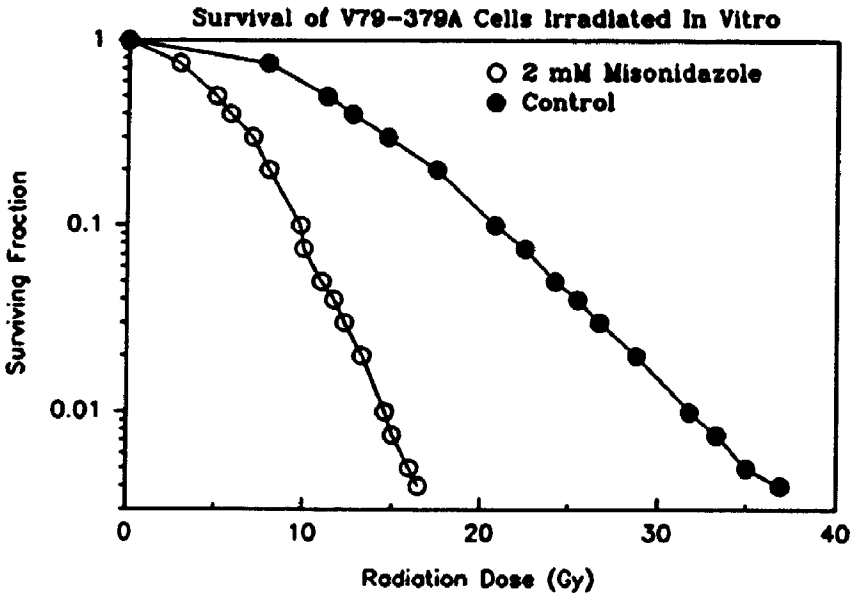

The mode of action of the nitroaromatic radiosensitizers is similar to that of Mitomycin C (Scheme 2.2).

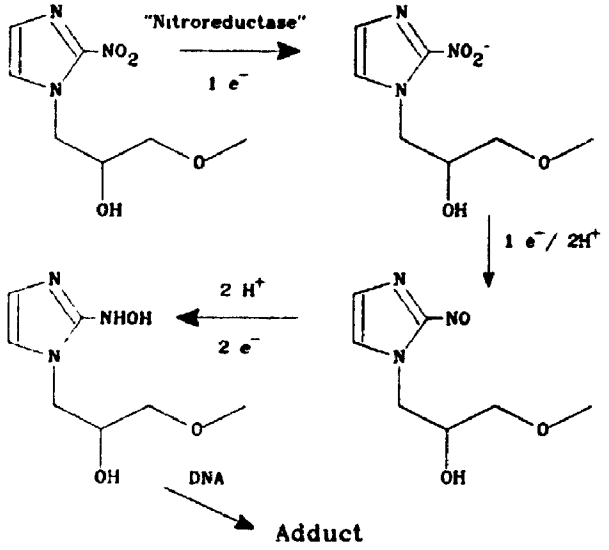

Scheme 2.2

The first stage in the bio-activation process is the diffusion of the sensitizer from the blood stream into the region of hypoxia. The nitro group then gains an electron via electron

transfer and the metabolic event is initiated. The radical anion would be quenched in the presence of oxygen leading to superoxide ion and back to starting misonidazole in a process called "futile cycling". In the hypoxic region however, no oxygen is present and thus the metabolic process can continue. The radical anion is further reduced to the dihydroxylamine which rapidly loses water to form the nitroso compound. The nitroso compound is then further reduced to the hydroxylamine and it is from this intermediate that Misonidazole is believed to exert its cytotoxic behaviour.

A number of products resulting from the fragmentation of Misonidazole have been reported[15]. Two products would seem to result from the attack of water on the hydroxylamine (Scheme 2.3).

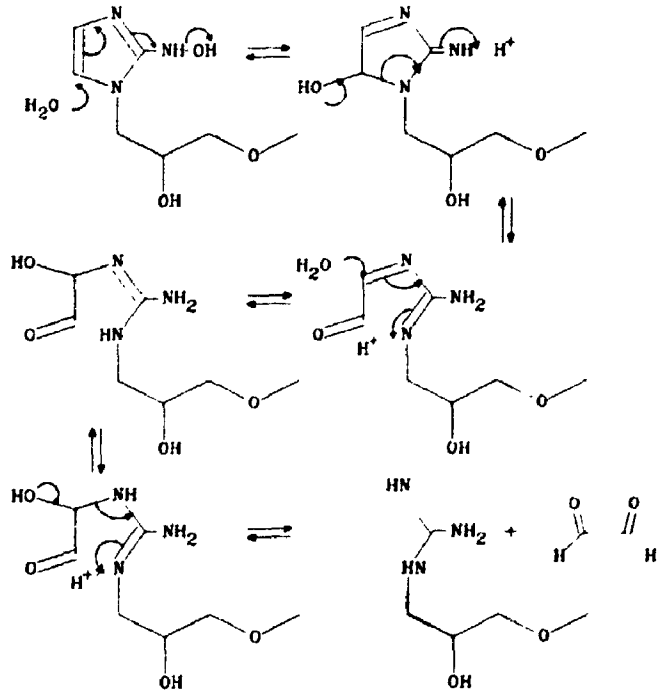

Scheme 2.3

Glyoxal has been identified[16] as a metabolite of Misonidazole and is known[17] to react readily with nucleic acids and proteins. When Chinese hamster ovary cells were exposed to Misonidazole under conditions of hypoxia in the presence of guanosine the following adduct was isolated from the media.

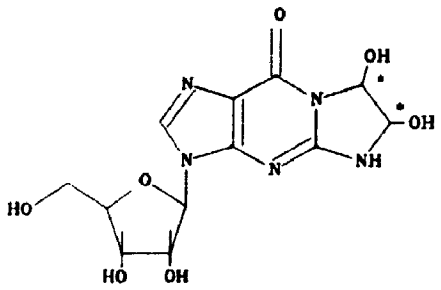

The asterisks indicate the glyoxal fragment believed to be derived from reduced Misonidazole. A number of other metabolites of Misonidazole have been identified which also possess alkylating activity. It is believed that Misonidazole exerts its radiosensitzing effects in a manner analogous to that of Mitomycin C by cross-linking complimentary strands of DNA in hypoxic cells and thereby functioning as a mitotic poison.

2.5 Radioactive Markers for Identification of Hypoxic Cells

A group of researchers from the Cross Cancer Institute published the seminal paper on hypoxia markers in 1981[18]. They were able to show by autoradiographic techniques that ^{14}C-labelled Misonidazole bound selectively to hypoxic regions in multicellular spheroids (an *in vitro* tumour model) and in the EMT-6 tumour model in Balb/c mice.

The authors recognized the value of a biochemical marker for hypoxia. Unfortunately, ^{14}C is a β-emitting radionuclide which can only be detected by autoradiography or liquid scintillation counting (a destructive technique). A much more useful marker would be labelled with an "imageable" isotope suitable for use in Nuclear Medicine.

2.6 Approaches to an Hypoxia Marker for Nuclear Medicine

The approach most often used in designing radiopharmaceuticals is to directly introduce a radionuclide into the structure of an existing drug. Indeed this approach has been used quite successfully in the labelling of Misonidazole. Misonidazole was directly brominated with ^{82}Br in 1982[19] (Scheme 2.4).

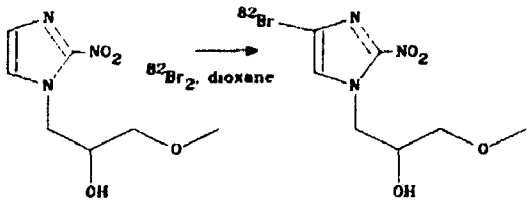

Scheme 2.4

The brominated analogue was tested *in vivo* and was found to sensitize tumours at a level equivalent to Misonidazole. In a tissue biodistribution experiment ^{82}Br-labelled compound was administered to balb/c mice bearing subcutaneous EMT-6 tumours. A high uptake of the drug was observed in the tumours but, unfortunately, the levels of drug in the blood were consistently higher than in the tumours throughout the experiment. In order for the agent to function as an hypoxic

cell imaging agent, the tumour to blood ratio must be significantly greater than unity so that one can adequately distinguish tumour activity due to hypoxia binding from activity due to the tumour blood pool.

The high blood activity may have been due to a number of factors. The investigators showed that the introduction of a bromine atom to the Misonidazole skeleton increased the lipophilicity of the resulting analogue as measured by its octanol-water partition coefficient (log P). The observed log P value for bromomisonidazole was 2.9 compared to 0.43 for misonidazole itself.

The octanol-water partition coefficient of a drug has been shown[20] to be an excellent predictor of the drug's behaviour *in vivo*. Compounds which are very water soluble tend to be excreted very rapidly from the body via the kidneys while compounds having a high partition coefficient tend to bind tightly to plasma proteins; the effective concentration of the drug is thus significantly reduced and it is excreted very slowly from the body. Very water insoluble compounds tend to exhibit their pharmacological activities very slowly owing to their low effective plasma concentrations.

The plasma binding of ^{82}Br-bromomisonidazole was determined and was found to be negligible. A plasma clearance experiment was undertaken and it was observed that bromomisonidazole was excreted in two components. A fast component was observed with a plasma half-life of 19 seconds along with a

slow component with a half-life of 6.3 hours. The fast component was found to be the clearance of parent compound from the bloodstream while the slow component was shown by a double-label experiment to be bromide ion. [^{3}H,^{82}Br]-bromo-Misonidazole was administered to mice and the radioactivity found in the bloodstream was monitored. The ratio of ^{82}Br activity to ^{3}H activity was found to increase with time; an indication of an accumulation of bromide ion in the blood.

Bromomisonidazole was later shown to be a useful *in vitro* marker for hypoxia in a spheroid tumour model[21] but its use as a radiopharmaceutical for nuclear medicine was precluded by its metabolic debromination [22].

The radiolabelling of the Misonidazole analogue 1-(2-phenoxyethyl)-2-nitroimidazole (PENI, Scheme 2.5) was reported in 1984[23].

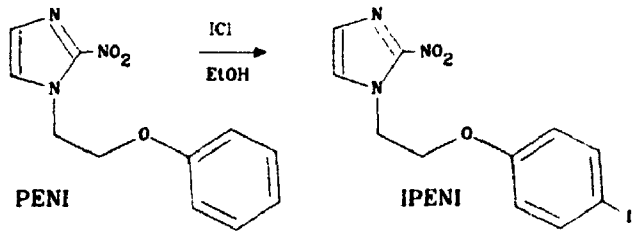

Scheme 2.5

Unfortunately the resulting compound was unacceptably lipophilic (log P=2.84) and its biodistribution was once again consistent with the very slow clearance of a water-insoluble compound.

A second approach to the iodination of a Misonidazole analogue has been attempted[24] (Scheme 2.6)

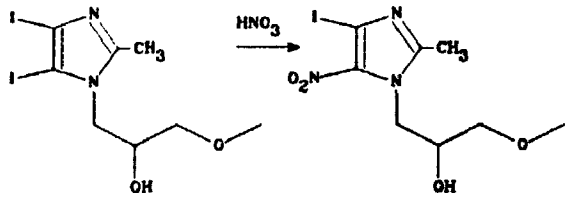

Scheme 2.6

The resulting iodinated nitroimidazole was found to have 5-10 times the activity of Misonidazole as a radiosensitizer. Unfortunately, the compound was also found to be metabolically deiodinated *in vitro* by both aerobic and hypoxic EMT-6 cells. It is possible that the dehalogenation occurs by a simple nucleophilic aromatic substitution pathway (Scheme 2.7).

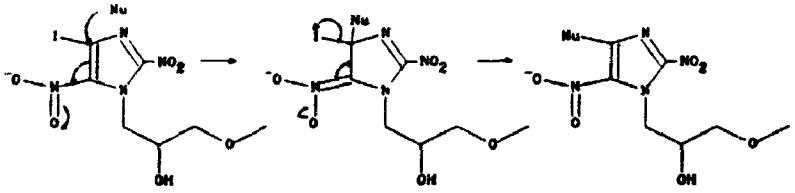

Scheme 2.7

The field of positron emission tomography (PET) has enjoyed the most success in the search for a hypoxic cell imaging agent. Three ^{18}F-labelled nitroimidazoles were reported in 1986[25]: [^{18}F] fluoro-normethoxy Misonidazole (^{18}F-MISO), 1-(2-[^{18}F]fluoroethyl)-2-nitroimidazole (^{18}F-ENI), and [^{18}F] fluoro-norhydroxy metronidazole (^{18}F-METRO).

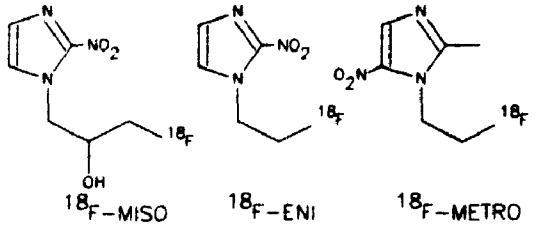

^{18}F-MISO is by far the most extensively tested of these agents. ^{18}F-MISO has been used to image spontaneous osteosarcomas in

dogs[26], hypoxic myocardium in isolated perfused rabbit heart and in dogs with acute coronary occlusion[27] and in human tumours of the brain[28]. ^{18}F-MISO continues to generate excitement as a valuable new diagnostic tool in the anti-cancer arsenal but its use will remain limited to the few centres around the world where PET procedures are performed. The success of this agent renders necessary the discovery of an hypoxia imaging agent suitably labelled with a γ-emitting radionuclide for use in single photon emission computed tomography (SPECT) techniques.

When we began our research toward such an agent it was not immediately apparent how a radiohalogen could be introduced into the Misonidazole skeleton in such a way that the label would be metabolically stable *and* such that the pharmacological properties of Misonidazole would be preserved. We made the decision to look beyond the nitroimidazole nucleus to other bioreductive alkylating agents in the search for an hypoxia label suitable for SPECT.

2.7 Nitrobenzyl Carbamates: Potential Bioreductive Alkylating Agents Labelled with Iodine

Teicher and Sartorelli[29] published a study on a series of *ortho* and *para* nitrobenzyl halides and carbamates as prototypical bioreductive alkylating agents in 1980. A total of twelve analogues were tested and all of these agents showed higher toxicity towards hypoxic than towards aerobic cells *in vitro*. Particularly noteworthy was the following compound 2.25:

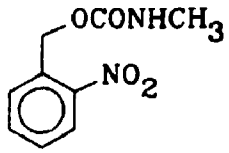

2.25

The ED_{50}* for this compound towards aerobic EMT-6 tumour cells in culture was 3.57 ug/ml while towards hypoxic tumour cells the value dropped to .006 ug/ml. The data would seem to indicate that 2.25 was nearly six hundred times more toxic to hypoxic cells than it was toward aerobic cells. The nature of this selective toxicity was believed to result from the reductive activation of the molecule in hypoxic tissue.

2.8 Activation of the p-Nitrobenzyl System: $S_{RN}1$?

Teicher and Sartorelli originally reported that the selective toxicity of some *ortho* and *para* nitrobenzyl halides and

---

*ED_{50} is defined as the concentration of drug required to achieve a 50% kill of EMT-6 cells *in vitro*.

carbamates was a result of the bioreductive process outlined in Scheme 2.8.

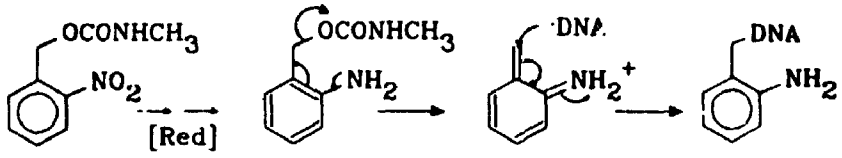

Scheme 2.8

Central to this process was the complete reduction of the nitro compound to the corresponding aniline. In light of the work of Kornblum and others[30] the following question has arisen[31]: Can nitroaromatic antineoplastics be activated by the $S_{RN}1$ mechanism?

2.8.1 The $S_{RN}1$ Mechanism

In a study of the alkylation of nitroparaffin salts an anomalous behaviour was observed[32] with some alkylating agents. The alkylation of a salt of 2-nitropropane with benzyl chloride proceeded in excellent yield to the product resulting from oxygen alkylation. The analogous alkylation of the same salt with 4-nitrobenzyl chloride was observed to undergo *carbon* alkylation in 92% yield (Scheme 2.9).

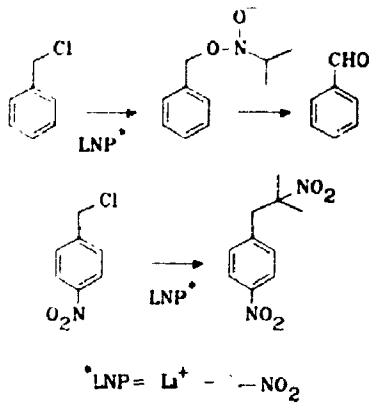

Scheme 2.9

It has been shown[33] that oxygen alkylation was a result of simple S_N2 attack on the alkyl halide but the carbon alkylation was a result of a different type of mechanism. The authors noted a change in the product distribution with a change in the leaving group on the nitrobenzyl halide (Table 2.1).

Table 2.1 Yields and rates for the alkylation of the lithium salt of 2-nitropropane with 4-nitrobenzyl halides (from ref. 33)

	para					meta
	% Yield Alkylate		Rates			Rate
Halide	C-	O-	k_t	k_C	k_O	k_t
Cl	92	6	.024	.022	.002	.0013
Br	17	57	.34	.058	.28	.28
I	7	86	1.9	.13	1.8	1.4

The insensitivity of the rate of carbon alkylation with respect to the halide was in contrast to the large change in the rate of oxygen alkylation observed with changes in the halide. The authors suggested that a free-radical mechanism might be responsible for the carbon alkylation. The authors

were able to show that the addition of one equivalent of *para*-dinitrobenzene as a free-radical trap in the alkylation of the lithium salt of 2-nitropropane with *para*-nitrobenzyl chloride changed the product distribution from 92% carbon alkylation to 72% oxygen alkylation. The proposed[34] mechanism is outlined in Scheme 2.10.

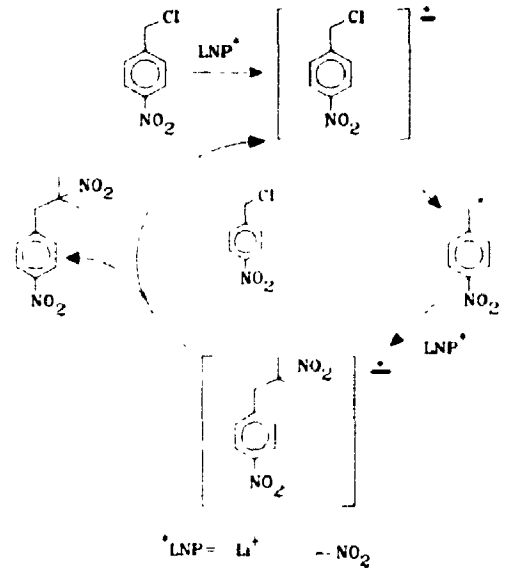

Scheme 2.10

The reaction has been shown to occur with a number of nucleophiles in addition to the nitroparaffin salts[35] and has been shown to be catalyzed by light[35]. The $S_{RN}1$ reaction has also been shown to occur with a variety of aromatic halides[36] (Scheme 2.11) and a variety of nucleofuges.

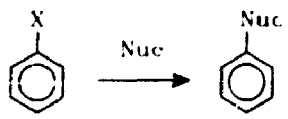

X=Cl, Br, I, $PO(OR)_2$

Nuc= NH_2, R , Ar

Scheme 2.11

The reaction is tolerant to a variety of substituents on the aromatic ring including alkyl, alkoxy, phenyl, carboxylate and benzoyl functionality. The reaction *does not*, however, proceed in the presence of dimethylamino, ionized hydroxy, or nitro groups. This final point was of crucial importance to the goal of our research.

An electrochemical study was undertaken[37] in order to investigate the metabolic activation of *ortho* and *para* nitrobenzyl alcohol derivatives. Sartorelli and co-workers showed that reduction of these compounds in the presence of nucleophiles led to products consistent with the $S_{RN}1$ mechanism (Scheme 2.12).

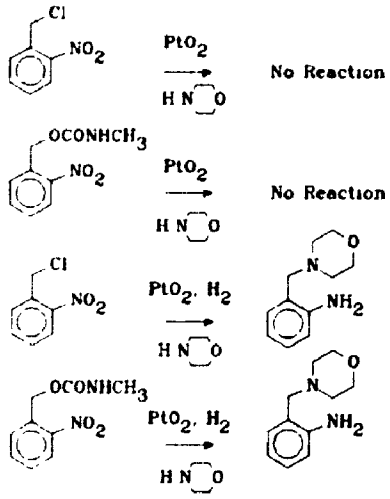

Scheme 2.12

Cyclic voltammetry was then used to further characterize the reduction process. The voltammograms of *o* and *p*-nitrobenzyl chlorides were characterized by the absence of an anodic wave corresponding to the reoxidation of the radical anion (Scheme 2.13).

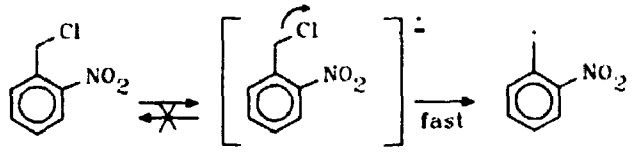

Scheme 2.13

In the presence of morpholine, the voltammograms were consistent with the formation of the morpholine adduct. The formation of the morpholine adduct was confirmed by standard chemical techniques following controlled potential electrolysis.

Unfortunately, the situation for the corresponding carbamates was not quite so clear. Cyclic voltammetry showed that these compounds undergo quasi reversible one-electron reduction (Scheme 2.14).

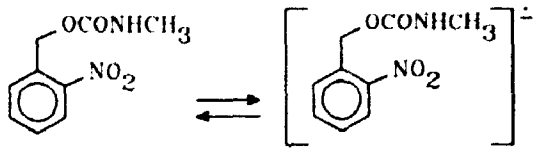

Scheme 2.14

Controlled potential electrolysis in the presence or absence of morpholine yielded only the starting nitro carbamates. The authors concluded that the reactive intermediate that undergoes substitution was formed after two or more electrons were added to the system. It seems that the originally postulated mechanism involving complete reduction of the nitro carbamate to the aniline may be correct. It is interesting to note that (*o*-nitrobenzyl)-6-thioguanine does not undergo carbon-sulfur cleavage when reduced in the presence of

morpholine (Scheme 2.15).

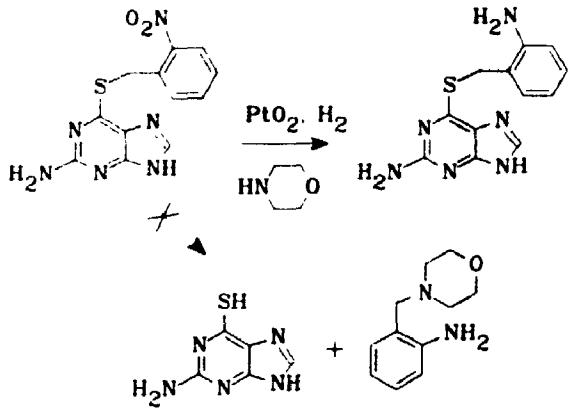

Scheme 2.15

This is an important result since it implies that carbon-sulfur bond formation at the subcellular level is an *irreversible* process. Thus DNA may be alkylated irreversibly by these agents.

Though the bioreductive alkylation of hypoxic cells was only implied in the toxic activity of the 2-nitrobenzyl carbamates, we believed the evidence was sufficiently strong to pursue the labelling of these agents with isotopes of iodine in the hopes that the resulting agents would serve as potential hypoxic cell imaging agents.

2.9 Chemistry

Ideally, the synthetic chemistry leading to a radiopharmaceutical should be designed in such a way that the radionuclide can be installed as the final step in the synthesis. This is especially important when using short-lived isotopes like ^{123}I. The halodemetallation reaction[38] has proven to be very useful in the case of halogen-containing radiopharmaceuticals (Scheme 2.16)

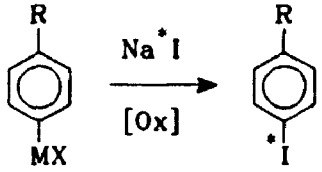

Scheme 2.16

A number of researchers[39] have enjoyed success with the halodemercuration reaction as a route to iodine containing radiopharmaceuticals. The availability of numerous synthetic routes to the required organomercury precursors encouraged us to pursue this route to the desired radiopharmaceuticals.

2.10 Target Molecule 2.7: Iodine *Para* to the Nitro Group

A survey of the literature suggested that compound **2.7** would be the most easily accessed of the iodinated 2-nitrobenzyl carbamates.

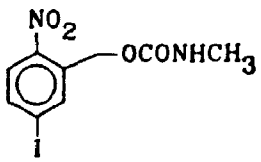

2.7

Since the corresponding aniline **2.5** is a common intermediate in the synthesis of the organomercury and the non-radioactive iodine compounds we chose this aniline as our first target molecule.

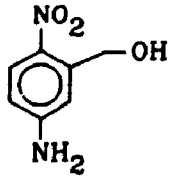

2.5

The aniline was first prepared in 1933[40] and the procedure was repeated with only a few minor modifications. Commercial 3-nitrobenzaldehyde was reduced with sodium borohydride[41] to the corresponding alcohol **2.1** which was further reduced to the corresponding aniline **2.2** with hydrazine in the presence of 10% palladium on charcoal[42] as catalyst (Scheme 2.17).

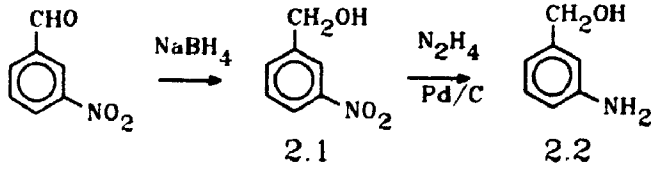

2.1 2.2

Scheme 2.17

The aminobenzyl alcohol **2.2** was then protected as the diacetate prior to nitration. The yield of the reaction was greatly improved by the addition of five mole percent 4-dimethylamino pyridine (DMAP) as a hypernucleophilic acylation catalyst[43] (Scheme 2.18).

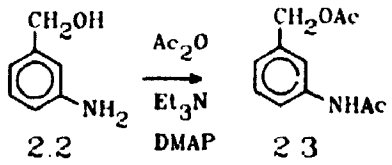

2.2 2.3

Scheme 2.18

The nitration of **2.3** in cold fuming nitric acid proceeded smoothly to yield three isomeric products (Scheme 2.19).

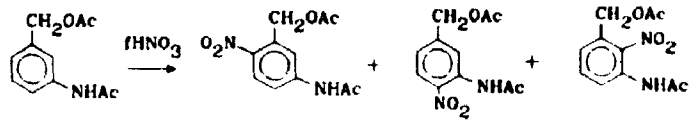

2.3 2.4 (4) 2.4a (2) 2.4b (1)

Scheme 2.19

The desired **2.4** was readily isolable from the mixture by recrystallization from benzene. The target aniline was then obtained by the hydrolysis of **2.4** in 50% sulfuric acid.

With the desired intermediate **2.5** in hand we synthesized the corresponding ^{127}I compound via the Sandmeyer[44] reaction (Scheme 2.20).

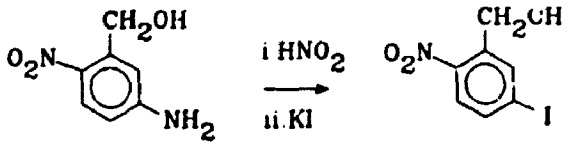

2.5 2.6

Scheme 2.20

We chose the method of Hu, Ni, and Kao[45] to synthesize the desired organomercury compound **2.8** because of the reported high yields of analogous reactions and the simplicity of the procedure (Scheme 2.21).

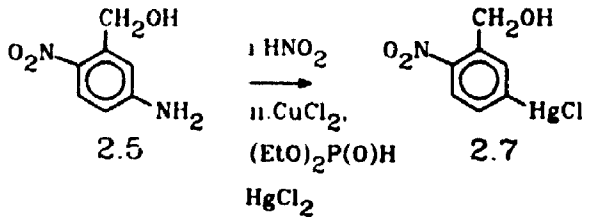

2.5 2.7

Scheme 2.21

The desired N-methyl carbamates **2.7** and **2.9** were obtained by reaction of the benzyl alcohols **2.6** and **2.8** with methyl isocyanate under catalysis by triethylamine (Scheme 2.22).

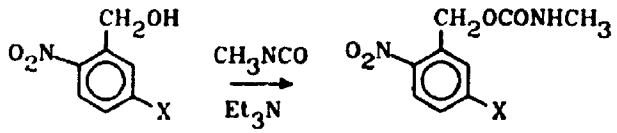

2.6 (X=I) 2.7 (X=I)
2.8 (X=HgCl) 2.9 (X=HgCl)

Scheme 2.22

Treatment of the chloromercury derivative **2.9** with $Na^{131}I$ in the presence of N-chlorosuccinimide as oxidant furnished radioactive **2.7** in 77% radiochemical yield after purification by HPLC. The identity of the radioactive material was confirmed by recrystallization to constant specific activity.

2.11 Target molecule 2.15: Iodine *Meta* to the Nitro Group

The preliminary biodistribution for [^{131}I] **2.7** data showed a high accumulation of radioiodide in the thyroid. Halogens substituted *ortho* and *para* to electron acceptors like nitro, cyano and carboxyl groups are activated to nucleophilic aromatic substitution[46]. In order to investigate this type of substitution as a possible mechanism for the *in vivo* deiodin-

ation we prepared the isomeric carbamate **2.15** in which the iodine atom is substituted *meta* to the nitro group.

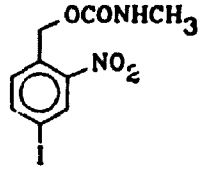

2.15

The isomeric carbamate **2.15** was prepared in a manner analogous to that of **2.7**. The synthesis of the corresponding aniline **2.13** has previously been reported[47] and we followed this route without modification.

Commercial benzyl chloride was nitrated with a cold fuming nitric acid/sulfuric acid mixture to yield the dinitrated derivative **2.10**. The dinitro derivative **2.10** was found to be difficult to handle due to its lachrymatory properties. As a result **2.10** was not purified but was instead converted directly to the acetate **2.11** (Scheme 2.23).

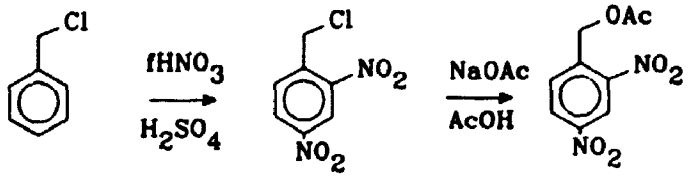

2.10 2.11

Scheme 2.23

Hydrolysis of the acetate **2.11** in 50% aqueous sulfuric acid gave rise to 2,4-dinitrobenzyl alcohol **2.12**. The nitro group at the 4-position was then selectively reduced by sodium hydrosulfide to yield the desired aniline **2.13** (Scheme 2.24).

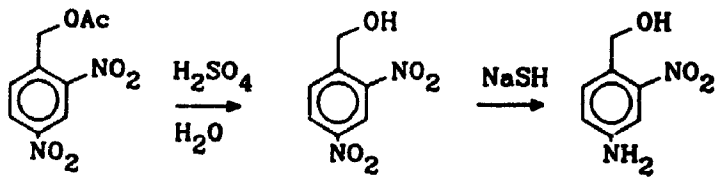

2.11 2.12 2.13

Scheme 2.24

The corresponding iodo and chloromercury derivatives **2.14** and **2.17** were synthesized by the previously described procedure and converted to the N-methyl carbamates **2.15** and **2.17** with methyl isocyanate and triethylamine (Scheme 2.25).

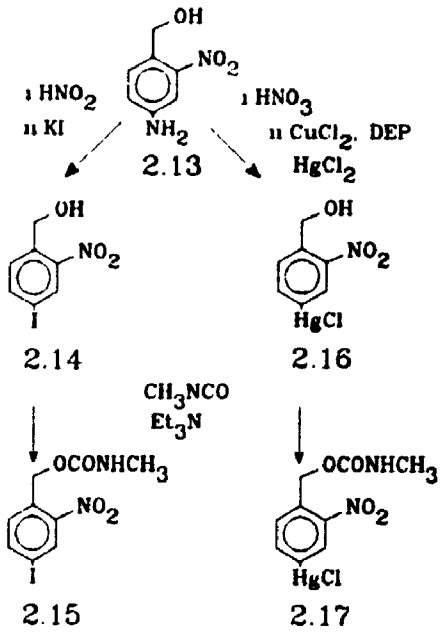

Scheme 2.25

2.12 Target Molecule 2.23: The Dinitro Analogue

The activity displayed by a compound as a radiosensitizer is related to the compound's reduction potential. With this in mind we pursued the synthesis of the di-nitrated derivative **2.23** in the hopes that the increased electron affinity of the

di-nitro derivative would result in a more effective bioreductive alkylating agent.

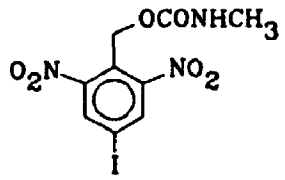

2.23

Commercial 2,6-dinitrotoluene was iodinated by the method of Arotsky, Butler, and Darby[48] with elemental iodine in the presence of fuming sulfuric acid (Scheme 2.26).

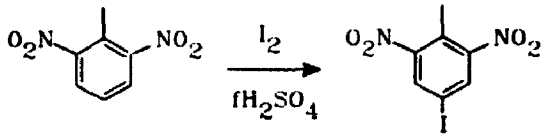

2.19

Scheme 2.26

Iodine is not normally regarded as a powerful electrophile. However, in the presence of fuming sulfuric acid the following reaction has been shown[49] to occur:

$$3I_2 + 2SO_3 + 2H^+ \rightarrow 2I_3^+ + SO_2 + H_2SO_4 \qquad \text{Eq. 2.1}$$

At room temperature I_3^+ is believed to function as the electrophile while at higher temperatures an even better electrophile I_2^+ is formed according to equation 2.

$$4I_3^+ + 2SO_3 + 2H^+ \rightarrow 6I_2^+ + SO_2 + H_2SO_4 \qquad \text{Eq. 2.2}$$

The desired 4-iodo-2,6-dinitrotoluene **2.19** was brominated by the method of Fieser and Doering[50]. Calcium carbonate, bromine, and the 4-iodo-2,4-dinitrotoluene were sealed in a Carius tube with a catalytic amount of pyridine and heated for six hours at 160°C (Scheme 2.27).

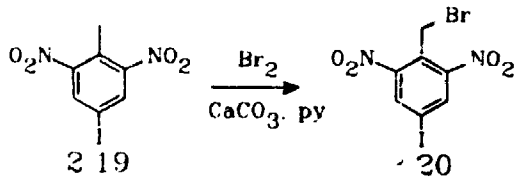

Scheme 2.27

Yields from the bromination reaction were consistently lower than 30%. This was in contrast to the results of Fieser and Doering who achieved an average yield of 71% in the bromination of 2,4,6-trinitrotoluene. The poor yields achieved in this reaction may result from cleavage of the carbon-iodine bond in the starting materials at the high reaction temperature. The energy required for homolytic bond cleavage in elemental bromine is 44 kcal/mol as compared to 64 kcal/mol for the sp^2 carbon-iodine bond in iodobenzene.

The yields achieved were sufficient to continue forward in the synthesis. The benzyl bromide **2.20** was converted to the acetate by reaction with sodium acetate in refluxing acetic acid. The acetate **2.21** was then hydrolyzed in aqueous sulfuric acid to the alcohol **2.22** (Scheme 2.28)

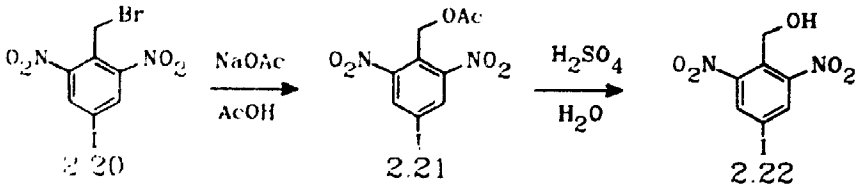

Scheme 2.28

The alcohol was then converted to the N-methyl carbamate **2.23** with methyl isocyanate and triethylamine (Scheme 2.29).

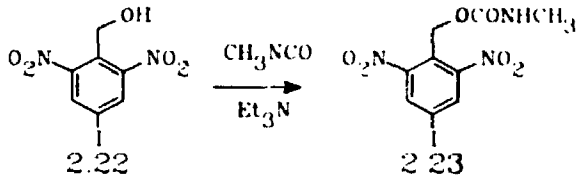

Scheme 2.29

We initially believed that the palladium catalyzed couplings of aryl iodides and hexaalkyl ditins were limited to activated aromatic systems. We were fortunate to learn that this methodology has been extended to highly deactivated systems by Beletskaya and co-workers[51]. Using π-allyl palladium chloride dimer they were able to convert *o*, *m*, and *p*-nitroiodobenzenes and 2,4-dinitroiodobenzene to the corresponding trimethylstannyl derivatives in good yield. With this in mind we attempted the coupling reaction with the iodo carbamate **2.24** (Scheme 2.30).

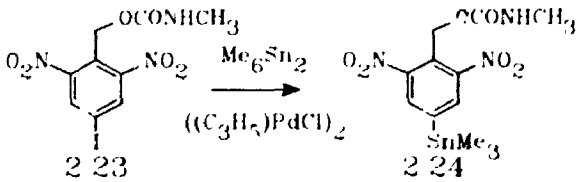

Scheme 2.30

The desired trimethylstannyl derivative **2.24** was obtained in 57% yield. The trimethylstannyl derivatives have some practical advantages over t' chloromercury derivatives in labelling reactions. The trimethylstannyl derivatives are more soluble in organic solvents, react more quickly (qualitatively) than the organomercury derivatives, and are more strongly retained by reversed-phase HPLC columns than the radioiodinated analogues produced from the trimethylstannyl

derivatives. This final point is worthy of further explanation. A typical radiolabelling reaction involves the treatment of approximately 500 μg of organotin compound with nanogram quantities of radioactive iodine. The radiopharmaceutical produced in the reaction is mixed with 10^5–10^6 times its weight in starting material. Organomercury precursors are slightly more polar than their iodinated analogues and elute ahead of the iodine radiopharmaceutical on reversed-phase HPLC columns. The iodine radiopharmaceutical is almost inevitably swamped by the organomercury compound. The purification of the radiopharmaceutical thus requires time-consuming re-injections. Trimethylstannyl derivatives are slightly less polar than the corresponding iodinated derivatives and elute behind the iodine radiopharmaceutical. The net result is that the purification step using organotin precursors is a single HPLC injection, an important advantage when time is a factor. The numerous practical advantages of radiolabelling via organotin precursors coupled with our success in obtaining the trimethylstannyl derivative **2.24** encouraged us to attempt the stannylation of the mono-nitro carbamate **2.15** (Scheme 2.31).

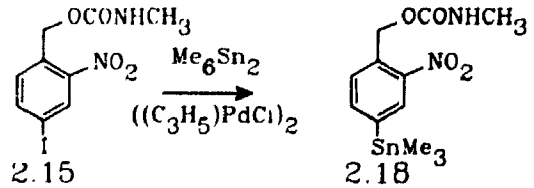

2.15 2.18

Scheme 2.31

The organotin derivative **2.18** was obtained in satisfactory yield.

The labelling of the trimethylstannyl derivatives **2.18** and **2.24** proved straightforward giving rise to the desired ^{125}I derivatives in yields of 70% and 76% respectively.

2.13 Partition Coefficients of the Target Molecules

The octanol-water partition coefficient (log P) has been shown to be an excellent measure of a compound's macroscopic behaviour *in vivo*[52]. Extremely lipophilic molecules (high log P) exhibit slow pharmacodynamics due to strong interactions with lipids and plasma proteins. Lipophilic molecules must be eliminated from the bloodstream via the hepatobiliary sytem (liver, gallbladder then intestine) or must be metabolized by the liver to more water soluble derivatives.

A systematic study[53] of a series of 2-nitroimidazoles did not indicate a strong correlation between biological activity and partition coefficient. The study did show, however, that the plasma half-life was strongly dependent on the partition coefficient. With this in mind we undertook the determination of the partition coefficients of compounds **2.7**, **2.15**, and **2.23**. Two approaches were used. In a more typical protocol ^{125}I-labelled compound was partitioned between pH 7.4 phosphate buffer and freshly distilled n-octanol. An aliquot of each layer was counted for radioactivity and the partition coefficient was calculated in the usual way. The values obtained in this manner are compiled in Table 2.2.

Table 2.2. Partition Coefficients of the test compounds.

Compound	Log P	Std. Dev.
2.7	1.16	0.12
2.15	2.66	0.04
2.23	1.25	0.04

The process of determining log P values is often complicated by large systematic errors. A method for the determination of log P values via HPLC chromatography has appeared[54] which has the advantage of comparing the retention time of a compound with an unknown log P on a reversed-phase column to the retention times of a series of compounds with known log P's in order to arrive at the log P of the test compound. The retention behaviour of a molecule under a given set of HPLC conditions is routinely expressed as k', the capacity factor, a term which is defined by equation 1:

$$k' = (t_r - t_o)/t_o \qquad 1)$$

The retention time for a retained peak is given by t_r while the retention time for an unretained peak is given by t_o. It has been shown[55] that, if simple partitioning is being observed, then the following expression (2) should hold:

$$\log P = \log K + \log k' \qquad 2)$$

The ratio of the log K for a given compound over the log K of benzene should remain constant for a given set of HPLC conditions. The HPLC experiment was performed and the results are shown graphically in Figure 2.4a.

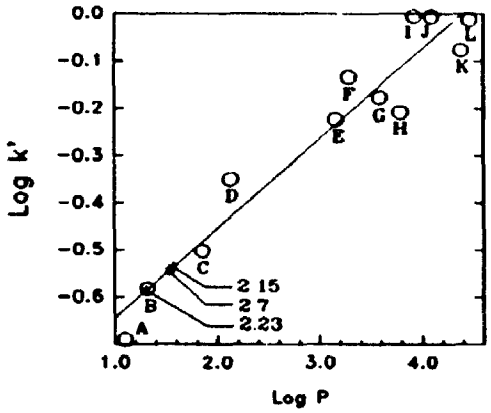

Figure 2.4a Plot for Log P Determination

The use of extensively silylated stationary phase in these log P determinations was recommended by the authors. Commercial reversed-phase HPLC packing consists of silica particles that have been functionalized with octadecylsilyl groups. The nature of the coupling reaction and the size of the silicon reagent dictates that many of the silanol groups originally present are not functionalized in the reaction. The result is that some basic molecules interact with the slightly acidic silanol groups and the HPLC peak widths are broadened. In the log P experiment the presence of silanols leads to scattering of the k' values due to interactions other than simple hydrocarbon partitioning. Commercial end-capped (extensively silylated) columns are available and these were used in the log P experiment. Our results show substantial scatter about the line of best fit; a result that was not observed by McCall in his original publication. Our results suggest that the

commercial columns may not be sufficiently silylated to give reliable log P values. The results of our experiment are given in Table 2.3.

Table 2.3. Retention data for Figure 2.4a.
Solvent system: 35% H_2O:65% (1% triethylamine in acetonitrile).

Compound	Label	k'	log k'	log P^{56}	log K	K_N
benzyl alcohol	A	0.204	-0.690	1.10	1.79	0.72
o-toluidine	B	0.262	-0.582	1.32	1.90	0.77
nitrobenzene	C	0.315	-0.502	1.85	2.35	0.95
benzene	D	0.447	-0.350	2.13	2.48	1.00
toluene	E	0.598	-0.223	3.16	3.38	1.36
iodobenzene	F	0.734	-0.134	3.29	3.42	1.38
napthalene	G	0.666	-0.177	3.59	3.76	1.52
chlorobenzene	H	0.619	-0.208	3.79	4.00	1.61
acenapthene	I	0.987	-0.005	3.92	3.93	1.58
biphenyl	J	0.986	-0.006	4.09	4.10	1.65
fluorene	K	0.840	-0.076	4.38	4.46	1.80
phenanthrene	L	0.973	-0.012	4.46	4.47	1.8[illegible]
2.7	*	0.286	-0.543	1.53		
2.15	*	0.291	-0.536	1.57		
2.23	*	0.260	-0.585	1.31		

Table 2.4. Linear regression values for Figure 2.4a.

Plot	a	b	r	σ(log P)
1	-0.8347	0.1902	0.9647	1.139

The log P values for compounds **2.7**, **2.15**, and **2.23** calculated from the HPLC experiment do not agree well with the values obtained in the simple partitioning experiment (Table 2.2). The large discrepancy between the values obtained by liquid-liquid partitioning for the structural isomers **2.7** and

2.15 suggests that this technique is the least reliable of the two used. The log P's for the three test compounds were calculated** by the method of Fujita, Iwasa, and Hansch[52] and are tabulated in Table 2.5.

Table 2.5. Comparison of experimental and calculated log P values.

Compound	Log P (HPLC)	Log P (calc'd)
2.7	1.53	1.66
2.15	1.57	1.66
2.23	1.31	1.38

The good agreement between the log P's calculated from the HPLC experiment and those calculated by the semi-empirical method of Leo, Iwasa, and Hansch suggests that, despite some scatter around the line of best fit, the HPLC method provides a good estimation of the log P's of the test compounds. Perhaps a greater strength of the HPLC method is the ability to directly compare a series of compounds under nearly identical conditions.

2.14 Electrochemical Studies

A linear relationship between radiosensitization efficiency and reduction potential has been established[57]. The half-wave reduction potentials for the compounds were determined by polarography in acetonitrile containing 1M tetraethyl ammonium perchlorate as electrolyte. A dropping mercury electrode served as the cathode while a 1 cm^2 tube of platinum foil served as the anode. A silver/silver chloride electrode

**Details of these calculations are given in Appendix 2.

served as the reference. The compounds were dissolved in triply-distilled (from P_2O_5) acetonitrile to a concentration of 0.1 mM and were thoroughly degassed with argon prior to the experiment. The cell configuration is shown in Figure 2.5.

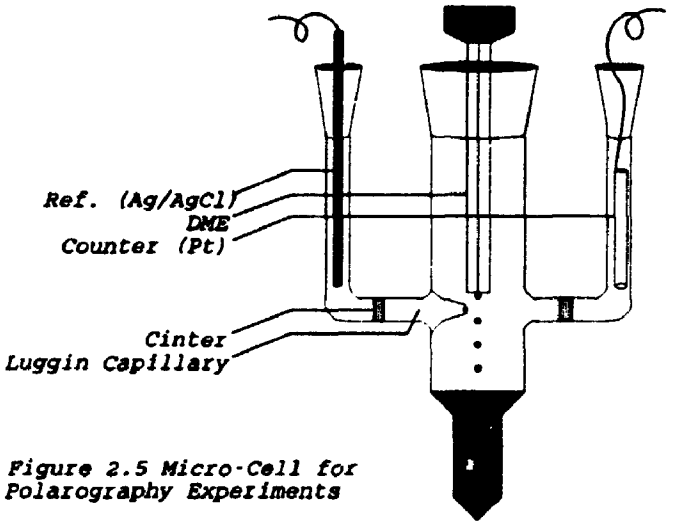

Figure 2.5 Micro-Cell for Polarography Experiments

The results of the polarography experiments are shown in Table 2.6.

Table 2.6 Polarography results for the test compounds. * SSC-silver/silver chloride electrode; ** (calculated); ***($E_{1/2}$ lit[56]); **** (lit[59]).

Compound	$E_{1/2}$ (vs SSC)*	$E_{1/2}$ (vs SCE)**
2.7	-0.994	-1.101
2.15	-0.988	-1.007
2.23	-0.784	-0.803
2.25	-1.128	-1.147
MISO	ND	-1.052***
Nitrobenzene	-1.118	-1.137
Nitrobenzene		-1.147****

A comparison of the half-wave reduction potentials for the test compounds and that of Misonidazole indicates that none of the test compounds are precluded on the basis of their reduction potentials alone.

2.15 Biological Studies

A preliminary investigation using [^{125}I]-**2.7** was undertaken to determine the organ distribution of this agent in healthy CD-1 mice. The results are represented graphically in Figure 2.6.

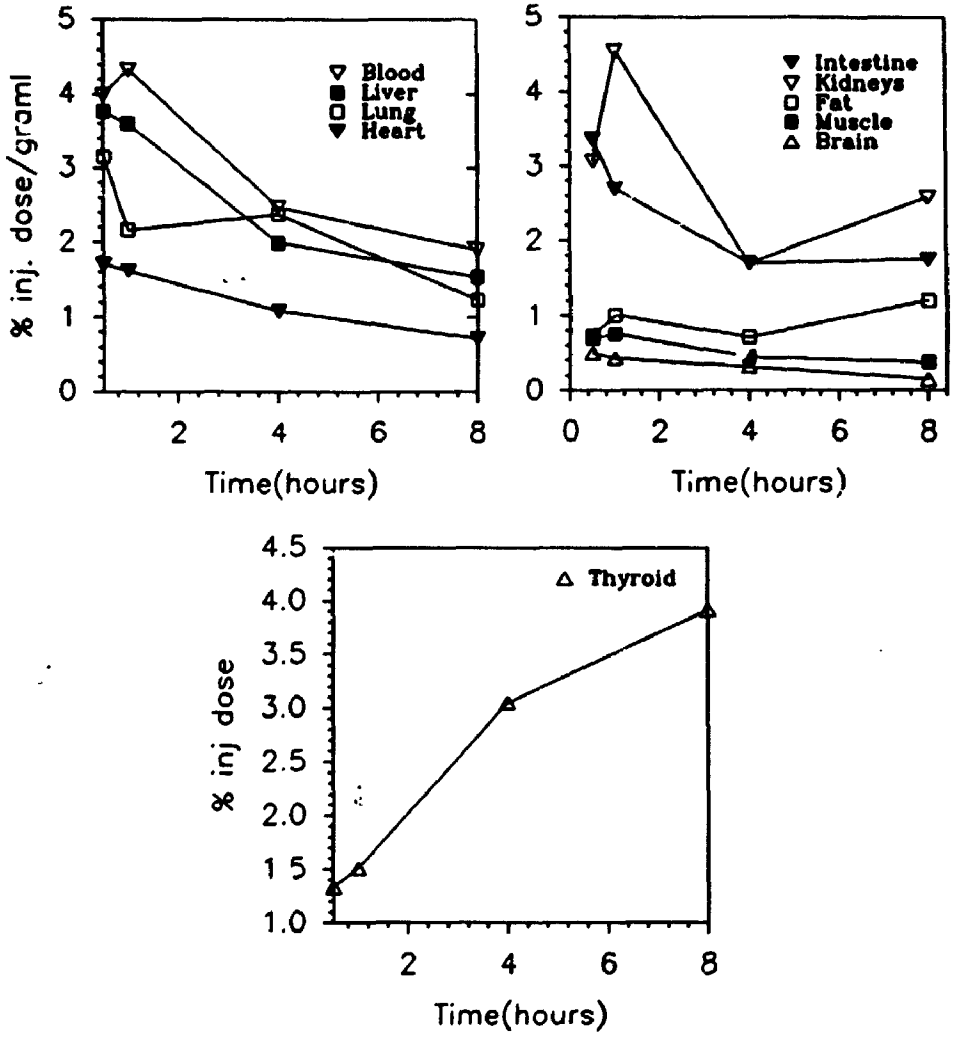

Figure 2.6 Healthy Biodistribution of [I-125]-2.7

The high thyroid uptake observed in this preliminary investigation was cause for concern. Thyroid uptake is given in units of percent injected dose in the whole organ by con-

vention. The small size of the organ coupled with the high uptake of iodide gives rise to unreasonable values (150-200%) for uptake on a per gram basis. Compound **2.7** is activated towards nucleophilic aromatic substitution because the iodine is substituted *para* to the nitro group (see section 2.11). We attempted to stabilize the molecule towards nucleophilic aromatic substitution by preparing the isomeric carbamate **2.15** in which the iodine is substituted *meta* to the nitro group. The results of a healthy biodistribution experiment with ^{125}I-labelled **2.15** are represented graphically in Figure 2.7.

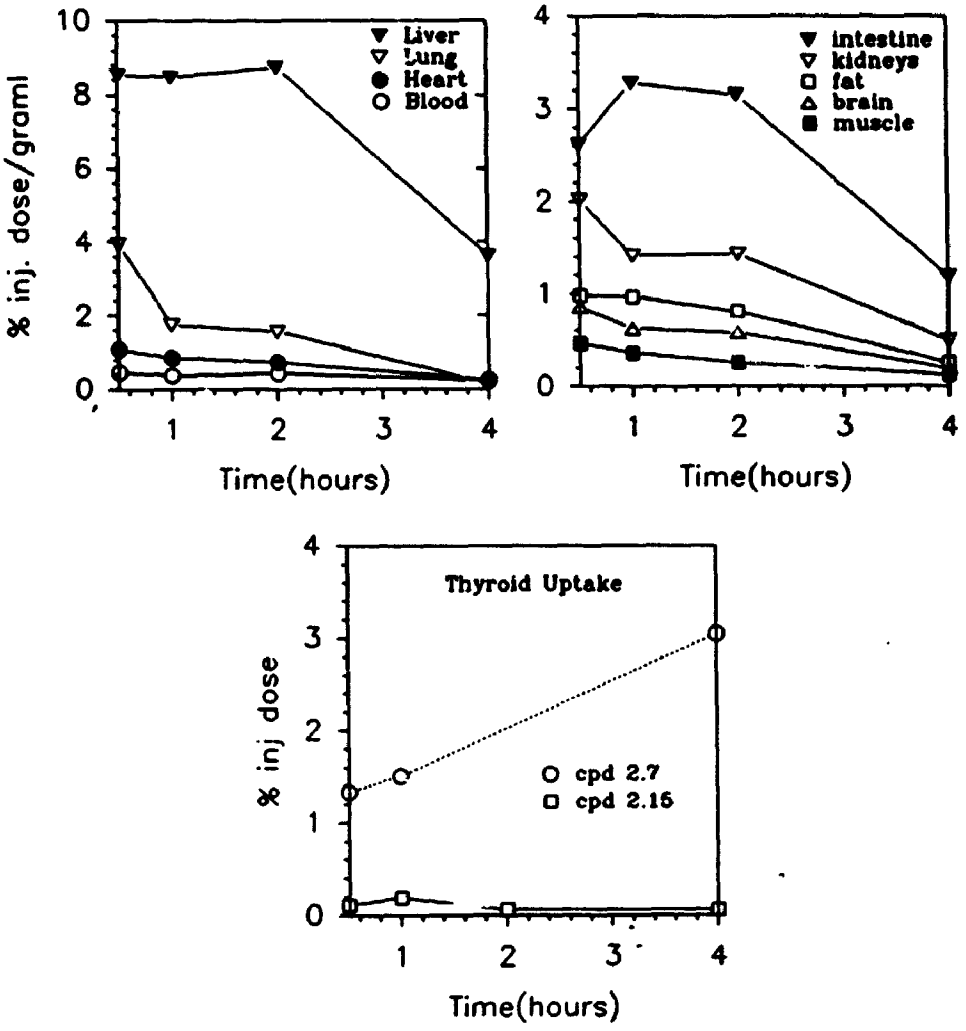

Figure 2.7 Healthy Biodistribution of [I-125]-2.15

The comparison of thyroid uptake clearly demonstrates that the *meta* substitution of the iodine relative to the nitro group has stabilized **2.15** relative to **2.7** with respect to *in vivo* deiodination. The improved stability of **2.15** convinced us to suspend further testing of **2.7** as a potential hypoxic cell imaging agent. Our attention turned to the testing of **2.15** using the EMT-6 tumour model in Balb/c mice. We encountered a number of technical difficulties in setting up this

system. The time interval spent solving these problems allowed us to pursue a third carbamate **2.23** which is the dinitrated analogue of **2.15**. The results of a biodistribution of **2.23** in healthy CD-1 mice is represented graphically in Figure 2.8.

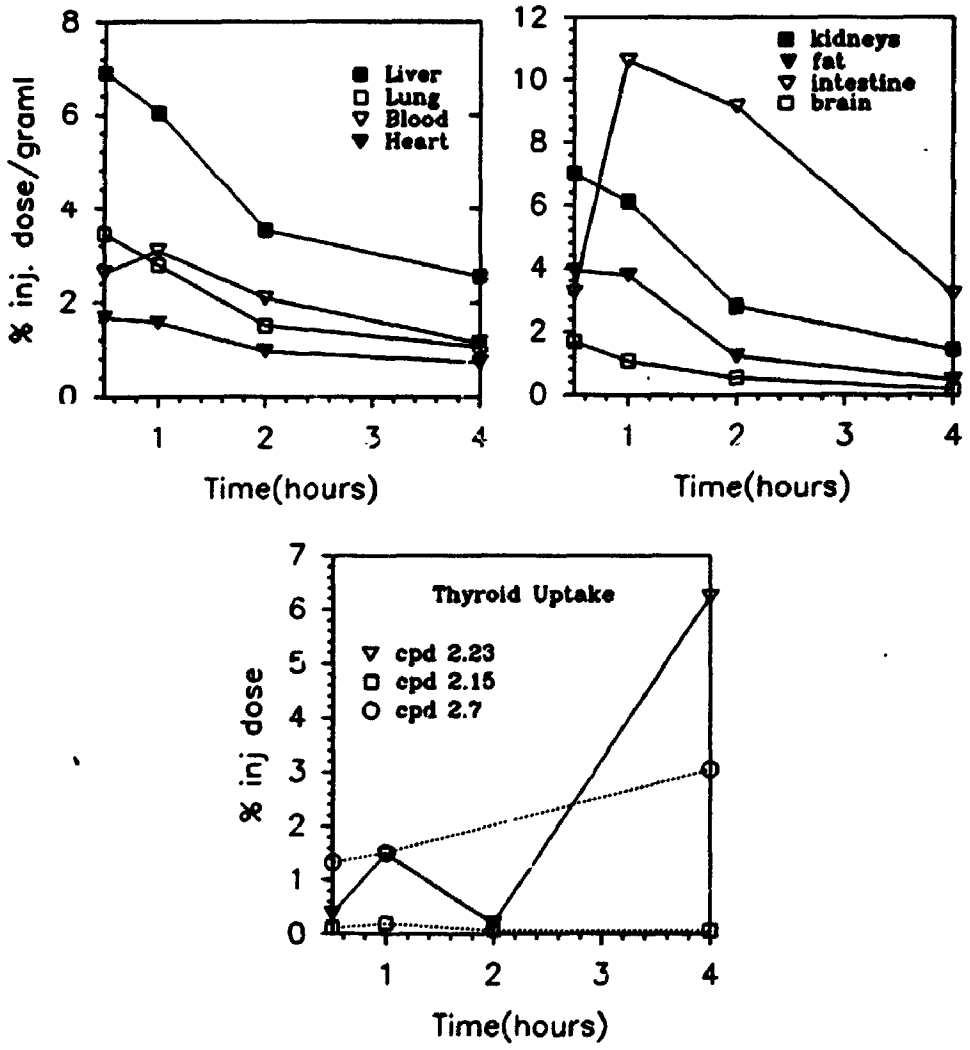

Figure 2.8 Healthy Biodistribution of [I-125]-2.23

We were suprised to find significant thyroid uptake following injection of ^{125}I-**2.23**. It is possible that the high electron affinity of the dinitro analogue renders is suscep-

tible to nucleophilic aromatic substitution despite the mutually *meta* substitution of the nitro groups relative to the iodine. It is also conceivable that an alternative mechanism for deiodination exists.

The EMT-6 tumour model was eventually established and we proceeded directly to the testing of compounds **2.15** and **2.23** using this system. The results for compound **2.15** are represented graphically in Figure 2.9.

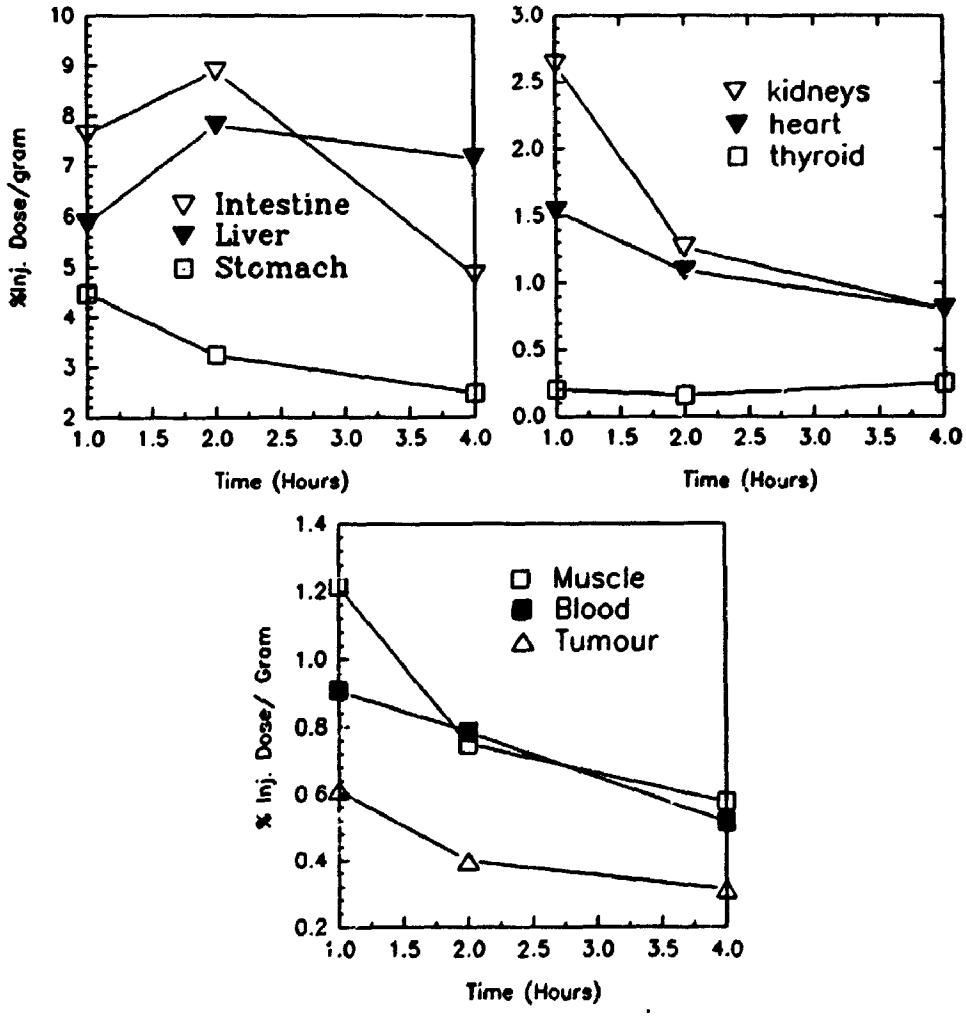

Figure 2.9 Biodistribution of [I-125]-2.15 in Balb/c Mice Bearing EMT-6 Tumours

The corresponding data for the dinitro analogue **2.23** is represented graphically in Figure 2.10.

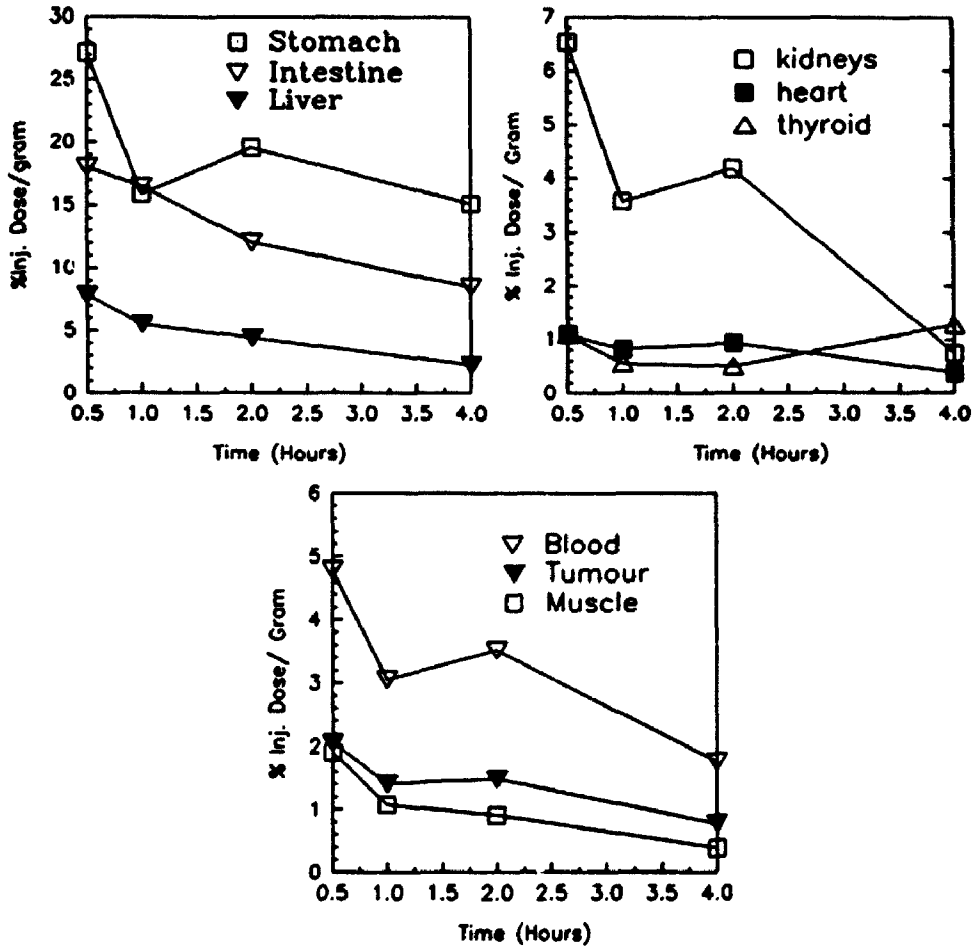

Figure 2.10 Biodistribution of [I-125]-2.23 in Balb/c Mice Bearing EMT-6 Tumours

2.16 Discussion

Since we began our studies two analogues of Misonidazole have been labelled with radioiodine with some success. Iodovinylmisonidazole (IVM) was reported in 1991[60] to be taken up by hypoxic cells at a level equivalent to ^{18}F-MISO. Few experimental details were divulged. A second agent iodoazomycin riboside (IAZR) was the subject of a full paper[61] in which its uptake in an *in vivo* tumour model was described.

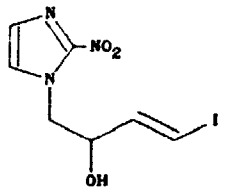

IVM

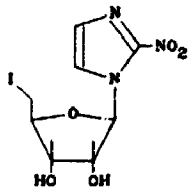

IAZR

The authors tabulated the tissue uptake and the tumour to blood ratios for a variety of the 2-nitroimidazole derivatives that have been reported. Table 2.7 is a reproduction of this table expanded to include the iodinated carbamates **2.15** and **2.23**.

Table 2.7 Biodistribution data for Potential Hypoxia Imaging Agents at one hour post-injection (from ref. 55). * -3 Hours post injection.

Cpd	Label	%Inj.dose/gr Tumour	%Inj.dose/gr Blood	T/B Ratio	Tumour Model
MISO	^{3}H	1.37± 0.45	0.73± 0.23	1.88	C3H/KHT
IAZR	^{131}I	0.28± 0.15	0.19± 0.02	1.47	BDF/LL
IAZR*	^{131}I	9.83± 3.20	1.79± 0.58	5.49	Balb/c EMT6
IAZA	^{125}I	2.55± 1.56	0.91± 0.20	2.80	Balb/c EMT6
Br-MISO	^{82}Br	1.10± 0.19	2.77± 1.05	0.40	Balb/c EMT6
F-MISO	^{3}H	1.29± 0.20	0.98± 0.07	1.31	Balb/c EMT6
2.15	^{125}I	0.40± 0.31	0.78± 0.44	0.51	Balb/c EMT6
2.23	^{125}I	1.49± 0.81	3.52± 1.79	0.52	Balb/c EMT6

The absolute tumour uptake and more importantly the tumour to blood ratios for both of the tested carbamates **2.15** and **2.23** are clearly unsatisfactory. There is little merit in any further consideration of these compounds as hypoxia imaging agents. We have, however, been successful in stabilizing the iodine atom to nucleophilic aromatic substitution in **2.15** relative to **2.7**. We have also been successful in establishing a benchmark against which further compounds may be tested.

The polarographic results indicate that the reduction potentials of **2.15** and **2.23** should be ideal. We believe that the lipophilicity of these analogues may be the root cause of their failure *in vivo*. A comparison of our log P values to the log P values of other compounds tested as hypoxic cell labels indicates that **2.15** and **2.23** are approximately five times too lipophilic to give an adequate tumour to blood ratio. If suitable structural changes were introduced to the 2-nitrobenzyl moiety such that additional water solubility could be imparted to the molecule then plasma binding due to lipophilic interactions with the blood might be reduced. The following derivatives **2.27**, **2.28** and **2.29** have been proposed as more hydrophilic analogues of **2.15**. Their synthesis has been undertaken by a current fourth year student and we hope to report on their biodistribution in Balb/c mice bearing EMT-6 tumours in the very near future.

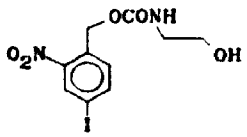

2 27

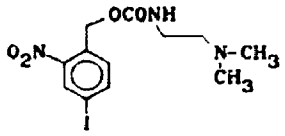

2 28

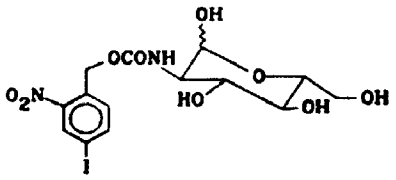

2.29

2.17 Experimental

3- Nitrobenzyl alcohol 2.1

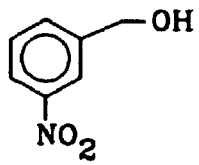

2.1

A solution of 3- Nitrobenzaldehyde (Alpha, 20 g, 0.13 mol) in 95% EtOH (50 mL) was added dropwise to a stirred solution of $NaBH_4$ (2.5 g, 0.066 mol) in distilled water (25 mL). On complete addition the mixture was cooled and then carefully acidified with concentrated HCl. The ethanol was removed *in vacuo* and the remaining aqueous solution extracted with diethyl ether (3 x 100 mL). The combined organic layers were dried (Na_2SO_4) and evaporated *in vacuo*. The residue was distilled to yield 3- nitrobenzyl alcohol **2.1** (15.32 g; 75%; bp. 118°C, 0.15 mm Hg, (lit.[62] 120-5 °C 0.05 mm Hg). HMR: $\delta(CDCl_3)$ 8.1 (m, 1H, H_{arom}), 8.07 (m, 1H, H_{arom}), 7.6 (m, 1H, H_{arom}), 7.5 (t, 1H, H_{arom}), 4.7, (s, 2H, $-CH_2O-$) 3.6 (br s, 1H, -OH). I.R. (neat) 3354 (O-H), 1527 ($-NO_2$), 1352 ($-NO_2$), 1043 (C-O) cm^{-1}.

3-Aminobenzyl alcohol 2.2

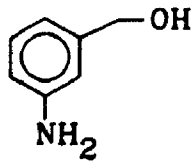

2.2

To a solution of 3-Nitrobenzyl alcohol **2.1** (15.0 g, 0.098

mol) in abs. ethanol (100 mL) was added 10% palladium on activated charcoal (Aldrich, 100 mg) and hydrazine hydrate (BDH, 7.38 mL, 0.196 mol) . The reaction mixture was then heated to 50°C for one hour. The catalyst was removed by filtration and the ethanol was removed *in vacuo*. The residue was recrystallized from benzene to yield 3-aminobenzyl alcohol **2.2** (10.29 g, 0.083 mol, 85%) m.p. 90-94°C (lit. 97°C[63]). HMR (acetone-d_6) δ 7.7 (m, 1H, H_{arom}), 7.6 (d,m 1H, H_{arom}), 7.3 (t, 1H, H_{arom}), 7.2 (d,m 1H, H_{arom}), 4.6 (s, 2H, $-CH_2O-$). I.R. (Nujol) 3250 (N-H), 3148 (C-H), 1458 (C=C) cm^{-1}.

(N-Acetyl)-3-aminobenzyl acetate 2.3

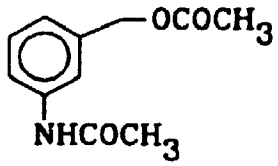

2.3

To a solution of 3-Aminobenzyl alcohol **2.2** (10.1 g, 0.08 mol), triethylamine (BDH, 15 mL, 0.10 mol) and 4-dimethyl-aminopyridine (Aldrich, 500 mg, 4 mmol) in dry methylene chloride (50mL), acetic anhydride (BDH, 20 mL, 0.21 mol) was added dropwise such that steady reflux was maintained. On complete addition the mixture was brought to reflux overnight. The mixture was then allowed to cool and washed with 8 N HCl (50 mL) and then with saturated Na_2CO_3 (50 mL). The methylene chloride layers were combined, dried (Na_2SO_4), and taken to dryness *in vacuo*. The residue was recrystallized from diethyl

ether/ 60-80° pet. ethers to yield (N-acetyl)-3-aminobenzyl acetate **2.3** (15 g; 0.072 mol; 76.5%), m.p. 74°C, (lit[2] 83°C). HMR ($CDCl_3$) δ 9.0 (bs, 1H, -NH-), 7.6 (s, 1H, H_{arom}), 7.5 (d, 1H, H_{arom}), 7.25 (t, 1H, H_{arom}), 7.00 (d, 1H, H_{arom}), 5.0 (s, 2H, $-CH_2-$), 2.15 (d, 3H, $-NCH_3$), 2.06 (s, 3H, $-CH_3$). IR. (Nujol) 3258 (N-H), 1743 (C=O), 1657 (C=O), 1612 (C=O), 1572 (C=C) cm^{-1}.

(N-Acetyl)-3-amino-6-nitrobenzyl acetate **2.4**

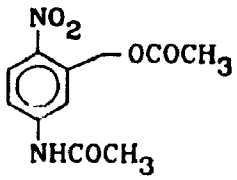

2.4

(N-acetyl)-3-aminobenzyl acetate **2.3** (2.24 g, 0.01 mol) was added to 86% fuming nitric acid (6.0 g, 0.08 mol) at -18°C at such a rate as to maintain a temperature of ≤-5°C. On complete disappearance of starting material (ca. 1 hr.), the reaction mixture was poured onto ice (100 g) and quickly extracted with ethyl acetate (3 x 50 mL). The combined organic layers were washed with water until the washings were neutral. The organic layers were dried (Na_2SO_4) and the solvent was removed *in vacuo*. HMR analysis indicated three mononitrated products: the desired **2.4**, as well as the 2-nitro and 4-nitro isomers in a ratio of 4:1:2. (N-Acetyl)-3-amino-6-nitrobenzyl acetate **2.4** was isolated by fractional recrystallization from benzene. Yield (828 mg, 3.3 mmol, 65%)

mp. 113°C (lit. 111°C[64]). HMR: δ(acetone d_6) 8.4 (br s, 1H, -NH-), 8.1 (d, 1H, H_{arom}), 7.8 (d, 1H, H_{arom}), 7.6 (dd, 1H, H_{arom}), 5.5 (s, 2H, $-CH_2O-$), 2.2 (d, 3H, $-NCH_3$), 2.2 (s, 3H, $-CH_3$). I.R.: (THF) 3280 (N-H), 1745 (C=O), 1700 (C=O), 1545 (NO_2), 1340 (NO_2) cm^{-1}.

3-Amino-6-nitrobenzyl alcohol 2.5

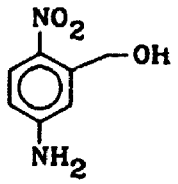

2.5

(N-Acetyl)-3-amino-6-nitrobenzyl acetate 2.4 (515 mg, 2.0 mmol) was taken up in 8 N HCl (5 mL) and brought to reflux for one hour. The mixture was then poured onto ice (10 g), neutralized with aqueous ammonia and extracted with ethyl acetate (3 x 10 mL). The combined organic layers were dried (Na_2SO_4) and taken to dryness *in vacuo*. The crude residue was recrystallized from benzene to yield 3-amino-6-nitrobenzyl alcohol 2.5 (211 mg, 1.25 mmol, 62%), mp. 140°C. (lit.[3] 143°C). HMR: δ(acetone, d_6) 8.0 (d, 1h, H_{arom}), 7.1 (m, 1H, H_{arom}), 6.0 (dd, 1H, H_{arom}), 6.0 (br s, 2H, $-NH_2$) 5.0 (s, 2H, $-CH_2O-$), 4.5 (br s, 1H, -OH). I.R.: (THF) 3450 (O-H), 3350 (N-H), 1577 (NO_2), 1300 (NO_2) cm^{-1}. HRMS: m/e calculated for $C_7H_8N_2O_3$: 168.0535, observed: 168.0531.

3-Iodo-6-nitrobenzyl alcohol 2.6

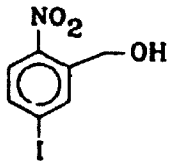

2.6

3-Amino-6-nitrobenzyl alcohol 2.5 (120 mg, 0.71 mmol) was taken up in distilled water (5 mL) containing 12 M HCl (250 μL, 3 mmol). The solution was cooled (0°C) and a slight excess of sodium nitrite (50 mg, 0.72 mmol) dissolved in water (1 mL) was then added dropwise. The solution was allowed to stir for 15 minutes at which point the excess nitrous acid was removed by addition of urea (20 mg, 0.33 mmol). After no more gas was evolved, a slight excess of potassium iodide (141 mg, 0.85 mmol) dissolved in water (1 mL) was added dropwise. The mixture was heated briefly to boiling to complete the reaction and was then allowed to cool. The cooled solution was extracted with chloroform (3 x 5 mL) and the combined chloroform layers were washed once with a dilute solution of sodium thiosulphate (5 mL) to remove any remaining iodine. The organic layers were combined, dried (Na_2SO_4) and taken to dryness *in vacuo*. The crude residue was dissolved in hot benzene, decolorized with charcoal, and on cooling the concentrated mixture crystalline 3-iodo-6-nitrobenzyl alcohol 2.6 (183 mg, 0.66 mmol, 92%) formed, mp. 118-120°C. HMR: $\delta(CDCl_3)$ 8.2 (m, 1H, H_{arom}), 7.2 (m, 2H, H_{arom}), 4.9 (s, 2H, $-CH_2O-$), 2.2 (br s, 1H, -OH). I.R.: (THF) 3200 (C-H), 2800 (C-H),

1558 (NO_2), 1344 (NO_2) cm^{-1}. HRMS: m/e calculated for $C_7H_6INO_3$: 278.9392, observed: 278.9390.

O-(N-Methyl carbamoyl), 3-iodo-6-nitrobenzyl alcohol 2.7

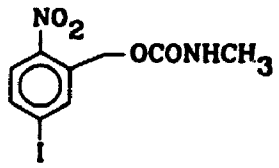

2.7

A solution of 3-Iodo-6-nitrobenzyl alcohol 2.6 (70 mg, 0.25 mmol) was prepared in methyl isocyanate (Aldrich, 200 μL, 3.4 mmol). Triethylamine (BDH, 200 μL, 1.43 mmol) was then added as a catalyst and the mixture was stirred until it solidified. The product could be recrystallized from acetone to yield O-(N-methyl carbamoyl), 3-iodo-6-nitrobenzyl alcohol 2.7 (85 mg, 0.25 mmol, 97%) mp. 106°C. HMR: δ(DMSO-d_6) 8.0 (s, 1H, -NH-), 7.96 (dd, 1H, H_{arom}), 7.84 (d, 1H, H_{arom}), 7.52 (d, 1H, H_{arom}), 5.30 (d, 1H, $-CH_2O-$), 2.59 (d, 3H, $-NCH_3$). IR. (THF) 3570 (N-H), 1740 (C=O), 1565 (NO2), 1347 (NO_2) cm^{-1}. MS m/e calculated for $C_9H_9IN_2O_4$: 335.9607, observed: 335.9600.

3-Chloromercury- 6-nitrobenzyl alcohol 2.8

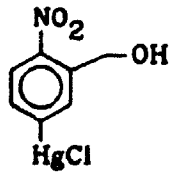

2.8

3-Amino-6-nitrobenzyl alcohol 2.5 (100 mg, 0.60 mol) was

treated with concentrated HCl (BDH, 300 μL, 3.6 mmol) in water (2 mL). $NaNO_2$ (BDH, 41 mg, 0.60 mol) dissolved in water (1 mL) was then added to the cooled (0°C) solution and the mixture was left to stir for 30 minutes. In the meantime, diethyl phosphite (Aldrich, 127 mg, 0.81 mmol), $HgCl_2$ (BDH, 197 mg, 0.73 mmol), and $CuCl_2$ (BDH, 20 mg, 0.15 mmol) were taken up in reagent grade acetone (2 mL). To this solution was added the diazonium salt solution and N_2 was evolved. After approximately one hour a curdy precipitate of 3-chloromercury, 6-nitrobenzyl alcohol **2.8** (121 mg, 0.31 mmol, 52%) formed which was collected by filtration but resisted attempts at recrystallization. HMR: δ(acetone d_6) 8.0 (d, 1H, H_{arom}), 7.87 (d, 1H, H_{arom}), 7.56 (dd, 1H, H_{arom}), 4.90 (s, 2H, $-CH_2O-$), 4.60 (s, 1H, -OH). IR. (THF) 3400 (O-H), 2800 (C-H), 1510 (NO_2), 1338 (NO_2) cm^{-1}. HRMS: m/e calculated for $C_7H_6ClHgNO_3$: 388.9742, observed: 388.9862.

O-(N-Methyl carbamoyl)-3-chloromercury-6-nitrobenzyl alcohol **2.9**

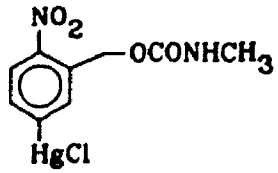

2.9

A solution of 3-chloromercury, 6-nitrobenzyl alcohol **2.8** (70 mg, 0.18 mmol) was prepared in freshly distilled THF (2 mL). Et_3N (BDH, 225 μL, 1.16 mmol) and CH_3NCO (Aldrich, 500

μL, 8.5 mmol) were then added and the mixture was stirred for one hour. The solvent and excess reagents were removed *in vacuo* to leave a solid residue which could be recrystallized from benzene to yield O-(N-methyl carbamoyl)-3-chloromercury-6-nitrobenzyl alcohol **2.9** (74 mg, 0.17 mmol, 93%), mp. 208-212°C. HMR: δ(DMSO d_6) 8.0, (d, 1H, -NH), 7.75 (s, 1H, H_{arom}), 7.68 (dd, 1H, H_{arom}), 7.22 (d, 1H, H_{arom}), 5.29 (s, 2H, $-CH_2O-$), 2.57 (d, 3H, $-NCH_3$). I.R.: 3510 (N-H), 2830 (C-H), 1748 (C=O), 1527 (NO_2), 1350 (NO_2), cm^{-1}.

2.4 Dinitrobenzyl chloride 2.10

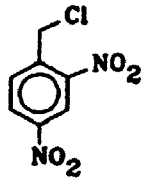

2.10

Benzyl chloride (Fisher, 40 mL, 0.35 mol) was added dropwise to a cooled (ice) mixture of fuming nitric acid (80 g, 1.09 mol) in concentrated sulfuric acid (180 g, 1.84 mol) at such a rate that the temperature did not rise above 20°C. On complete addition, the mixture was allowed to warm to room temperature and stirring was continued overnight. The mixture was then poured onto crushed ice (250 g) and extracted with diethyl ether (3 x 100 mL). The combined organic layers were washed with water until they were neutral. The combined ether layers were dried (Na_2SO_4) and evaporated *in vacuo* to yield crude 2,4-dinitrobenzyl chloride **2.10** (71 g, 0.33 mol, 94%).

HMR: δ(acetone d_6) 8.86 (d, 1H, H_{arom}), 8.62 (dd, 1H, H_{arom}), 8.16 (d, 1H, H_{arom}), 5.19 (s, 2H, $-CH_2O-$).

2,4-Dinitrobenzyl acetate 2.11

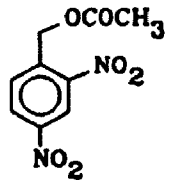

2.11

Crude 2,4-dinitrobenzyl chloride 2.10 (71 g, 0.33 mol) in glacial acetic acid (500 mL) with anhydrous sodium acetate (Baker, 53 g, 1.09 mol) was refluxed overnight. The following morning the mixture was filtered to remove the NaCl and the acetic acid was stripped *in vacuo*. The residue was recrystallized from methanol to yield 2,4-dinitrobenzyl acetate 2.11 (77g, 0.32 mol, 97%) mp. 89-91 °C (lit.[65] 96-97°C). HMR: δ(acetone-d_6) 8.9 (d, 1H, H_{arom}), 8.6 (dd, 1H, H_{arom}), 8.1 (d, 1H, H_{arom}), 5.61 (s, 2H, $-CH_2O-$), 2.2 (s, 3H, $-CH_3$). IR: (CH_2Cl_2) 3110 (C-H), 2830 (C-H), 1750 (C=O), 1535 (NO_2), 1340 (NO_2), cm^{-1}.

2,4-Dinitrobenzyl alcohol 2.12

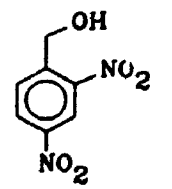

2.12

A suspension of 2,4-dinitrobenzyl acetate 2.11 (8.0g,

0.03 mol) in 50% H_2SO_4 (200 mL) was heated to 120°C at which point a solution was obtained. The mixture was then cooled in ice and extracted with ethyl acetate (3 x 50 mL). The organic layers were combined, dried (Na_2SO_4) and taken to dryness *in vacuo*. The residue was recrystallized from water to yield 2,4-dinitrobenzyl alcohol **2.12** (5.5 g, 0.028 mol, 83%) mp. 110-17°C (lit[4] 115.5-16°C). HMR: δ(acetone-d_6) 8.85 (d, 1H, H_{arom}), 8.61 (dd, 1H, H_{arom}), 8.28 (d, 1H, H_{arom}), 5.14 (s, 1H, -CH_2O-), 3.07 (bs, 1H, -OH). I.R.: (CH_2Cl_2) 3380 (O-H), 3120 (C-H), 2830 (C-H), 1525 (NO_2), 1340 (NO_2) cm^{-1}.

4-amino-2-nitrobenzyl alcohol 2.13

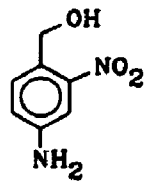

2.13

Concentrated aqueous ammonia (500 μL), 2,4-dinitrobenzyl alcohol **2.12** (2.0 g, 0.01 mol), and NH_4Cl (BDH, 3.2 g, 0.06 mol) and were dissolved in distilled water (100 mL) and heated to 75°C. A solution of $Na_2S.9H_2O$ (7.27 g, 0.03 mol) was then added dropwise at such a rate that the temperature was maintained at 75°C. On complete addition, the mixture was vacuum filtered to remove precipitated sulfur. The filtrate was extracted with ethyl acetate and the combined organic layers combined, dried (Na_2SO_4), and evaporated *in vacuo*. The residue was recrystallized from benzene to yield 4-amino-2-

nitrobenzyl alcohol **2.13** (822 mg, 4.9 mmol, 48%) mp. 86-88°C (lit[66] 87-88°C). HMR: δ(acetone-d_6) 7.5 (d, 1H, H_{arom}), 7.3 (d, 1H, H_{arom}), 7.0 (dd, 1H, H_{arom}), 5.2 (bs, 2H, $-NH_2$), 4.78 (d, 2H, $-CH_2O-$), 4.26 (t, 1H, -OH). IR: (CH_2Cl_2) 3435 (O-H), 3350 (N-H), 1632 (C=O), 1522 (NO_2), 1340 (NO_2) cm^{-1}. HRMS: m/e calculated for $C_7H_8N_2O_3$: 168.0535, observed: 168.0536.

4-Iodo-2-nitrobenzyl alcohol **2.14**

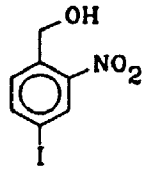

2.14

Concentrated hydrochloric acid (1.5 mL, 18 mmol) and 4-amino-2-nitrobenzyl alcohol **2.13** (1.0 g, 5.9 mmol) were dissolved in distilled water (20 mL) and the mixture was cooled (0°C). $NaNO_2$ (BDH, 823 mg, 11.9 mmol) dissolved in distilled water (2 mL) was then added and the mixture was stirred for 15 minutes. Urea (358 mg, 6.0 mmol) was then added to consume the excess nitrous acid followed by the dropwise addition of sodium iodide (1.16 g, 7.7 mmol) dissolved in distilled H_2O (5 mL). The resulting suspension was allowed to stir overnight and heated briefly on a steam bath the following day to complete the reaction. The mixture was extracted with methylene chloride (3 x 25 mL) and the combined organic layers were washed with dilute sodium thiosulfate solution (10 mL), dried (Na_2SO_4) and taken to dryness *in vacuo*. The residue was

recrystallized from diethyl ether/ 60-80°C petroleum ethers to yield 4-iodo-2-nitrobenzyl alcohol **2.14** (956 mg, 3.42 mmol, 58%), mp. 75-77°C, (lit.[61] 85-86°C). HMR: $\delta(CDCl_3)$ 8.36 (d, 1H, H_{arom}), 8.14 (dd, 1H, H_{arom}), 7.74 (d, 1H, H_{arom}), 4.94 (s, 2H, $-CH_2O-$), 4.73 (bs, 1H, -OH). IR: (CH_2Cl_2) 3390 (O-H), 2810 (C-H), 1520 (NO_2), 1335 (NO_2) cm^{-1}. HRMS: m/e calculated for $C_7H_5INO_3$: 278.9392, observed: 278.9392.

O-(N-Methyl carbamoyl)-4-iodo-2-nitrobenzyl alcohol **2.15**

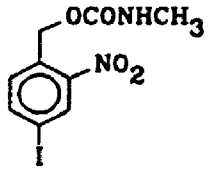

2.15

A solution of 4-Iodo-2-nitrobenzyl alcohol **2.14** (586 mg, 2.1 mmol) in excess CH_3NCO (Aldrich, 5 mL, 85 mmol) and Et_3N (BDH, 1 mL, 7.2 mmol) as catalyst was stirred for one hour at which time the excess reactants were removed *in vacuo*. The resulting solid was recrystallized from aqueous ethanol to yield the desired O-(N-methyl carbamoyl)-4-iodo-2-nitrobenzyl alcohol **2.15** (421 mg, 1.25 mmol, 60%), mp 103-104°C. HMR: δ(acetone-d_6) 8.4 (d, 1H, H_{arom}), 7.94 (dd, 1H, H_{arom}), 7.31 (d, 1H, H_{arom}), 6.42 (bs, 1H, -NH), 5.43 (s, 2H, $-CH_2O-$), 2.83 (d, 3H, $-NCH_3$). IR: (CH_2Cl_2) 3510 (N-H), 2820 (C-H), 1743 (C=O), cm^{-1}. HRMS: m/e calculated for $C_9H_9IN_2O_4$: 335.9607, observed: 335.9605.

4-Chloromercury-2-nitrobenzyl alcohol **2.16**

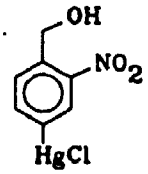

2.16

Concentrated hydrochloric acid (1.5 mL, 18 mmol) and 4-amino-2-nitrobenzyl alcohol **2.13** (1.02 g, 6.0 mmol) were dissolved in distilled water (10 mL). To this cooled (0°C) solution was added $NaNO_2$ (770 mg, 11.0 mmol) dissolved in distilled water (2 mL) and the mixture was left to stir for 15 minutes. In the meantime, diethyl phosphite (1.28 g, 9.20 mmol), mercuric chloride (1.99 g, 7.30 mmol), and cupric chloride (211 mg,1.60 mmol) were combined in reagent grade acetone (20 mL) and the mixture was heated to reflux. Urea (190 mg, 3.2 mmol) was added to the diazonium salt solution to discharge the remaining nitrous acid and the mixture was added dropwise to the refluxing acetone solution. On complete addition the mixture was allowed to cool and stirring was maintained overnight. The resulting solid was filtered and recrystallized from toluene to yield the desired 4-chloromercury-2-nitrobenzyl alcohol **2.16** (975 mg, 2.50 mmol, 42%), mp. 218-22°C. HMR: δ(acetone d_6) 8.32 (s, 1H), 7.94 (s, 2H), 4.99 (d, 2H), 4.63, (t, 1H). IR. (THF) 3560 (O-H), 2810 (C-H), 1422 (NO_2), 1340 (NO_2) cm^{-1}. MS. m/e calculated for $C_7H_6ClHgNO_3$: 388.9742, observed: 388.9672.

O-(N-Methyl carbamoyl)-4-chloromercury-2-nitrobenzyl alcohol **2.17**

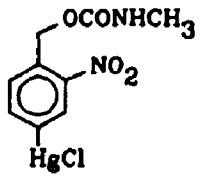

2.17

A solution of 4-chloromercury-2-nitrobenzyl alcohol **2.16** (99 mg, 0.25 mmol) was prepared in dry THF (3 mL). CH_3NCO (Aldrich, 500 μL, 8.5 mmol) and Et_3N (BDH, 100 μL, 0.72 mmol) were then added. The solution was stirred overnight and the solvent was then removed *in vacuo*. The resulting solid was recrystallized from toluene to yield O-(N-methyl carbamoyl)-4-chloromercury-2-nitrobenzyl alcohol **2.17** (77 mg, 0.17 mmol, 68%), mp. 260-264°C. HMR: δ(1:1 acetone d_6: DMSO d_6) 8.34 (s, 1H, H_{arom}), 7.93 (d, 1H, H_{arom}), 7.63 (d, 1H, H_{arom}), 7.10 (bs, 1H, -NH), 5.40 (s, 2H, $-CH_2O-$), 2.6 (s, 3H, NCH_3). IR: (THF) 3560 (N-H), 2800 (C-H), 1728 (C=O), 1520 (NO_2), 1337 (NO_2) cm^{-1}.

O-(N-Methyl carbamoyl)-2-nitro-4-trimethylstannylbenzyl alcohol **2.18**

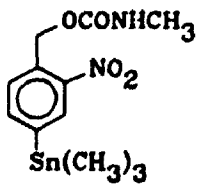

2.18

O-(N-methyl carbamoyl)-4-iodo-2-nitrobenzyl alcohol **2.15**

(55.0 mg, 0.16 mmol) and π-allyl palladium chloride dimer (Aldrich, 5.0 mg, 14 μmol) were taken up in dry methylene chloride (5 mL) under an atmosphere of argon. Hexamethylditin (66.7 mg, 0.203 mmol) was then added in one portion. The reaction was allowed to proceed for one hour at which time the mixture was filtered through a plug of Celite. The methylene chloride was stripped *in vacuo* and the resulting solid was recrystallized from diethyl ether/ 60-80°C petroleum ethers to yield the desired O-(N-methyl carbamoyl)-2-nitro-4-trimethylstannylbenzyl alcohol **2.18** (32.6 mg, 0.087 mmol, 55%) mp. 89-90°C. HMR: $\delta(CDCl_3)$ 8.14 (s, 1H, H_{arom}), 7.73 (d, 1H, H_{arom}), 7.53 (d, 1H, H_{arom}), 5.49 (s, 2H, $-CH_2O-$), 4.77 (bs, 1H, -NH), 2.83 (d, 3H, NCH_3), 0.35 (s, 9H, $Sn(CH_3)_3$). HRMS: m/e calculated for $C_{12}H_{18}N_2O_4Sn$: 374.0289, observed: 374.0287.

4-Iodo-2,6-dinitrotoluene **2.19**

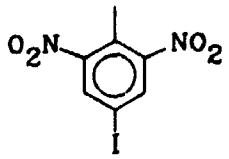

2.19

The method of Arotsky, Butler and Darby[67] was used to prepare 4-Iodo-2,6-dinitrotoluene **2.19**. Iodine (BDH, 1.4 g, 5.5 mmol), 2,6-dinitrotoluene (Aldrich, 1.0 g, 5.5 mmol), and fuming sulfuric acid (BDH, 13.8 g, 140 mmol) were heated at 100°C for one hour. The mixture was allowed to cool and then poured onto crushed ice (250 g). The solution was then ex-

tracted with ethyl acetate (4 x 100 mL). The ethyl acetate layers were combined and washed with saturated sodium thiosulfate solution (100 ml) in order to remove any remaining iodine. The combined ethyl acetate layers were dried (Na_2SO_4) and taken to dryness *in vacuo*. The solid residue was recrystallized from diethyl ether/ hexanes to yield 4-iodo-2,6-dinitrotoluene **2.19** (9.2 g, 0.03 mol, 54%) mp. 76-77°C (lit.[67] 91°C). HMR: $\delta(CDCl_3)$ 8.26 (s, 2H, H_{arom}), 5.46 (s, 3H, $-CH_3$). IR: (CH_2Cl_2) 3050 (C-H), 2980 (C-H), 1531 (NO_2), 1340 (NO_2) cm^{-1}.

α-Bromo-4-iodo-2,6-dinitrotoluene **2.20**

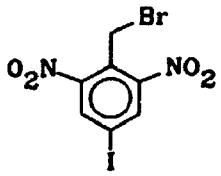

2.20

Calcium carbonate (1.24 g, 0.012 mol), 2,6-dinitro-4-iodotoluene **2.19** (3.82 g, 0.012 mol) and bromine (BDH, 2.29g, 0.014 mol), and pyridine (200 μL, 2.47 mmol) were sealed in a Carius tube (10 mL) and heated at 150°C for eight hours. The Carius tube was allowed to cool and was then further cooled for 15 minutes in liquid nitrogen. The Carius tube was then carefully opened and inverted into an Erlenmeyer flask. The contents were allowed to thaw and then washed with ethyl acetate (3 x 10 mL) and water (3 x 10 mL). The organic layer was separated from the aqueous layer which was washed with

ethyl acetate (3 x 25 mL). The combined ethyl acetate layers were dried (Na_2SO_4) and taken to dryness *in vacuo*. The crude residue consisted of a mixture of product and starting material in the ratio of ca. 2:1 as shown by proton NMR. The residue was dissolved in a minimum of diethyl ether and decolorized with charcoal at which point sufficient hexanes were added to induce crystallization. α-Bromo-4-iodo-2,6-dinitrotoluene **2.20** (1.3 g, 3.36 mmol, 28%) was isolated mp. 86-89°C. HMR: $\delta(CDCl_3)$ 8.36 (s, 2H, H_{arom}), 4.834 (s, 2H, $-CH_2Br$). IR: (CH_2Cl_2) 3090 (C-H), 1545 (NO_2), 1343 (NO_2), cm^{-1}. HRMS: m/e calculated for $C_7H_4BrIN_2O_4$: 395.8399, observed: 385.8392.

4-Iodo-2,6-dinitrobenzyl Acetate **2.21**

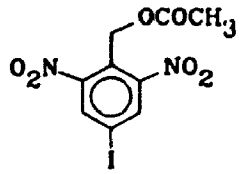

2.21

α-Bromo-2,6-dinitro-4-iodotoluene **2.20** (20 mg, 0.05 mmol) and sodium acetate (8.5 mg, 0.10 mmol) were taken up in acetic acid (5 mL) and brought to reflux overnight. The acetic acid was removed *in vacuo* and the resulting solid was taken up in ethyl acetate (10 mL). The ethyl acetate was washed with water (2 x 5 mL) and the combined water layers were washed with ethyl acetate (2 x 5 mL). The organic layers were combined, dried (Na_2SO_4), and the ethyl acetate was stripped *in*

vacuo. The resulting solid could be recrystallized from diethyl ether/hexanes to yield 4-iodo-2,6-dinitrobenzyl acetate **2.21** (14 mg, 0.038 mmol, 75%) mp. 76-78°C. HMR: $\delta(CDCl_3)$ 8.33 (s, 2H, H_{arom}), 5.44 (s, 2H, $-CH_2O-$), 2.00 (s, 3H, $-CH_3$). IR: (CH_2Cl_2) 3040 (C-H), 1673 (C=O), 1463 (NO_2), 1270 (NO_2) cm^{-1}. HRMS: m/e calculated for $C_9H_7IN_2O_6$: 365.9349, observed: 365.9344.

4-Iodo-2,6-dinitrobenzyl alcohol **2.22**

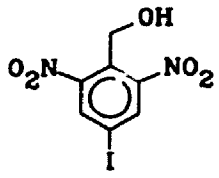

2.22

A solution of 4-iodo-2,6-dinitrobenzyl acetate **2.21** (25.5 mg, 0.07 mmol) was prepared in 50% aqueous tetrahydrofuran (4 mL). Concentrated sulfuric acid (2 mL) was then added while the mixture was vigorously stirred. The mixture was brought to reflux for one hour, cooled in ice, and extracted with ethyl acetate (3 x 10 mL). The organic layers were combined, dried (Na_2SO_4), and taken to dryness *in vacuo*. The residue was recrystallized from diethyl ether/ 60-80° petroleum ethers to yield 4-iodo-2,6-dinitrobenzyl alcohol **2.22** (18.0 mg, 0.06 mmol, 80%) mp. 108-110°C. HMR: $\delta(CDCl_3)$ 8.37 (s, 2H, H_{arom}), 4.92 (d, 2H, J=7.0 Hz, $-CH_2O-$), 2.65 (t, 1H, J=7.0 Hz, -OH). IR: (CH_2Cl_2) 3600 (O-H), 1535 (NO_2), 1342 (NO_2), 1028 (C-O) cm^{-1}.

O-(N-Methyl carbamoyl)-4-iodo-2,6-dinitrobenzyl alcohol **2.23**

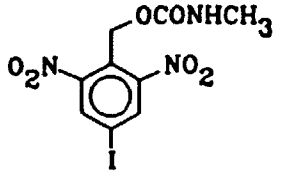

2.23

A solution of 4-iodo-2,6-dinitrobenzyl alcohol **2.22** (20 mg, 0.06 mmol) was prepared in dry methylene chloride (2 mL). Methyl isocyanate (Aldrich, 20 μl, 0.34 mmol) and triethylamine (BDH, 20μL, 0.14 mmol) were then added with stirring. The reaction was allowed to proceed for one hour at which point the solvent and excess reagents were removed *in vacuo*. The crude residue was recrystallized from diethyl ether/ hexanes to yield O-(N-methyl carbamoyl)-4-iodo-2,6-dinitrobenzyl alcohol **2.23** (20 mg, 0.05 mmol, 93%) mp. 126-128°C. HMR: $\delta(CDCl_3)$ 8.37 (s, 2H, H_{arom}), 5.46 (s, 2H, $-CH_2O-$), 2.73 (d, 3H, $-N-CH_3-$). IR: (CH_2Cl_2) 3520 (N-H), 3125 (C-H), 1766 (C=O), 1573 (NO_2), 1380 (NO_2), cm^{-1}. HRMS: m/e calculated for $C_9H_8IN_3O_6$: 380.9457, observed: 380.9466.

O-(N-Methyl carbamoyl)-2,6-dinitro-4-trimethylstannylbenzyl Alcohol **2.24**

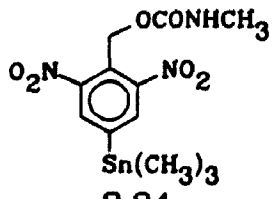

2.24

O-(N-Methyl carbamoyl)-4-iodo-2,6-dinitrobenzyl alcohol

2.23 (31.5 mg, 0.083 mmol) was dissolved in dry methylene chloride (2 mL). π-Allyl palladium chloride dimer (Aldrich, 5 mg, 14 μmol) was added and the mixture was stirred. Hexamethyl ditin (27 mg, 0.083 mmol) were then added at which point the yellow solution immediately turned black as a fine precipitate formed. The reaction was allowed to proceed for 30 minutes at which point the palladium black was removed by filtration through a plug of Celite. The product was purified by preparative thin layer chromatography (neutral alumina 0.25mm, 20% ethyl actetate in hexanes, R_f=0.56) to yield O-(N-methyl carbamoyl)-2,6-dinitro-4-trimethylstannylbenzyl alcohol **2.24** (17.9 mg, 0.042 mmol, 52%) as a yellow oil which was shown to be pure by NMR. HMR: $\delta(CDCl_3)$ 8.03 (s, 2H, H_{arom}), 5.50 (s, 2H, $-CH_2O-$), 4.60, (bs, 1H, -NH), 2.72 (d, 3H, NCH_3), 0.422 (s, 9H, $-Sn(CH_3)_3$. IR: (CH_2Cl_2) 3450 (N-H), 3050 (C-H), 2920 (C-H), 1725 (C=O), 1538 (NO_2), 1342 (NO_2), cm^{-1}. HRMS: m/e calculated for $C_{12}H_{17}N_3O_6Sn$: 419.0139, observed: 419.0142.

2.18 Radiolabelling

O-(N-Methyl carbamoyl)-3-[^{131}I]iodo-2-nitrobenzyl alcohol 2.7a

O-(N-methyl carbamoyl)-3-chloromercury-2-nitrobenzyl alcohol **2.9** (1 mg, 2.2 μmol) and N-chlorosuccinimide (1 mg, 7.4 μmol) were dissolved in freshly distilled THF (250 μL) in a small stoppered test tube (Vacuutainer, Becton Dickinson, 5 mL) equipped with a stirring flea. Na^{131}I solution (10 μL, 392 μCi, chemical grade, Merck Frosst) and the mixture was allowed to stir overnight. The reaction was quenched by addition of 10% sodium thiosulfate solution (1 mL) and the mixture was extracted with chloroform (3 x 1 mL). The combined organic layers were assayed for radioactivity in a dose calibrator (342 μCi, 94%) and compared to the combined aqueous layers (22 μCi, 6%). The chloroform layers were evaporated in a stream of air and the residue injected onto a LC-18 reverse phase HPLC column (Supelco) eluted with 3:2 methanol:water. The radioactive peak corresponding to a previously injected cold standard was collected to yield the desired O-(N-methyl carbamoyl)-3-[^{131}I]iodo-2-nitrobenzyl alcohol **2.7** (279 μCi, 82%) in an overall radiochemical yield (uncorrected for decay) of 77%.

2.19 Recrystallization to Constant Specific Activity

Crude O-(N-methyl carbamoyl)-3-[^{125}I]iodo-2-nitrobenzyl alcohol **2.7b** (6660 dps) was placed in a tared vial with O-(N-methyl carbamoyl)-3-[^{127}I]iodo-2-nitrobenzyl alcohol 2.7 (19.85 mg, 59 μmol). The two compounds were then dissolved in a minimum of hot ethyl acetate. On cooling crystals appeared which were collected in a plugged Pasteur pipette and washed twice with ice cold ethyl acetate. The residual crystals were washed from the plug with hot THF and the solution collected in a second tared vial. The solvent was removed to yield O-(N-methyl carbamoyl)-3-[$^{125/127}$I]iodo-2-nitrobenzyl alcohol **2.7/2.7b**(12.59 mg, 37 μmol) which was counted for radioactivity (2300 dps, 55%). The procedure was repeated to yield (8.70 mg, 26 μmol) whose radioactivity was again counted (1557 dps, 97%) and repeated again to yield (5.7 mg, 17 μmol) with a radioactivity of (999 dps, 98%).

2.20 Partition Coefficients

The partition coefficients were determined by the method of Fujita[68]. Freshly distilled n-octanol (BDH, 1.00 mL) and freshly prepared pH 7.4 phosphate buffered saline (Sigma, 1.00 mL) were placed in each of 10 disposable centrifuge tubes (Baxter, 15 mL). The test compound was dissolved in n-octanol (100 μl) to a concentration of ca. 1μCi/10μl. An aliquot of the stock solution (10 μl, 1 μCi) was added to each of the ten centrifuge tubes. The tubes were then placed in a rotating

mixer for one hour. The tubes were then centrifuged for two minutes at 1000 rpm. to effect sharp separation of the two phases. An aliquot of each phase (500 μL) was then placed in a tared scintillation vial, the mass of the aliquot determined and the radioactivity was assayed in a well counter.

2.21 Biological Studies

Healthy Biodistributions

The HPLC-purified compound was dissolved in pH 7.4 phosphate buffered saline and taken up in one-piece insulin syringes (Terumo, 0.25 mL, 30 guage). The filled syringes were assayed for radioactivity *pre* and *post*-injection in a thyroid probe equipped with a NaI(Th) detector in order to accurately determine the injected dose. The radioactive drug was injected via tail vein into male CD1 mice. The animals were sacrificed via CO_2 asphyxiation at the time points indicated. The whole carcass was exsanguinated by atrial puncture followed by whole-body perfusion with heparinized Ringer's lactate solution injected via the left ventricle. The tissues of interest were then isolated by dissection and placed in tared disposable scintillation vials (Baxter, 15 mL). The organs were weighed and then assayed for radioactivity in a well-counter. The data for ^{125}I-**2.7**, ^{125}I-**2.15**, and ^{125}I-**2.23** are tabulated in tables 2.8, 2.9 and 2.10.

Table 2.8. Healthy Biodistribution data for ^{125}I-2.7 in male CD1 mice. Uptake is expressed as % injected dose per gram of tissue except thyroid uptake which is expressed as % injected dose. Errors reported are standard deviations from a sample of 3 mice per time point.

	Time (Hours)			
Organ	0.50	1.00	4.00	8.00
Blood	3.99± 0.72	4.33± 0.26	2.47± 1.12	1.90± 0.11
Heart	1.71± 0.21	1.61± 0.23	1.08± 0.35	0.71± 0.10
Lung	3.15± 1.88	2.16± 0.63	2.38± 0.52	1.23± 0.21
Liver	3.76± 1.10	3.59± 0.04	1.99± 0.61	1.54± 0.17
Kidneys	3.06± 0.42	4.55± 2.46	1.69± 0.64	2.58± 1.93
Intestine	3.36± 1.64	2.70± 0.71	1.70± 0.25	1.75± 0.55
Fat	0.73± 0.16	1.00± 0.15	0.72± 0.19	1.20± 1.18
Muscle	0.70± 0.17	0.75± 0.10	0.45± 0.11	0.38± 0.21
Brain	0.49± 0.12	0.43± 0.02	0.32± 0.15	0.15± 0.02
Thyroid*	1.33± 0.25	1.51± 0.45	3.05± 0.46	3.91± 0.91

Table 2.9. Healthy Biodistribution data for ^{125}I-2.15 in male CD1 mice. Uptake is expressed as % injected dose per gram of tissue except thyroid uptake which is expressed as % injected dose. Errors reported are standard deviations from a sample of 3 mice per time point.

	Time (Hours)			
Organ	0.50	1.00	2.00	4.00
Blood	0.46± 0.13	0.38± 0.15	0.43± 0.09	0.22± 0.16
Heart	1.08± 0.14	0.86± 0.14	0.73± 0.20	0.26± 0.15
Lung	3.95± 1.76	1.76± 0.81	1.55± 0.62	0.46± 0.27
Liver	8.54± 1.87	8.47± 0.79	8.74± 1.52	3.63± 2.26
Kidneys	2.02± 0.60	1.40± 0.20	1.43± 0.11	0.50± 0.27
Intestine	2.62± 0.12	3.28± 0.70	3.15± 0.71	1.19± 0.72
Fat	0.98± 0.26	0.96± 0.07	0.81± 0.14	0.25± 0.15
Muscle	0.46± 0.23	0.36± 0.06	0.26± 0.03	0.12± 0.05
Brain	0.56± 0.08	0.62± 0.14	0.58± 0.15	0.19± 0.11
Bone	0.37± 0.13	0.34± 0.06	0.28± 0.09	0.14± 0.07
Stomach	1.03± 0.25	0.79± 0.14	0.74± 0.03	0.62± 0.35
Thyroid*	0.11± 0.19	0.19± 0.20	0.06± 0.02	0.06±0.04

Table 2.10. Healthy Biodistribution data for ^{125}I-2.23 in male CD1 mice. Uptake is expressed as % injected dose per gram of tissue except thyroid uptake which is expressed as % injected dose. Errors reported are standard deviations from a sample of 3 mice per time point.

	Time (Hours)			
Organ	0.50	1.00	2.00	4.00
Blood	2.64± 0.73	3.09± 0.34	2.09± 0.32	1.14± 0.70
Heart	1.69± 0.39	1.57± 0.35	0.97± 0.06	0.73± 0.10
Lung	3.46± 0.94	2.79± 0.73	1.51± 0.15	1.06± 0.10
Liver	6.91± 2.14	6.04± 0.52	3.55± 0.74	2.55± 0.57
Kidneys	7.00± 1.21	6.12± 1.11	2.78± 0.20	1.42± 0.16
Intestine	3.24± 0.43	10.6± 2.80	9.12± 3.27	3.18± 2.18
Fat	3.93± 0.95	3.78± 1.19	1.22± 0.24	0.47± 0.09
Brain	1.68± 0.24	1.07± 0.29	0.54± 0.16	0.17± 0.02
Stomach	6.00± 1.54	16.2± 7.19	13.8± 3.43	10.0± 1.87
Thyroid*	0.38± 0.13	1.49± 0.56	0.19± 0.19	6.24± 1.74

Biodistributions in Tumor-Bearing Mice

The EMT-6 experimental tumor model is an anaplastic sarcoma derived from an outgrowth of a transplanted preneoplastic nodule of the murine mammary tumour KHJJ. The tumour model has been described in great detail elsewhere[69]. Briefly, EMT-6 cells obtained from the London Regional Cancer Clinic were cultured as monolayers in Alpha minimum essential medium (MEM, Gibco) supplemented with 5% fetal calf serum in an atmoshpere of 95% air/5% CO_2 and 100% humidity at 37°C. When nearly confluent (ca. 3 days) the cells were trypsinized (Sigma) and resuspended in a miniumum of the Alpha MEM. An aliquot of the cell suspension was counted on a haemocytometer and sufficient suspension was

drawn up in syringes such that each syringe contained approximately 10^5 cells in 25 μl of medium. Male Balb/c mice were restrained in a modified 50 mL disposable syringe (Baxter) and the cell suspension was injected subcutaneously in the right rear flank. Tumours were palpable in one to two weeks and reached experimental volumes (500-1000 mm^3) in three to four weeks. Biodistributions were performed for ^{125}I-2.15, and ^{125}I-2.23 as previously described. The results appear in tables 2.11, 2.12 and 2.13.

Table 2.11. Biodistribution of ^{125}I-2.15 in Balb/c mice bearing EMT-6 tumours. Uptake is expressed as % injected dose per gram of tissue except thyroid uptake which is expressed as % injected dose. Errors reported are standard deviations from a sample of 3 mice per time point.

	Time (Hr)		
Organ	1.00	2.00	4.00
Blood	0.91± 0.59	0.79± 0.45	0.52± 0.34
Heart	1.54± 0.66	1.09± 0.49	0.81± 0.44
Liver	5.87± 4.20	7.80± 2.57	7.15± 1.45
Kidneys	2.64± 1.99	1.26± 0.58	0.81± 0.47
Intestine	7.63± 1.55	8.88± 3.67	4.83± 2.22
Stomach	4.48± 1.16	3.24± 0.93	2.47± 0.87
Tumour	0.61± 0.40	0.40± 0.31	0.31± 0.33
Muscle	1.22± 0.60	0.75± 0.42	0.57± 0.45
Thyroid	0.20± 0.22	0.16± 0.23	0.25± 0.24

Table 2.12. Biodistribution of ^{125}I-2.23 in Balb/c mice bearing EMT-6 tumours. Uptake is expressed as % injected dose per gram of tissue except thyroid uptake which is expressed as % injected dose. Errors reported are standard deviations from a sample of 3 mice per time point.

	Time (Hours)			
Organ	0.50	1.00	2.00	4.00
Blood	4.79± 1.01	3.06± 0.92	3.52± 1.79	1.76± 0.78
Heart	1.10± 0.26	0.82± 0.47	0.93± 0.67	0.38± 0.31
Liver	7.85± 2.86	5.50± 1.32	4.41± 3.77	2.23± 0.99
Kidneys	6.53± 2.11	3.57± 1.01	4.18± 3.88	0.74± 0.44
Intestine	18.0± 6.55	16.5± 1.93	12.1± 4.81	8.51± 5.73
Stomach	27.1± 2.91	15.8± 7.35	19.6± 2.99	15.1± 7.12
Tumour	2.06± 1.73	1.41± 0.57	1.49± 0.81	0.78± 0.50
Muscle	1.90± 0.26	1.08± 0.72	0.91± 0.64	0.38± 0.31
Thyroid	1.09± 0.72	0.56± 0.62	0.49± 0.68	1.28± 1.20

Table 2.13. Biodistribution of ^{125}I-2.23 in Balb/c mice bearing EMT-6 tumours--later time points. Uptake is expressed as % injected dose per gram of tissue except thyroid uptake which is expressed as % injected dose. Errors reported are standard deviations from a sample of 3 mice per time point.

	Time (Hr)		
Organ	4.00	8.00	24.00
Blood	1.15± 0.23	0.49± 0.11	0.25± 0.08
Heart	0.22± 0.02	0.11± 0.01	0.02± 0.02
Liver	1.79± 0.46	0.69± 0.06	0.49± 0.18
Kidneys	0.92± 0.17	0.25± 0.06	0.14± 0.05
Intestine	4.55± 2.43	0.64± 0.30	0.17± 0.09
Stomach	3.69± 1.15	1.11± 0.32	0.22± 0.11
Tumour	0.46± 0.14	0.17± 0.04	0.07± 0.02
Muscle	0.25± 0.08	0.09± 0.02	0.04± 0.01

2.22 References

1.Cancer Facts and Figures, 1989, American Cancer Society, Atlanta, Georgia.

2.Thomlinson, R.H., Gray, L.H., *Br. J. Cancer*, 1955, *9*, 539.

3.Hewitt, H.B., Wilson, C.W., *Br. J. Cancer*, 1959, *13*, 675.

4.Suit, H.D., Maeda, *Am. J. Roentg.*, 1966, *96*, 177.

5.Porter, J.R., *Bacterial Chemistry and Physiology*, 1946, *John Wiley and Sons*, p. 56-57.

6.Kennedy, K.A., Teicher, B.A., Sartorelli, A.C., *Biochem. Pharmac.*, 1980, *29*, 1-8.

7.Rasey, J.S., Grunbaum, Z., Shankland, E.G., Krohn, K.A., Mathis, C.A., *J. Nucl. Med.*, 1987, *28*, 594.

8.Martin, G.V., Rasey, J.S., Caldwell, J.S., Grunbaum, Z., Krohn, K.A., *J. Nucl. Med.*, 1987, *28*, 668.

9.Wakaki, S., Marumo, H., Tomoika, K., Shunuzu, G., Kato, E., Kanada, H., Kudo, S., Fujimoto, Y., *Antibiot. Chemotherapy*, 1958, *8*, 228.

10.Schwartz, H.S., Sodergren, J.E., Philips, F.S.,; *Science*, 1963, *142*, 1181-1183.

11.Iyer, V.N., Szybalski, W., *Proc. Nat. Acad. Sciences*, 1963, *50*, 355.

12.Moore, H.W., *Science*, 1977, *197*, 527-532.

13.Iyer, V.N., Szybalski, W., *Science*, 1964, *145*, 55.

14.Nakatsubo, F., Cocuzza, A.J., Keeley, D.E., Kishi, Y., *J. Amer. Chem. Soc.*, 1977, *99*, 4835-4836.
Fukuyama, T., Nakatsubo, F., Cocuzza, A.J., Kishi, Y., *Tet. Lett.*, 1977, *49*, 4295-4298.

15.Franko, A.J., *Int. J. Radiation Oncology. Biol. Phys.*, 1986, *12*, 1195-1202.

16.Raleigh, J.A., Liu, S.F.; *Int. J. Radiation Oncology, Biol. Phys.*, 1984, *10*, 1337-1340.

17.Carmichael, G.G., McMaster, G.K., *Methods in Enzymology*, 1980, *65*, 383-389.

18.Chapman, J.D., Franko, A.J., Sharplin, J., *Br. J. Cancer*, **1981**, *43*, **546.**

19.Rasey, J.S., Krohn, K.A., Freauff, S., *Radiation Research*, **1982**, *91*, **542-554.**

20.Leo, A., Hansch, D., Elkins, D., *Chem. Rev.*, **1971**, *71*, 525-516.

21.Rasey, J.S., Krohn, K.A., Grunbaum, Z., Conroy, P.J., Bauer, K., Sutherland, R.M., *Radiation Research*, **1985**, *102*, **76-85.**

22.Grunbaum, Z., Freauff, S.J., Krohn, K.A., Wilbur, D.S., Magee, S., Rasey, J.S., *J. Nucl. Med.* **1987**, *28*, **68-75.**

23.Wiebe, L.I., Jette, D.C., Chapman, J.D., *Nuklearmedizin*, **1984**, *23*, **62-67.**

24.Wiebe, L.I., Jette, D.C., Mercer, J.R., Samuel, B., Flanagan, R.J., Lee, J., Meeker, B.E., Chapman, J.D., in Mitta, A.E.A., Caro, R.A., Canellas, C.O. (eds), *Proc. Fifth Int. Symp. Radiopharmacology*, **1987**, **108-127.**

25.Jerabek, P.A., Patrick, T.B., Kilbourn, M.R., Dischino, D.D., Welch, M.J., *Appl. Radiat. Isot.*, **1986**, *37*, **599-605.**

26.Rasey, J.S., Koh, W.-J., Grierson, J.R., Grunbaum, Z., Krohn, K.A., *Int. J., Radiation Oncology, Biol. Phys.*, **1989**, *17*, **985-991.**

27.a) Shelton, M.E., Dence, C.S., Hwang, D.-R., Welch, M.J., Bergmann, S.R., *J. Nucl. Med.*, **1989**, *30*, **351-358.**
b) Martin, G.V., Rasey, J.S., Caldwell, J.C., Grunbaum, Z., Krohn, K.A., *J. Nucl. Med.*, **1987**, *28*, **668.**

28.Rasey, J.S., Grunbaum, Z., Shankland, E.G., Krohn, K.A., Mathis, C.A., Yano, Y., Budinger, T.F., *J. Nucl. Med.*, **1987**, *28*, **594.**

29.Teicher, B.A., Sartorelli, A.C., *J. Med. Chem.*, **1980**, *23*, **955-960.**

30.Kornblum, N., in Feuer, H.(ed); *The Chemistry of the Nitro and Nitroso Groups*, **1969**, Interscience, New York, **361-393.**

31.Wardman, P; *Int. J. Radiat. Biol.*, **1989**, *55*, 175-190.

32.Kerber, R.C., Urry, G.W., Kornblum, N., *J. Amer. Chem. Soc.*, **1964**, *86*, **3904.**

33.Kornblum, N., Pink, P., Yorka, K.V., *J. Amer. Chem. Soc.*, **1961, *83*, 2779.**

34.Kornblum, N., in Feuer, H.(ed); *The Chemistry of the Nitro and Nitroso Groups*, **1969,** Interscience, New York, **361-393.**

35.Russel, G.A., Danen, W.C., *J. Amer. Chem. Soc.*, **1966, *88*, 5663-5664.**

36.Bunnett, J. F., *Acc. Chem. Res.*, **1978, *11*, 413-420.**

37.Kirkpatrick, D.L., Johnson, K.E., Sartorelli, A.C., *J. Med. Chem.*, **1986, *29*, 2048-2052.**

38.Kabalka, G.W., Varna, R.J., *Tetrahedron*, **1989, *45*, 6601-6621.**

39.Flanagan, R.J., Charleson, F.P., Synnes, E.I., Wiebe, L.I., *J. Nucl. Med.*, **1986, *27*, 1165-1171.**
Baranowska-Kortylewicz, J., Kinsey, B.M., Layne, W.W., Kassis, A.I., *Appl. Radiat. Isot.*, **1988, *39*, 335-341.**

40.Fourneau, M.E., de Lestrange, Y., *Bull. Soc. Chim. France*, **1933, *53*, 330-340.**

41.Patai, S., (ed); *The Chemistry of the Carbonyl Group*, **1966,** *New York, Interscience*, **507-566.**

42.Furst, A., Berlo, R.C., Hooton, S., *Chem. Rev.*, **1965, *65*, 51-68.**

43.Hofle, G., Steglich, W., Vorbruggen, H., *Angew. Chem. Int. Ed. Engl.*, **1978, *17*, 569-583.**

44.Singh, P.R., Kuamr, R., *Aust. J. Chem.*, **1972, *25*, 2133.**

45.Hu, H.-N., Ni, J.-S., Kao, T.-S., *Huaxne Xuchao*, **1979, *37*, 10-13.**

46.Bunnett, J.F., Zahler, R.E., *Chem. Rev.*, **1951, *49*, 273-412.**

47.Gal'bershtam, M.A., Budarina, Z.N., *J. Org. Chem. U.S.S.R.*, **1969, *5*, 938.**

48.Arotsky, J., Butler, R., Darby, A.C., *J. Chem. Soc. (C)*, **1970,** *1480-1485.*

49.Symons, M.C.R., *J. Chem. Soc.*, **1957,** *2186.*

50.Fieser, L.F. Doering, W. von E.; *J. Amer. Chem. Soc.*, **1946, *68*, 2252-2253.**

51.Kashin, A.N., Bumagina, I.G., Bumagin, N.A., Bakuin, V.N., Beletskaya, I.P., *J. Org. Chem. U.S.S.R.*, **1981**, *17*, **905.**

52.Fujita, T., Iwasa, J., Hansch, C., *J. Amer. Chem. Soc.*, **1964**, *86*, **5175.**

53.Brown, J.M., Workman, P., *Radiation Research*, **1980**, *82*, **171-190.**

54.McCall, J.M., *J. Med. Chem.*, **1975**, *18*, **549-552.**

55.E.C., Bate-Smith, Westfall, R.G., *Biochem. Biophys. Acta.*, **1950**, *4*, **427.**

56.L., Albert, Hansch, C., Elkins, D., *Chem. Rev.*, **1971**, *71*, **525-613.**

57.Adams, G.E., Clarke, E.D., Flockhart, I.R., Jacobs, R.S., Sehmi, D.S., Stratford, I.J., Wardman, P., Watts, M.E., Parrick, J., Wallace, R.G., Smithen, C.E., *Radiat. Biol.*, **1979**, *35*, **133-150.**

58.Breccia, A., Berilli, G., Rofia, S., *Int. J. Radiat. Biol.* **1979**, *36*, **85-89.**

59.Maki, A. H., Geske, D.H., *J. Am. Chem. Soc.*, **1961**, *83*, **1852.**

60.Biskupiak, J.E., Grierson, J.R., Rasey, J.S., Martin, G.V., Krohn, K.A., *J. Labelled Cpds. Radiopharmaceuticals*, **1991**, *30*, **408.**

61.Mannan, R.H., Somayaji, V.V., Lee, J., Mercer, J.R., Chapman, J.D., Wiebe, L.I., *J. Nucl. Med.*, **1991**, *32*, **1764-1770.**

62.Thorp, J.; *J. Amer. Chem. Soc.*, **37**, *373*, **1915.**

63.Grice, R.; *J. Chem. Soc.*, **1963**, *1947*

64.Fourneau, M.E., de Lestrange, Y.; *Bull. Soc. Chim. France*, **1933**, *53*, **330.**

65.Williams, G.; *J. Chem. Soc.*, **1956**, **1304.**

66.Gal'bershtam, M.A., Budarina, Z.N., *J. Org. Chem. U.S.S.R.*, **1969**, *5*, **938.**

67.Arotsky, J., Butler, R., Darby, A.C.; *J. Chem. Soc. (C)*, **1970**, *1480-1485.*

68.Fujita, T., Iwasa, J., Hansch, C., *J. Am. Chem. Soc.*, 1964, *86*, 5175-5180.

69.Rockwell, S., *Laboratory Animal Science*, 1977, *27*, 831-851.

Chapter 3. 1-(4-[^{123}I]-iodophenyl)-2,6,7-trioxabicyclo-[2.2.2]octane as a Potential Imaging Agent for the GABA$_A$ Receptor.

3.1 Introduction

In 1950, three papers were published in volume 187 of the Journal of Biological Chemistry which fundamentally changed our understanding of the brain. Each of these papers dealt with the discovery of a remarkably simple molecule, later shown to play a crucial role in neuronal transmission, γ-amino butyric acid (GABA).

GABA

The first of these papers[1] reported the chromatographic isolation of a crystalline material from the ethanol extract of mouse brain homogenate. The material was tentatively identified as γ-amino butyric acid by its chromatographic behaviour and by the elemental analysis of the corresponding silver salt.

The second paper[2] described the isolation of the same material and its tentative identification as γ-amino butyric acid. The same paper detailed an elegant radiochemical determination of the origin of GABA from glutamic acid. Glutamic acid, extensively labelled with ^{14}C, was incubated with brain homogenate and the products were analyzed by paper chromatography. The authors were able to show that the only labelled products were GABA and glutamine. GABA is now accepted to be derived exclusively from glutamic acid in the

brain.

The third paper[3] dealt with the further proof of the identity of the unknown chemical as GABA. Roberts and Frankel were concerned that the unknown compound might be a mixture of two chromatographically similar amino acids. This problem had been encountered in other studies with leucine and isoleucine, valine and norvaline. Convincing proof that the unknown was a single compound was provided by Udenfriend using a double labelling technique.

3.2 Receptor Pharmacology

The role of GABA remained a mystery for quite some time following its discovery in the mouse brain in 1950. The report by Hayashi and Suhara[4] in 1956 that topically applied GABA exerted an inhibitory effect on electrical activity in the brain suggested that this remarkably simple molecule played a very important role in neuronal function. An understanding of the role of GABA in neurophysiology requires some knowledge of receptor pharmacology.

A receptor is a macromolecule* to which a bioactive molecule attaches and thereby elicits a response[5]. Receptors are generally located on the plasma membrane but are also associated with the cytoplasm and the nuclear compartments of the cell. The role of receptors is extremely important in

---

* In all cases studied to date, the macromolecule is a protein.

biology since they function as the primary site for regulating cellular activity in all organs and tissues.

3.2.1 Receptor Binding Molecules[6]

Agents which bind to the receptor recognition site and elicit a maximal response are called *Receptor Agonists* (Figure 3.1).

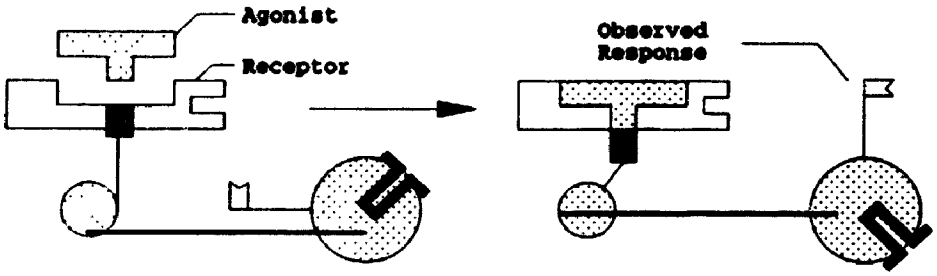

Figure 3.1. Schematic Representation of the Receptor-Receptor Agonist Interaction.

The receptor-ligand interaction is usually investigated by exposing biological tissues to various concentrations of ligand and observing the frequency or magnitude of a specific response (represented schematically by a flag).

A *Partial Agonist* binds to the receptor but elicits a less-than-maximal response (Figure 3.2).

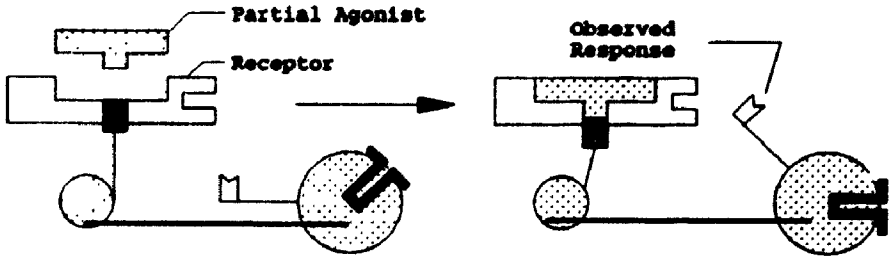

Figure 3.2. Schematic Representation of the Receptor-Patial Agonist Interaction.

An agent that occupies the recognition site but fails to elicit a response is called a receptor *Antagonist* (Figure 3.3)

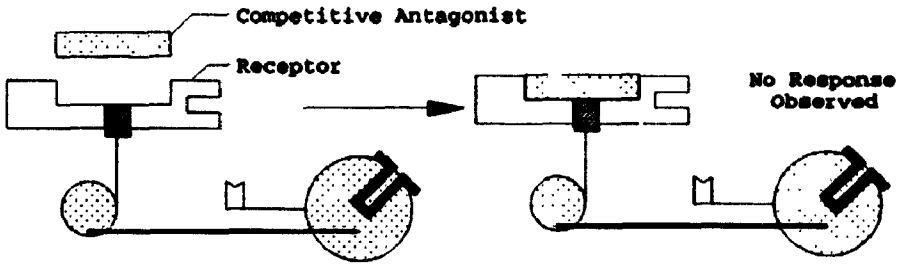

Figure 3.3. Schematic Representation of the Receptor-Competitive Antagonist Interaction.

An agent which binds to the receptor at a position removed from the recognition site yet elicits a response is called a *Non-competitive Agonist* (Figure 3.4).

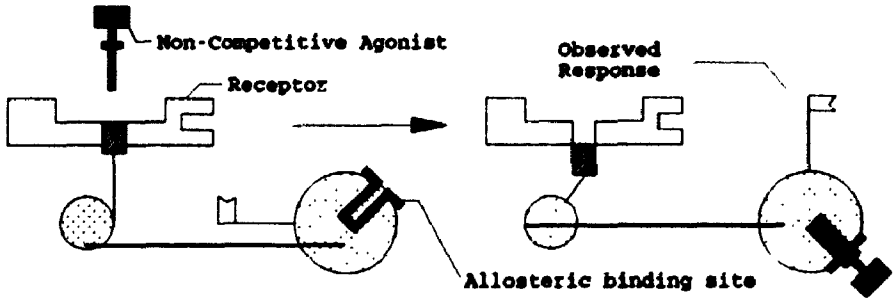

Figure 3.4. Schematic Representation of the Receptor-Non-Competitive Agonist Interaction.

Analogously, an agent which binds to the receptor at a position removed from the recognition site but blocks the effect of co-administered *Agonist* is called a *Non-competitive Antagonist* (Figure 3.5).

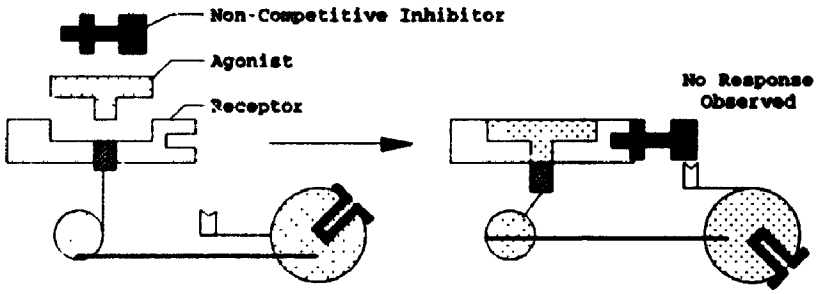

Figure 3 5. Schematic Representation of the Receptor-Non-Competitive Antagonist Interaction

Information about receptors is most often acquired by a systematic study of agents which bind to the receptor. Often the endogenous substance which binds to the receptor is not known and the receptors are classified according to the exogenous ligands which bind to it. Muscarinic and nicotinic receptors belong to this category. In other cases the endogenous ligand was discovered in advance of the receptor and the receptor is classified by the endogenous substance. GABA and dopamine receptors belong to this category.

3.3 The Theoretical Model of Receptor Binding[7]

The following assumptions are necessary in order to develop a simple theoretical model of receptor binding.

1. The amount of ligand taken up by the receptor is negligible relative to the total amount available.

2. Ligand molecules are adsorbed at a set of identical, non-interacting sites.

3. Response is proportional to receptor occupancy. ie. $R_A = y_A$ where R_A is the response observed and y_A is the fractional occupancy corresponding to this response.

When the receptor sites are saturated: $R_A=R_{MAX}$ and $y_A=R_A/R_{MAX}$. If these expressions hold, then the ratio of observed response to maximum response is equal to the fraction of receptors occupied by the drug.

When equilibrium is reached between the ligand and the receptor then:

$$RL \overset{K_D}{\rightleftharpoons} R + L$$

where R is the receptor, L is the ligand and RL is the ligand-receptor complex. The equilibrium dissociation constant is then:

$$K_D=k_{-1}/k_1= [R][L]/[RL] \qquad 1)$$

The rate constants for the formation and the dissociation of the ligand-receptor complex are given by k_1 and k_{-1} respectively. The experimentally measurable quantities are usually [L] and [LR]. Substituting $B_{MAX}=c([R]+[LR])$ and $B=c[LR]$ into equation 1 where B is the amount bound, B_{MAX} is the amount of ligand bound at saturation and c is a factor to convert from concentration per unit volume to amount of ligand per unit weight of tissue. One obtains the following expression:

$$B=[L]B_{MAX}/(K_D+[L]) \qquad 2)$$

A plot of B versus [L] has the following form (Figure 3.6):

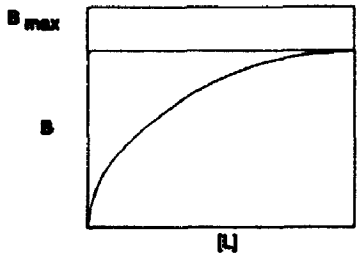

Figure 3.6. Plot of bound receptor versus ligand concentration.

At the ligand concentration required to give 50% response (y_A=0.5):

$$0.5= 1/(1+K_D/[L]) \qquad 3)$$

Thus at this level of response $K_D=[L]_{50}$. The dissociation constant can be easily determined from a concentration-response relationship provided the original assumptions hold (Figure 3.7).

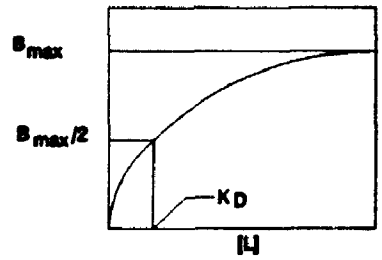

Figure 3.7. Determination of K_D from plot of B versus [L].

A low value for K_D (typically in the nanomolar range) implies a highly specific ligand-receptor interaction. Equation 2 can be transformed into the following expression:

$$B/[L]=-B/K_D + B_{MAX}/K_D \qquad 4)$$

A plot of B/[L] versus B should yield a straight line with slope of $-1/K_D$ and a y intercept of B_{MAX}/K_D. This type of plot

is called a Scatchard Plot[8] (Figure 3.8).

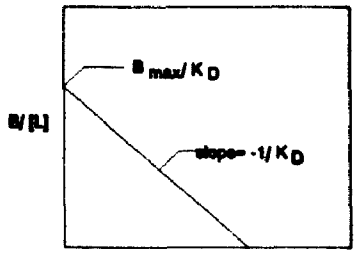

Figure 3.8. The Scatchard Plot.

The linearity of the Scatchard plot indicates whether the original assumptions hold and whether simple receptor binding is being observed. As might be expected simple receptor binding is rare. Scatchard plots are most often curved indicating that a more complicated mechanism is responsible for the observed binding. It has been observed that nearly every molecule shows some affinity for biological tissues. This affinity arises from ionic and lipophilic interactions and is referred to as *non-specific binding*. Non-specific binding is relatively easy to distinguish from specific binding. Specific binding is, by definition, a saturable process while non-specific binding depends only on the concentration of ligand not on the quantity of receptor.

3.4 The Kinetics of Receptor Binding

In principle, it is a straightforward procedure to study the kinetics of receptor binding:

$$L + R \underset{k_{-1}}{\overset{k_1}{\rightleftharpoons}} LR \qquad 5)$$

Equation 5 yields the second order rate expression:

$$\text{Rate} = d[LR]/dt = k_1[L][R] \qquad 6)$$

Which on integration yields equation 7:

$$1/([L_o]-[R_o]) \ln \frac{[R_o]([L_o]-[LR])}{[L_o]([R_o]-[LR])} = k_1 t \qquad 7)$$

A plot of $\ln \frac{[R_o]([L_o]-[LR])}{[L_o]([R_o]-[LR])}$ versus t should give rise to a straight line through the origin with a slope of k_1. It is also possible to measure the dissociation rate:

$$LR \overset{k_{-1}}{\rightarrow} L + R \qquad 8)$$

which follows the first order rate expression:

$$\text{Rate} = -d[LR]/dt = k_{-1}[LR] \qquad 9)$$

Equation 9 can be integrated to yield equation 10:

$$\ln([R_o]/[LR]) = k_{-1}t \qquad 10)$$

A plot of $\ln([R_o]/[LR])$ versus t should yie. . a straight line with slope equal to k_{-1}. Once k_1 and k_{-1} are determined K_D can be recalculated using the expression:

$$K_D = k_{-1}/k_1 \qquad 11)$$

This procedure will furnish an independent check on the value of K_D obtained by equilibrium analysis.

3.5 Practical Aspects of Receptor Pharmacology

The binding of ligands to receptors is usually studied using radioactive ligands. The first such study was reported by Jensen and Jacobsen in 1962[9] who reported the binding of ^{3}H-labelled estradiol to estrogen receptors.

Problems were encountered in the early research conducted into receptor binding due to ligands whose specific activity was too low. Specific activity refers to the quantity of radioactivity which is emitted per unit mass of ligand. The quantity is most often expressed as the number of Curies per millimole of ligand (S.I. units Bq/mmol). The specific activity actually refers to the ratio of radioactive ligands to non-radioactive ligands in a given preparation. The importance of specific activity in receptor pharmacology can perhaps best be illustrated by Figure 3.9:

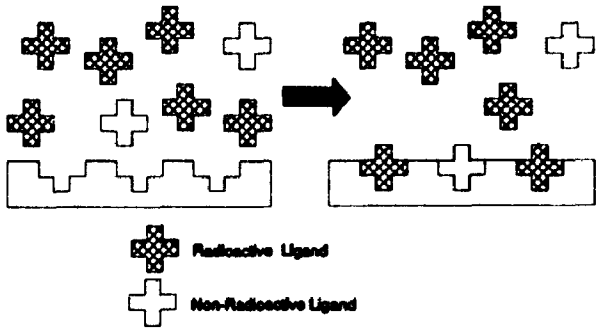

Figure 3.9. Receptor Labelling with a high specific activity ligand.

In the case of a high specific activity ligand the unoccupied receptor has a high probability of interacting with a radioactive ligand and thus the isolated ligand-receptor complex will retain a high amount of radioactivity.

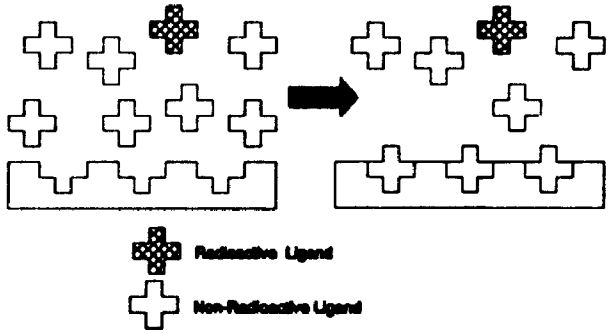

Figure 3.10. Receptor labelling with a low specific activity ligand.

In the case of a low specific activity ligand (Figure 3.10) the unoccupied receptor is exposed to relatively few radioactive ligands and the isolated ligand-receptor complex contains proportionately less radioactivity than the high specific activity case. The use of low-specific activity ligands often results in unacceptable signal to noise ratios resulting from poor counting statistics and interference due to background radiation.

3.6 Assays for Receptor Binding

As mentioned previously, the most easily measured quantities in the equilibrium equation 1 are [L] the free ligand concentration and [LR] the concentration of ligand-receptor complex. The free ligand concentration is easily determined by direct assay of the radioactivity in solution but determining the concentration of the ligand-receptor complex requires specialized techniques. The most common of these techniques are equilibrium dialysis and filter assays.

3.7 Equilibrium Dialysis

The equilibrium dialysis technique is the least sensitive of the two techniques and requires that the receptor not be able to pass through the membrane and that the ligand be able to diffuse freely through the membrane. The procedure is as follows:

1. The receptor and media are placed in a dialysis bag and dialysed against a bath containing radiolabelled ligand.

2. Once equilibrium has been reached the bath and the bag are analyzed for radioactivity.

The bag radioactivity is equal to [L] + [LR] and the bath radioactivity yields [L]. To achieve acceptable signal to noise there should be at least a 10% excess of bag activity over bath activity. This requires that [R] must be at least 10% of K_D. From equation 1:

$$[LR]/[L] = [R]/K_D \qquad 12)$$

The ratio $[R]/K_D$ is greatest when the concentration of unoccupied receptor [R] is greatest. This situation occurs when the concentration of ligand is very low. The result is, that for dialysis detection, binding can most readily be detected when the concentrations of ligand are low relative to the K_D for the ligand.

3.8 Filter Assays

A more sensitive technique is the filter assay. The only

requirement is that the receptor-ligand complex be retained by a membrane filter while any free ligand should pass through the filter. In the simplest case the concentration of ligand-receptor complex can be determined by assaying the radioactivity retained by the filter and the concentration of free ligand is determined by assaying the filtrate.

3.9 Competitive Binding

Once the baseline binding of a radioactive ligand to a receptor has been established the pharmacology of a receptor binding site is further studied through *competitive inhibition*. *Competitive inhibition* describes the measurement of the displacement of a labelled ligand by incubation of the receptor-ligand complex with a different non-radioactive ligand. In the simplest case the following equilibria exist:

$$R + L \overset{K_D}{\rightleftharpoons} RL \qquad 13)$$

$$R + I \overset{K_I}{\rightleftharpoons} RI \qquad 14)$$

Where L is the radioactive ligand being displaced from the recognition site and I is the non-radioactive inhibitor which is competing with L for the binding sites. Using the expressions for K_D and K_I the following expression can be derived:

$$B = \frac{B_{MAX}[L]}{([L] + K_D(1 + [I]/K_I))} \qquad 15)$$

If [I] is held constant and [L] is varied the resulting

Scatchard plot is a straight line having an apparent $K_D' = K_D(1 + [I]/K_I)$.

If true competitive inhibition exists then the K_D value is expected to change but B_{MAX} (the quantity of available binding sites) must remain constant. Since B_{MAX} cannot change, the x-intercept of the Scatchard plot (B_{MAX}) must remain constant.

A more common method for representing competitive binding data is to plot the fractional binding of radioligand versus the logarithm of the inhibitor concentration. The shape of the resulting plot is as follows (Figure 3.11):

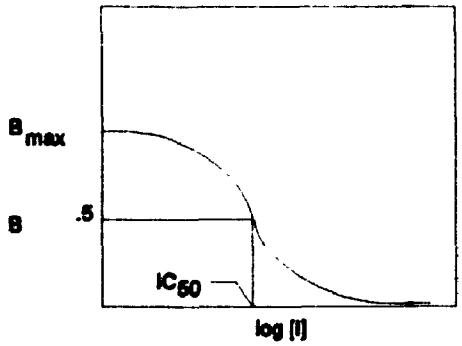

Figure 3.11. Competitive Inhibition Plot.

The inhibitory strengths of numerous ligands are conveniently compared using the concentration of ligand necessary to displace 50% of the radioactive ligand (IC_{50}). The shape of the plot of fractional displacement versus log [I] renders it difficult to determine whether simple inhibition is occurring. A more easily interpreted representation is that of the *Hill plot* which furnishes a straight line when simple competitive inhibition is observed.

From equation 15, if one varies [I] while holding [L] constant, then the amount of binding in the absence of inhibitor (B_o) is just:

$$B_o = \frac{B_{MAX}[L]}{(K_D + [L])} \qquad 16)$$

Which on substitution into equation 13 yields the following:

$$B/B_o = \frac{([L] + K_D)}{(([L] + K_D(1 + [I]/K_I))} \qquad 17)$$

Equation 17 can be converted to equation 18 which is the form of the Hill plot[10] (Figure 3.12).

$$\log \frac{(B_o - B)}{B} = \log \frac{K_D}{(K_i[L] + K_D[L])} + \log[I] \qquad 18)$$

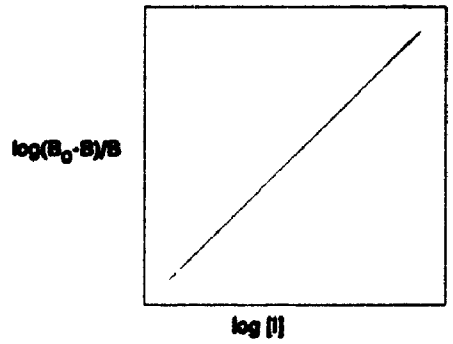

Figure 3.12. The Hill Plot.

Thus, if simple competitive inhibition is observed, a plot of $\log\{(B_o-B)/B\}$ versus $\log[I]$ is a straight line with a slope of 1.0.

Simple competitive inhibition is the exception. Hill slopes different from unity are often observed. Slopes of

Hill plots (Hill Coefficients) of less than unity have been interpreted in terms of negative cooperativity (for the inhibitor) or by the presence of sites with differing affinities for the receptor. Hill coefficients greater than unity may represent positive cooperativity or irreversible binding of the inhibitor. GABA provides an excellent example of these concepts. The Hill coefficient for [^{14}C]-GABA was found[11] to be 2.2 in a study of its binding to a receptor preparation isolated from rat cerebellum. This result has been interpreted in terms of a *positive cooperativity* between GABA and the GABA receptors. Evidence suggests[12] that two molecules of GABA may fit into the recognition site of the GABA receptor in a head-to-tail fashion giving rise to the observed cooperativity.

3.10 The Pharmacology of GABA Receptors

The pharmacology of GABA receptor binding has been extensively studied using the techniques outlined previously. GABA has been shown[13] to inhibit the firing of stimulated receptor neurons in the isolated crayfish stretch receptor . Elliott and Florey found that in the absence of GABA the stretch receptor neuron (in the crayfish tail) fired about five times per second in response to a physical stretch imparted to the tail. The nerve firings were detected by amplifying the electrical signal then displaying the resulting spikes on an oscilloscope. The signals were also converted to

sound via a loudspeaker. The topical application of solutions of GABA at various concentrations caused partial or complete blockage of the nerve impulses. These first experiments provided compelling evidence that GABA functioned as an inhibitory neurotransmitter but it took many years for this concept to gain widespread acceptance.

At the microscopic level GABA functions as an inhibitory neurotransmitter following its release from the pre-synaptic neuron by binding to the post-synaptic GABA receptor [14].

The binding of GABA to the receptor results in an increase in the permeability of the membrane to chloride ions. This increase in permeability is a result of the opening of the chloride ion channel. The net result of the influx of chloride ions is to hyperpolarize the membrane and in so doing reduce the probability that a neuron will produce an impulse (action potential).

The understanding of the role of GABA that has been acquired to date has been aided to a very large extent by the study of ligands--other than GABA--which bind to the GABA receptor. Many hundreds of molecules have been tested and show some affinity for the GABA receptor. We need consider only four of these compounds muscimol, bicuculline, baclofen and picrotoxin in order to classify most of the tested compounds.

3.11 Muscimol

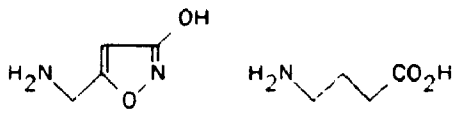

Muscimol GABA

Muscimol is a naturally occurring hallucinogenic drug which was first isolated from the mushroom *Amanita muscaria*[15]. Muscimol acts as a potent CNS depressant, as a sedative and as an antiemetic[16] in addition to its hallucinogenic activity. The structural similarity between GABA and Muscimol immediately suggests that Muscimol may be a GABA-mimetic acting at the GABA recognition site. Hill analysis[17] of the competitive inhibition of [^{3}H]-muscimol by various ligands has shown that muscimol is a GABA *agonist* (a substance which binds to the GABA receptor and gives rise to the same response observed with GABA) with a higher affinity for the GABA receptor than GABA itself.

The IC_{50} values for various GABA agonists and antagonists on [^{3}H]-muscimol binding are listed in Table 3.1.

Table 3.1. Competitive inhibition data for Muscimol binding. * Did not inhibit [^{3}H]-Muscimol binding at solubility limit of ligand.

Ligand	IC_{50} (Mouse P_2, μM)
Muscimol	0.02
GABA	0.20
Bicuculline	13
Baclofen	>1000*
Picrotoxin	>1000*

3.12 Bicuculline

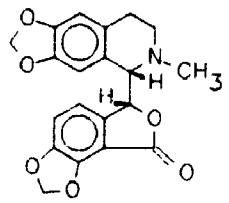

Bicuculline

A new alkaloid was reported in 1932 by Richard Manske[18], then of the National Research Laboratories in Ottawa. The alkaloid was isolated from the dried tubers of the *Dicentra cucullaria* plant. Only minute quantities were isolated in Manske's early work, limiting the degradation which could be performed to determine the structure. A tentative molecular formula and a melting point were reported. A second paper[19] was published the following year in which Manske reported the isolation of larger quantities of this alkaloid. By degradation work, Manske deduced the correct structure for the new alkaloid which he named *bicuculline*.

In 1970, it was shown[20] that neurons in the feline cerebral cortex and cerebellum, when treated with bicuculline, were resistant to the inhibitory effects of iontophoretically* administered GABA. Bicuculline was shown to function as a GABA *competitive antagonist,* a ligand which binds to the GABA receptor and blocks the action of GABA. Curtis *et al* showed that the blocking effect was reversible and that it was specific for the GABA receptor. Bicuculline had no effect on the binding of the other inhibitory neurotransmitter *glycine*.

Through construction of Dreiding models, the authors concluded that the nitrogen atom and the carboxylate group in GABA can be exactly isosteric with the nitrogen and the O=C-O- in bicuculline.

Bicuculline methiodide is a more stable form of bicuculline which has been shown[21] to have similar binding to that of bicuculline. The tritiated analogue was prepared and was shown[22] to be an excellent biochemical probe for the GABA receptor. Scatchard analysis yielded a K_D value of 380 nM and a B_{MAX} of 4.5 pmol/mg of receptor protein obtained from rat brain homogenate. The Hill coefficient for competitive binding was found to be 0.95 indicating a lack of cooperative action between binding sites and hence a simple association mechanism.

---

*Iontophoresis is the process whereby an ionized drug is forced to migrate through a cell membrane under the effect of a galvanic current applied across the membrane.

The discovery of the antagonist properties of bicuculline was a very important step in the understanding of GABA receptor pharmacology. The binding of GABA to brain membranes is complicated by the re-uptake of GABA at the synapse[23]. Sodium dependent and sodium independent GABA binding has been observed and it is now believed that the sodium dependent uptake is not receptor mediated but may represent a metabolic reabsorption route for GABA previously released from the post synaptic receptor. The net result is that studies of the GABA receptor using radioactive GABA as the ligand are complicated by metabolic elimination. The use of bicuculline methiodide as ligand in these studies eliminates the complication.

3.13 Baclofen

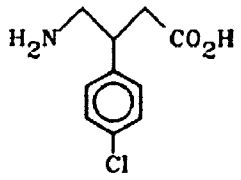

± Baclofen

The pharmacology of GABA was further complicated by the 1981 report that a new type of receptor for GABA had been discovered[24]. Baclofen, (±) β-(p-chlorophenyl)-γ-amino butyric acid, is a clinically important muscle relaxant which has been in use since 1966. Hill and Bowery conducted a study of the binding of [^{3}H]-baclofen in the presence and absence of Ca^{2+} and Mg^{2+} ions. They observed saturable binding in the presence of $CaCl_2$. Scatchard analysis gave a straight line

yielding a K_D value of 132 nM and a B_{MAX} value of 1.1 ρmol/mg of receptor protein. In the absence of Ca^{2+} ions, no saturable binding was observed. Competitive binding experiments showed that the (-) Baclofen isomer was over 500 times more potent than the (+) isomer. A striking result of the competitive binding experiments was the observation that bicuculline methobromide did not displace [^{3}H]-baclofen from the GABA receptor. This result provided convincing evidence that two types of GABA receptor exist; one which binds bicuculline and another which binds baclofen (Figure 3.13).

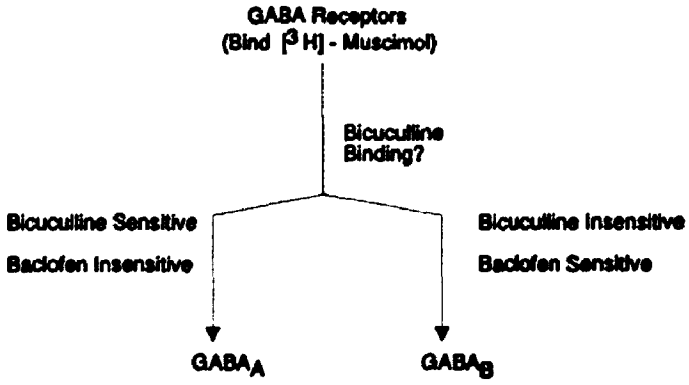

Figure 3.13. Classification of GABA Receptors

Bicuculline sensitive GABA receptors are now classified as the "A" subtype and baclofen sensitive GABA receptors are classified as the "B" subtype.

3.14 Picrotoxin

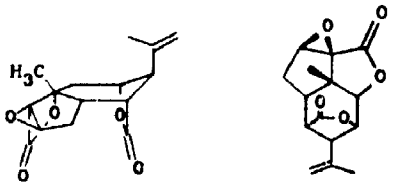

Picrotoxin

Picrotoxin is a sesquiterpene isolated from a poisonous plant of the moonseed family native to India. Its chemical history began in the early nineteenth century but its use as a poison or drug has been traced to the early sixteenth century[25]. Picrotoxin was first used to stun fish and to kill body lice.

The pharmacology of picrotoxin has been studied extensively throughout this century due to its extreme potency as a convulsant. Despite many studies, its mode of action was not well understood until relatively recently. The crayfish[26] once again played a key role in the elucidation of the mode of action of picrotoxin. Studies on the effects of various agents on the crayfish claw muscle inhibitory nerve showed that picrotoxin blocked the inhibitory effect of GABA applied to the nerve. The observed blocking suggested that picrotoxin was acting as a competitive inhibitor of GABA.

Structural work on picrotoxin[27] showed that the compound was an equimolar mixture of two components picrotoxinin and picrotin. Picrotin is the analogue of picrotoxinin hydrated at the isopropenyl group. Picrotoxinin is the active component having over 100 times the potency of picrotin.

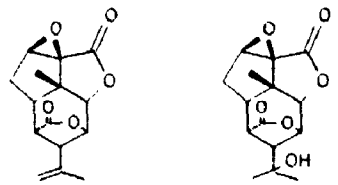

Picrotoxinin Picrotin

Picrotoxin binds to brain membranes[28] and appears to block the inhibitory effects of GABA as measured by the uptake of ^{36}Cl ion. Picrotoxin does not inhibit the binding of GABA (or Muscimol or Bicuculline) to the GABA recognition site to any appreciable extent. Picrotoxin acts as a *non-competitive GABA inhibitor* and acts at an *allosteric binding site*• called the *convulsant binding site* of the GABA receptor. Picrotoxin is called an *heterotropic ligand* because it binds to the receptor and elicits a response apparently without interacting to any significant extent with the primary binding site of the receptor.

The convulsant binding site is the GABA receptor component of central interest to our research. In 1978 a new class of compounds, the cage convulsants, was reported[29] to inhibit the binding of picrotoxinin to brain membranes.

•An allosteric binding site implies that the site of action is physically removed from the primary binding site of the receptor.

3.15 Cage Convulsants

In 1973 Casida and Bellet[30] reported that 4-alkyl-2,6,7-trioxa-1-phosphabicyclo [2.2.2] octanes **3.12** were highly toxic in mice.

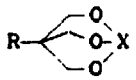

3.12

The authors found that the phosphites (X=P), the phosphates (X= P=O) and the thionophosphates (X= P=S) were of similar toxicity for the same alkyl group R but that the toxicity is greatly dependant on the nature of R. In their original communication they reported that the most potent compound had R as isopropyl **3.13**.

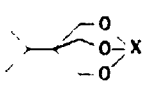

3.13

X	LD_{50} (mg/kg)
P	22
P=O	18
P=S	26

It was known that the bicyclic phosphites and thionophosphates were easily oxidized to the phosphates *in vivo* implying that the toxic effect was exerted by the same compound in all three cases. The authors also deduced that, unlike other phosphoric esters*, the toxic effects were not due to the inhibition of cholinesterase. Even at high doses, the brain cholinesterase activity was not at all inhibited. The authors extended the structure- activity relationship in a subsequent paper[31] and found that the most potent compound

---

*ie. parathion, diisopropyl fluorophosphate.

was obtained when the alkyl group was t-butyl **3.14**.

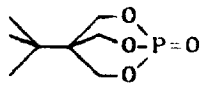

3.13

This compound had an LD_{50}* of 0.053 mg/kg in male Swiss Webster mice. Bowery *et al*[32] showed that administration of bicyclic phosphate esters antagonized the hyperpolarization effect of γ-amino butyric acid (GABA). Mattsson *et al*[33] showed that the Phosphorous Trioxa Bicyclo Octane (PTBO) derivatives caused an increase in the level of cyclic guanidine mono phosphate (GMP) in the brains of poisoned rats. The authors took this as an indication that the PTBO derivatives blocked the inhibitory action of GABA which in turn led to an overproduction of cyclic GMP. The PTBO derivatives were also found to inhibit the binding of picrotoxin to brain homogenate suggesting that both compounds bind to the convulsant binding site of the chloride ion channel[34].

Having established that the PTBO esters were highly selective GABA antagonists it became immediately apparent that a radiolabelled analogue might prove to be a useful biochemical probe for the GABA receptor. The first such radioligands were prepared by Milbrath *et al*[35]. They labelled the 4-methyl and 4-*t*-butyl analogues (**3.12** R=CH_3, *t*-But, X=

---

*LD_{50} is the dose of drug (usually given in mg of drug per kg of animal) necessary to kill 50% of a given group of animals in a given time period.

P=O) with ^{32}P and examined their metabolic fate in mice, rats and rabbits. The authors found that the radioactivity from both the methyl and *t*-butyl phosphates was very rapidly excreted in the first 12 hour urine of all three species. There were notable species differences in the metabolism of the compounds (Table 1).

Table 1. Percent of injected dose excreted in urine--as parent compound--at up to 48 hours post injection.

	R = Me	R = *t*-Butyl
Mouse	70	6
Rat	90	24
Rabbit	16	18

Particularly noteworthy was the observation that much less of the tertiary-butyl bicyclophosphate was present intact in the urine in all species as compared to the methyl derivative. In addition, the authors noted that of the ^{32}P activity in the rabbit (for the methyl derivative) which was not excreted was almost entirely retained in the liver and the bone. The bone uptake was believed to result from the complete hydrolysis of the parent compound to phosphate. In addition to the bicyclic phosphoric esters, two other classes of compounds were added to the list of GABA inhibitors: the silatranes[36] **3.15**, and the bicyclic orthocarboxylate esters[37] **3.16**.

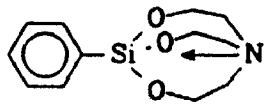

3.15

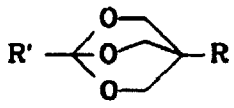

3.16

It was soon shown[38] that, of the bicyclic orthocarboxylates tested, the benzoic orthocarboxylates (3.16 R'=C_6H_5) showed particular toxicity.

Casida *et al*[39] tested nearly 100 bicyclic orthobenzoates and found that the most toxic compounds were those having a tertiary butyl group at the 4 position. In addition they found that the toxicity and the receptor binding efficiency could be greatly improved by introducing an additional substituent on the benzene ring.

Table 3.2 lists a number of substituents and the corresponding IC_{50}, and LD_{50} values for the 4'-substituted *t*-butyl orthobenzoates (TBOB's).

Table 3.2. LD_{50} and receptor IC_{50} vs. ^{35}S TBPS values for a series of 4'-substituted 4-*t*-butyl orthobenzoates.

X	IC_{50} (nM)	LD_{50}(mg/kg)
H	49	1.3
F	42	0.77
Cl	7	1.1
Br	10	1.2
CF_3	92	38
NO_2	55	2.9
CN	3	0.060
N_3	315	15
t-C_4H_9	2200	84

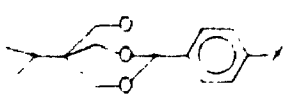

The extreme toxicity of these compounds is immediately striking. A dose of 25 μg per mouse (administered by i.p. injection) of the 4-Cl derivative is sufficient to kill 50% of the mice in a given population. The 4'-CN compound **3.18** is an order of magnitude more toxic than the original *t*-butyl bicyclophosphate ester **3.17**.

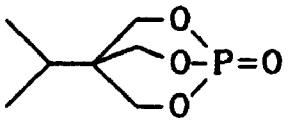

3.17

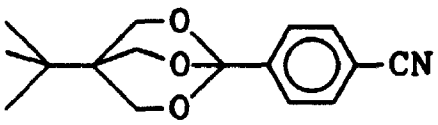

3.18

The same year, 4'-^{3}H-TBOB **3.19** was reported as a radioligand for the $GABA_A$ receptor[40].

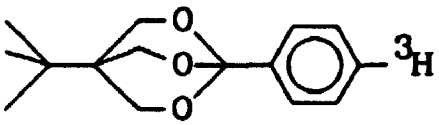

3.19

Following this result, we proposed molecule **3.20**, 4'-[^{123}I]-TBOB as an *in vivo* marker for the $GABA_A$ receptor.

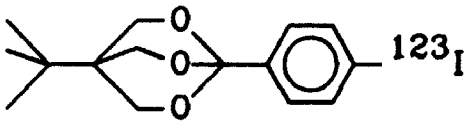

3.20

We proposed that the molecule be labelled with ^{123}I since this isotope is ideal for imaging in the nuclear medicine clinic[41]. In addition, we felt that the available data suggested that substitution amongst the halogens did not

greatly alter the toxicity of the compounds as measured by LD_{50}, nor did it have a large effect on the receptor binding as measured by the receptor IC_{50} (see Table 3.2). Since we began our studies we have learned[42] that compound **3.20** has an IC_{50} value of 12 nM in competition with ^{35}S TBPS.

3.16 Why Image the $GABA_A$ Receptor?

Changes in the number of GABA receptors has been linked to a number of neurological disorders[43] including Huntington's disease, epilepsy, alcoholism, Alzheimer's disease, and Parkinson's disease. These changes in GABA binding have been observed using autoradiography and the receptor binding techniques described earlier. Both of these techniques involve the analysis of post-mortem or surgically resected brain specimens. Clearly, a much more useful technique would be the *in vivo* monitoring of these changes in receptor quantity using Nuclear Medicine techniques. The Nuclear Medicine method for monitoring dopamine receptor populations has been extremely successful in shedding new light on diseases such as schizophrenia and Parkinson's[44].

Predictably, the changes in GABA receptor populations observed in different diseases do not follow simple patterns. The decrease in GABA binding in Huntington's disease was originally interpreted as a decrease in receptor concentration due to cell loss. This cell loss was restricted to specific regions of the brain. Recent evidence[45] indicates that cell

loss may occur sometime after the first changes in GABA binding are observed. The implication is that changes occur in the cell membrane which decrease GABA binding prior to cell death. This observation opens up the possibility of pharmacological rescue if the disease is diagnosed in its early stages.

If changes in the number of GABA receptors, as measured by *in vivo* receptor binding, are an excellent predictor of disease then surely the best ligand for nuclear medicine would be GABA itself. Unfortunately, a number of factors preclude radioactive GABA as a Nuclear Medicine probe; the most important of which is drug delivery. GABA is zwitterionic and as such cannot cross the blood-brain-barrier (BBB). Thus, though ^{11}C-labelled GABA could be relatively easily produced for PET, once the radioactive drug was injected into the bloodstream it could be detected everywhere in the body--except the brain. A more appropriate ligand might be muscimol a drug which is known to cross the BBB. The labelling of a GABA agonist is not sufficient however, to provide definitive diagnoses of diseases involving changes in GABA concentration. When neuronal loss occurs, a process called *denervation hypersensitivity* appears to cause an increase in the number of GABA receptors in the brain. We believe that the use of a labelled *non-competitive* inhibitor of the $GABA_A$ receptor might allow the Nuclear Medicine clinician to distinguish between decreases in GABA binding due to changes in the cell membrane

in the early stages of disease from decreases in GABA binding due to the loss of neurons during the latter stages of disease.

Chugani and Olsen[43] have compiled a list of criteria a ligand must meet in order to provide a suitable marker for receptor quantification using Nuclear Medicine.

1. The ligand must have high lipid solubility and low protein binding so that it crosses the BBB easily.

2. The ligand must bind selectively to the receptor with high affinity.

3. The ligand must have low non-specific binding.

4. The ligand must remain bound to the receptor long enough to allow imaging (low dissociation rate).

5. The ligand should not be significantly metabolized prior to tomographic imaging.

6. The ligand should be relatively simple to synthesize.

7. The ligand must be produced with relatively high specific activity.

If these criteria are met the authors predict that:

> "The successful quantitative imaging of receptors in humans may eventually allow early detection and characterization of receptor alterations in some diseases and ultimately lead to improved diagnosis, subclassification, treatment selection, and management of these disorders."

The balance of this chapter will outline our attempts to discover to what extent radioiodinated 4'-iodo TBOB **3.20** meets the above criteria.

3.17 Chemistry

We believed that the radioactive material could most easily be obtained in high specific activity via halodestannylation of the 4'-trimethylstannyl derivative **3.10** (Scheme 3.1)[46].

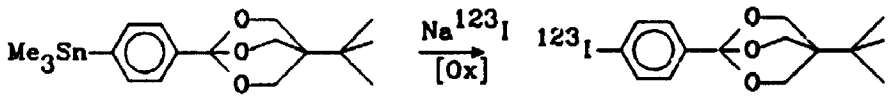

3.10 Scheme 3.1 3.20

Since the bicyclic ortho ester functionality has been shown[47] to provide protection for the carboxylate group under strongly basic conditions we felt that lithiation followed by transmetalation[48] would provide an ideal route to the trimethylstannyl derivative **3.10** (Scheme 3.2).

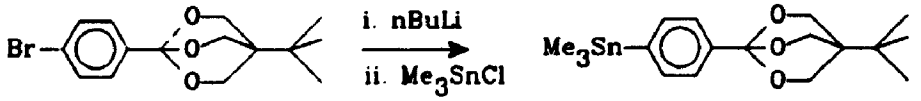

3.9 Scheme 3.2 3.10

We chose to lithiate the corresponding bromo compound **3.9** in order to eliminate the possibility of reduced specific activity arising from dilution of the radioactive iodo compound with non-radioactive starting material. The desired 4'-trimethylstannyl TBOB **3.9** was obtained in 96% yield by this method.

The brominated precursor **3.9** and the non-radioactive 4'-iodo TBOB **3.8** were obtained via the Lewis-acid catalysed rearrangement of the corresponding oxetane esters **3.7** and **3.6** respectively (Scheme 3.3).

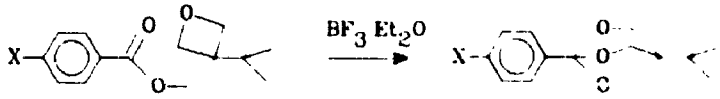

3.6 X=I
3.7 X=Br

Scheme 3.3

3.8 X=I
3.9 X=Br

The rearrangement is believed[47] to occur via the following mechanism (Scheme 3.4):

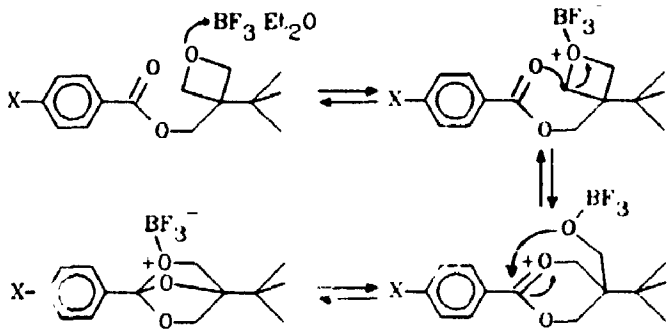

Scheme 3.4

The driving force for the reaction is believed to be the relief of ring strain occurring when the oxetane is converted to the bicyclooctane system.

The oxetane alcohol **3.5** was obtained via the pyrolysis of the carbonate ester **3.4a** derived from the reaction of the triol **3.4** with diethyl carbonate and catalytic amounts of ethanolic potassium hydroxide (Scheme 3.5)[48].

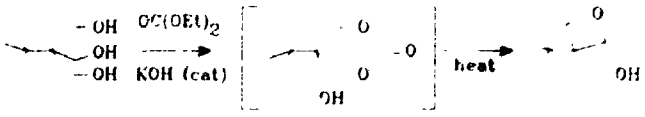

3.4 3.4a 3.5

Scheme 3.5

The triol **3.4** was originally prepared by the method of Cooper, and co-workers[50] (Scheme 3.6).

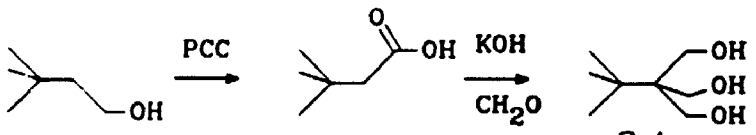

3.4

Scheme 3.6

This route gave rise to very poor yields[51] of triol **3.4** from relatively expensive starting material. The alternative synthesis of Ozoe and Eto[52] (Scheme 3.7) was successfully used to prepare the triol **3.4** in moderate yield from the less expensive starting material diethyl malonate.

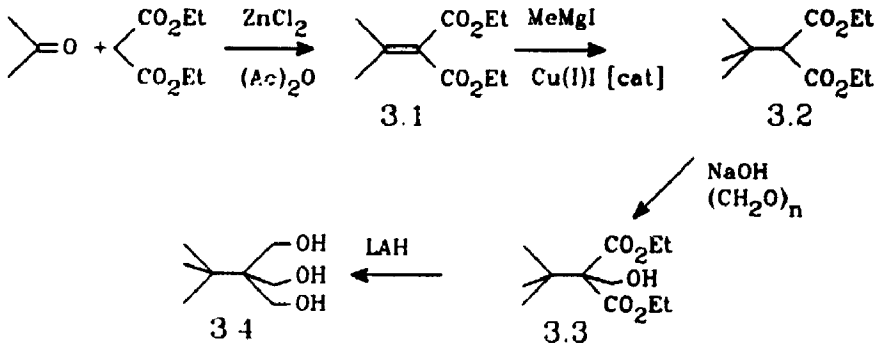

3.1 3.2 3.3 3.4

Scheme 3.7

3.18 Results and Discussion

Treatment of 4'-trimethylstannyl TBOB with $Na^{131}I$ and N-chlorosuccinimide gave rise to good yields of the desired **3.8** following purification by HPLC. ^{131}I-labelled **3.8** was dissolved in phosphate buffered saline and injected into female CD1 mice via tail vein. The mice were sacrificed at pre-determined time points by CO_2 asphyxiation. The carcasses were exsanguinated with heparinized Ringers lactate (ca. 10 mL) perfused via the left ventricle following clipping of the atrium. Each carcass was dissected and the organs of interest weighed and assayed for radioactivity in a well-counter. The results are represented graphically in Figure 3.14.

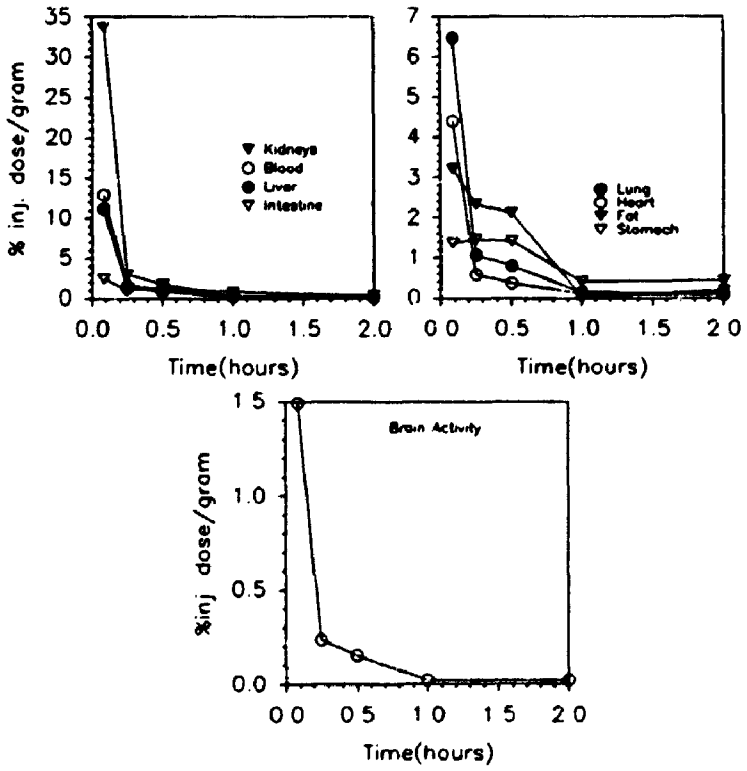

Figure 3.14. Biodistribution of [131-I] 3.8 in female CD-1 mice.

The very rapid washout of the compound is immediately striking. We were surprised to observe that the highest initial uptake was in the kidneys; on closer examination this result proved to be quite plausible. The biodistribution data for the kidneys, blood, liver, intestine, lung, heart *and* brain are all consistent with an extremely rapid metabolic elimination of the injected radioactivity. The only tissues to exhibit any retention of radioactivity were the stomach and the fat. The source of the stomach activity is not clear but may be a reabsorption of metabolically-released iodide. The activity observed in the fat is consistent with the absorption of a highly lipophilic molecule in lipophilic tissue.

We were disappointed by the very rapid wash-out of the drug and the extremely low brain activity. We initially suspected that the drug was undergoing rapid hydrolysis in the bloodstream. The *in vivo* activity of the tertiary butyl orthobenzoates argues against this conclusion since the compounds exert their toxic effects following intra-peritoneal injection. In order to investigate the stability of **3.11** in the bloodstream the ^{123}I analogue was incubated in human plasma for up to four hours then subjected to HPLC analysis. The parent compound could be isolated in greater than 95% purity at all time points tested (Figure 3.15).

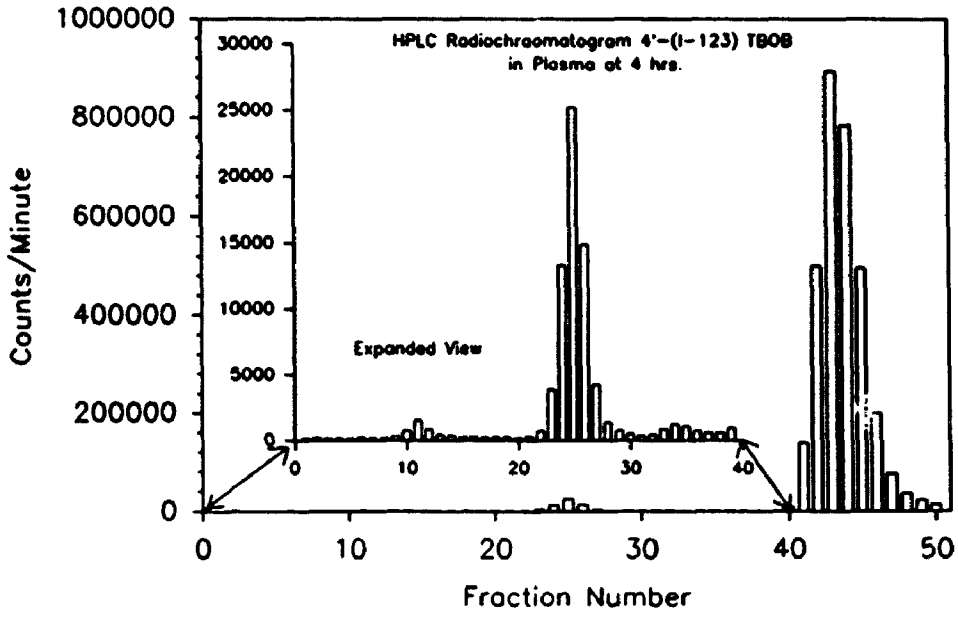

Figure 3.15. HPLC Radiochromatogram of 4'-[123-I] TBOB after four hours incubation in human plasma.

Figure 3.15 was created by collecting the HPLC effluent following an injection of an ethyl acetate extract of one of the plasma samples. The effluent was collected by an auto-collector such that 50 samples were collected over the 12 minute run. The effluent samples were assayed for radioactivity in a γ-well counter. The activity observed for each fraction was then plotted versus the fraction number to arrive at Figure 3.15. A previously injected, non-radioactive **3.8** standard was found to have a retention time of 11.3 minutes (corresponding to fraction 47 of the radiochromatogram). We believe that the radioactivity appearing in fractions 41-47 (amounting to 98% of the total activity injected) is the parent molecule [^{123}I]- **3.11**. The activity observed in fractions 1-40 was expanded by a factor

of approximately 30 in the inset of Figure 3.15. It is apparent that at least two additional radioactive peaks are present. We anticipated that some of the hydrolysis product, the triol ester **3.21**, might be observed in the plasma extract.

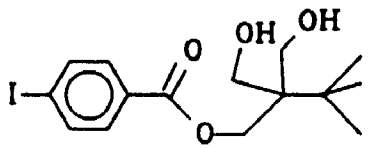

3.21

Authentic **3.21** was prepared from 4-iodobenzoyl chloride and the triol **3.4** and subjected to HPLC analysis. Under the same HPLC conditions, the triol ester **3.21** eluted at 6.8 minutes (corresponding to fraction 28 in the radiochromatogram). We believe the activity in fractions 22-28 of the radiochromatogram (amounting to 2% of the total activity injected) is due to the hydrolysis product [^{123}I]-**3.21**. Authentic 4-iodobenzoic acid was not retained by the solvent system employed in our investigation. An unretained peak eluted at 2.5 minutes under the same conditions (corresponding to fractions 10 and 11). We believe that the radioactivity appearing in fractions 9-13 (amounting to 0.1% of the total activity injected) is due to [^{123}I]-4-iodobenzoic acid but it may be due to free iodide or some other unidentified species. We did not pursue the identity of this compound. We believe these experiments show that, over the time course of our biodistribution experiments, the parent compound did not undergo significant hydrolysis in the plasma.

A sample of urine was collected in an early biodistribution study and was analyzed for radioactivity. We were surprised to find over 40% of the injected dose in a very small volume (ca. 100 μl) of urine. Clearly the drug or its metabolites were being excreted via the kidney. This was a surprising result since very lipophilic molecules are usually cleared via the hepatobiliary system (liver, gall bladder then intestine). This result is, however, consistent with the high levels of radioactivity observed in the kidneys at the earliest time point. We turned our attention to the identification of the radioactive compounds in the urine. A new experiment was performed in which mice were injected with 4'[123-I]-TBOB **3.11** and kept in metabolism cages so that urine could be collected. The urine was pooled at various time points and subjected to HPLC analysis in order to determine the retention time of the radioactive fraction (Figure 3.16).

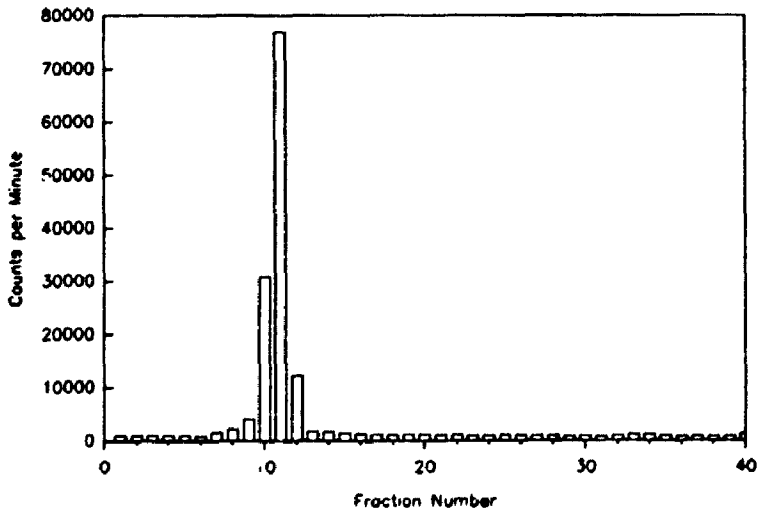

Figure 3.16. HPLC radiochromatogram of 4'[123-I] TBOB isolated from mouse urine at one hour post-injection.

Figure 3.16 was constructed in a manner exactly analogous to that of Figure 3.15. The retention time of the parent compound eluted with an 80% methanol to 20% water solvent system on a 25-cm C-18 reversed-phase column was 11.3 minutes. This retention time corresponds to fraction 37 of the radiochromatogram. Since there is no mechanism for the clearance of lipophilic molecules via the kidney we did not expect to observe parent molecule **3.11** in the urine. There appears to be some activity in fractions 35-37 but this activity represents only 0.2% of the total. This activity may result from contamination of the HPLC injector port. We did expect to find the more water soluble hydrolysis product **3.21** in the urine. This assumption also proved to be incorrect.

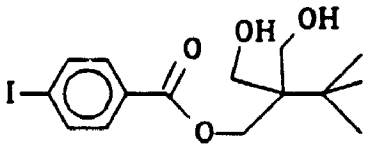

3.21

Under the same HPLC conditions the triol ester **3.21** elutes at 6.8 minutes corresponding to fraction 20 in the radiochromatogram. Figure 3.16 shows that, as early as one hour post-injection, very little, if any, triol ester was being excreted. Unfortunately, the HPLC conditions used in the experiment were not suitable for the identification of the radioactive metabolites eluting in fractions 6-14. An unretained peak eluted at 2.4 minutes under these conditions (corresponding to fraction number 8 in the radiochromatogram).

Figure 3.16 shows that the radioactive fraction (amounting to 85% of the total activity injected) was not retained under these conditions. We were unable to identify the metabolites found in the urine but a recent publication[53] may shed some light. Tritiated TBOB **3.19** was administered to rats via stomach tube and the urine and faeces were examined for the presence of metabolites. The authors were able to tentatively identify benzoic acid and hippuric acid as metabolites by comparing the R_f's of authentic samples to the R_f's of the radioactive metabolites. The administration route used in this experiment is indeed questionable since the authors point out that the half-life for hydrolysis of TBOB is on the order of minutes at pH 2-3. It is not clear why the authors chose this administration route except to perhaps explain the lack of oral toxicity observed for this class of compounds. Though not directly transferrable to our study, the metabolism data for 4'-[^{3}H]-TBOB suggests that the polar metabolites may be 4-iodobenzoic acid or 4-iodohippuric acid.

3.19 Specific Activity Determination

A limited number of receptor sites are available to bind the radioactive ligand. It was therefore necessary to determine the specific activity of a typical radioligand preparation. A standard solution of [127-I] **3.8** was prepared and aliquots were subjected to HPLC analysis. The area counts observed for a number of different amounts of [127-I] **3.8** were

obtained and related back to the original concentration of the standard solution in order to construct a standard curve (Figure 3.17).

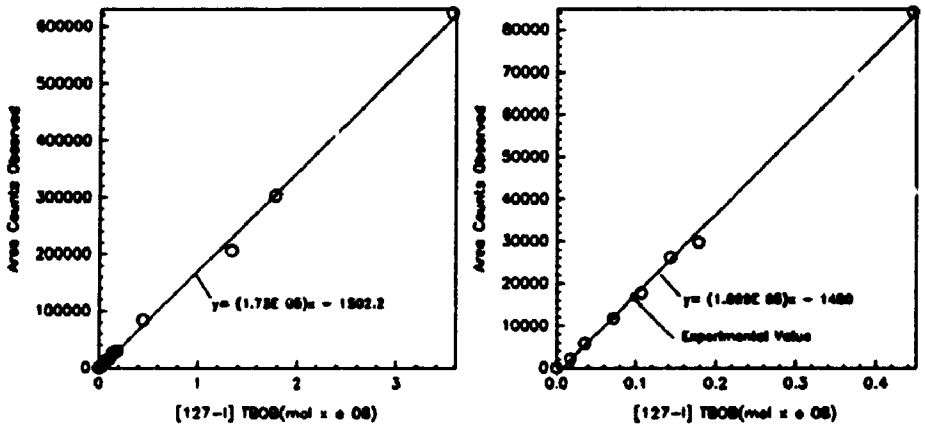

Figure 3.17. Standard Curve for 4' [127-I] TBOB

The standard curve displays excellent linearity throughout the range of concentrations tested. The number of area counts observed for a preparation of ^{123}I-3.20 was 16816 corresponding to 1 ρmol of ^{127}I-3.20. The specific activity of the preparation was calculated to be 413 Ci/mmol (S.I. 15.3 x 10^{13} Bq/mmol). The value is three orders of magnitude lower than the theoretical maximum for ^{123}I radiopharmaceuticals (2.4 x 10^{5} Ci/mmol[54], 8.9 x 10^{15} Bq/mmol) but is not out of line with values obtained by other researchers in this field[55]. The specific activities of radiopharmaceuticals differ greatly from the theoretical maximum due to the presence of significant levels of contamination from non-radioactive isotopes. Contamination may arise from a number of sources, the most serious of which is probably the injector port of the

HPLC. When we began these studies our purification procedure using HPLC employed the same column and injection ports for both the radioactive and the non-radioactive compounds. In retrospect, this is an unacceptable procedure since non-radioactive material may be carried over into the purification of the radioactive sample thereby decreasing the specific activity of the final radioactive compound. Our protocol has been changed so that two columns and two injection ports are now used; one for the radioactive preparation and one for the non-radioactive sample. It is interesting to note that these precautions have not improved the specific activity of other radiopharmaceuticals labelled with ^{123}I. It appears that the contamination may originate at the source of the ^{123}I. At present we have no method for the determination of the specific activity of commercial $Na^{123}I$ solutions. A project has been initiated with our group to study this question using ion chromatography, an extremely sensitive analytical tool. Unfortunately, ion chromatography is subject to many of the same sources of contamination that plague HPLC. It is not clear that the source of contamination can ever be identified with any confidence.

3.20 Plasma Binding

The HPLC retention of the target molecule **3.9** coupled with its low polarity (recrystallization from hexanes) led us to predict a high level of plasma binding for the molecule.

Highly lipophilic molecules tend to have a stronger affinity for plasma proteins than for the aqueous portion of plasma. The result is that highly lipophilic molecules bind tightly to plasma proteins and are unavailable for interaction with receptors on cell membranes. The extent of plasma binding of **3.9** was determined by incubating the drug with human plasma and separating the plasma proteins from the aqueous fraction by ultrafiltration at various time points. The data is compiled in Table 3.3.

Table 3.3. Protein binding data for 4'-[^{123}I]-TBOB. (* -radioactive counts observed)

Time Point	Protein Bound*	Free*	% Protein Bound
30 min	754959	14227	98.2
90 min	681441	15711	97.7
180 min	567657	13789	97.6

Table 3.3 clearly demonstrates that a very large fraction of the injected radioactivity (probably 100% within experimental error) is bound to plasma proteins immediately after injection. Experience has shown[56] that such a high level of plasma binding precludes *any* biological activity since no drug is available to interact with enzymes or receptors outside the blood.

3.21 Partition Coefficient Determination

The octanol-water partition coefficient (log P) has been shown to be an excellent measure of a compound's macroscopic behaviour *in vivo*[57]. Extremely lipophilic molecules (high log P) exhibit slow pharmacokinetics due to strong interactions

with lipids and plasma proteins. Lipophilic molecules must be eliminated from the bloodstream via the hepatobiliary system (liver, gallbladder then intestine) or must be metabolized by the liver to more water soluble derivatives. We believed that the determination of the partition coefficient for **3.8** might shed some light on the *in vivo* behaviour of the compound. Two approaches were used. In a more typical protocol ^{123}I-labelled **3.8** was partitioned between pH 7.4 phosphate buffer and freshly distilled n-octanol. An aliquot of each layer was counted for radioactivity and the partition coefficient was calculated in the usual way. The value obtained in this manner was 2.19 ±0.03. The process of determining log P values is often complicated by large systematic errors. We believed the log P value of 2.19 for **3.8** was too low given the long HPLC retention time and the high plasma binding observed. A method for the determination of log P values via HPLC chromatography has appeared[58] which has the advantage of comparing the retention time of a compound with an unknown log P on a reversed-phase column to the retention times of a series of compounds with known log P's in order to arrive at the log P of the test compound*. The HPLC experiment was performed and the results are shown graphically in Figure 3.18.

---

*The method was discussed previously in chapter 2.13.

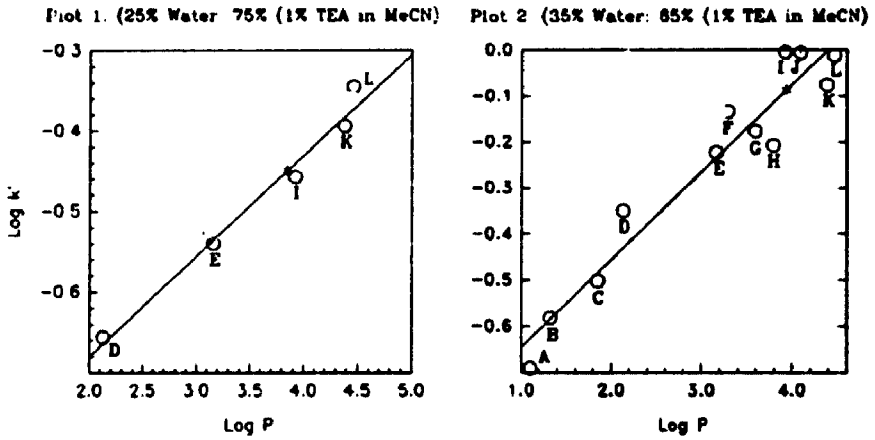

Figure 3.18. Plots for Log P Determination.

As discussed in chapter 2.13, our results show substantial scatter about the line of best fit; a result that was not observed by McCall in his original publication. Our results indicate that the commercial columns may not be sufficiently silylated to give reliable log P values. The results of our experiment are given in Table 3.4 and 3.5.

Table 3.4. Retention data for plot one of Figure 3.18.
Solvent system: 25% H_2O:75% (1% triethylamine in acetonitrile).

Compound	Label	k'	log k'	log P^{59}	log K	K_N
Benzene	D	0.221	-0.656	2.13	2.78	1
Toluene	E	0.288	-0.540	3.16	3.70	1.33
Acenapthene	I	0.349	-0.457	3.92	4.38	1.58
Fluorene	K	0.404	-0.394	4.38	4.77	1.72
Phenanthrene	L	0.452	-0.345	4.46	4.80	1.73
3.9	*	0.356	-0.449	3.85*		

Table 3.5. Retention data for plot two of Figure 3.18. Solvent system: 35% H_2O:65% (1% triethylamine in acetonitrile).

Compound	Label	k'	log k'	log P^{oct}	log K	K_N
benzyl alcohol	A	0.204	-0.690	1.10	1.79	0.72
o-toluidine	B	0.262	-0.582	1.32	1.90	0.77
nitrobenzene	C	0.315	-0.502	1.85	2.35	0.95
benzene	D	0.447	-0.350	2.13	2.48	1.00
toluene	E	0.598	-0.223	3.16	3.38	1.36
iodobenzene	F	0.734	-0.134	3.29	3.42	1.38
naphthalene	G	0.666	-0.177	3.59	3.76	1.52
chlorobenzene	H	0.619	-0.208	3.79	4.00	1.61
acenapthene	I	0.987	-0.005	3.92	3.93	1.58
biphenyl	J	0.986	-0.006	4.09	4.10	1.65
fluorene	K	0.840	-0.076	4.38	4.46	1.80
phenanthrene	L	0.973	-0.012	4.46	4.47	1.80
4'-I-TBOB	*	0.818	-.087	3.93*		

Table 3.6. Linear regression values for plot one and two in Figure 3.18.

Plot	a	b	r	σ(log P)
1	-0.9297	0.1250	0.9895	0.872
2	-0.8347	0.1902	0.9647	1.139

The log P value for **3.8** calculated from the HPLC experiment was 3.89 ±1.14. This value is much larger than the value of 2.19 ±0.03 found using a liquid-liquid partitioning experiment. The high plasma binding observed for **3.8** argues in favour of the higher of the two log P values. The method of Hansch (see appendix I) was used to estimate a log P value of 4.30 for compound **3.8** providing additional evidence to support a higher value for the log P of **3.8**. Despite the large uncertainty in the value for the log P of **3.8** we believe

that the high plasma binding and hence the very low uptake of the radioactive molecule by the brain can be rationalized in terms of the molecule's high lipophilicity.

3.22 Summary

It is appropriate at this point to return to the original criteria and examine which of these we have accomplished and which criteria have not been met. We can state with confidence that the target molecule **3.8** is a high affinity ligand which can be labelled at high specific activity relatively easily. Unfortunately, in all other aspects this project has failed. The target molecule **3.8** is unacceptably lipophilic for use as an *in vivo* receptor probe. The molecule binds too tightly to plasma proteins and thus, cannot leave the bloodstream and cross the blood-brain-barrier. Further, the cage convulsants seem to undergo rapid metabolism *in vivo* resulting in extremely short plasma half-lives. It is not at all clear that a solution exists to these problems save the abandoning of this entire group of compounds as potential non-competitive $GABA_A$ antagonists suitable for use as radioligands for SPECT.

3.23 Experimental:

Diethylisopropylidene Malonate 3.1

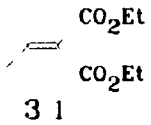

3.1

Diethylisopropylidene malonate **3.1** was prepared according to the procedure of Knoeber *et al*[61]. Diethyl malonate (BDH, 49.2 g, 0.31 mol), acetone (BDH, 26.6 g, 0.46 mol), acetic anhydride (BDH, 39.4 g, 0.39 mol) and anhydrous zinc chloride (BDH, 6.0 g, 0.046 mol) were brought to reflux under an argon atmosphere for 24 hours. The resulting dark solution was diluted with benzene (50 mL) and washed with water (2 x 50 mL). The combined aqueous layers were washed with benzene (2 x 50 mL). The combined organic layers were dried (Na_2SO_4) and the benzene was removed *in vacuo*. The residue was distilled through a 20-cm Vigreux column to yield diethylisopropylidene malonate **3.1** (41.2 g, 0.21 mol, 66%) b.p. 75-80 °C.(0.1 mm Hg) lit.[47]110-115°C (9-10 mm Hg). HMR: $\delta(CDCl_3)$ 4.11 (q, 4H, CH_2CH_3), 1.94 (s, 6H, $C(CH_3)_2$), 1.17 (t, 6H, $-CH_2CH_3$). IR: (CH_2Cl_2) 2965 (C-H), 1705 (C=O), 1628 (C=O) cm^{-1}.

Diethyl-t-butylmalonate 3.2

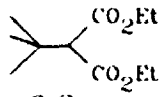

3.2

Diethyl *t*-butylmalonate **3.2** was also prepared according to the method of Knoeber *et al*[61]. Methyl magnesium iodide was prepared in the usual manner from magnesium turnings (Aldrich, 18.3 g, 0.75 mol) and methyl iodide (Fisher, 113.5 g, 0.80 mol) in freshly distilled diethyl ether (150 mL). The solution was cooled to 0°C in an ice-salt bath and copper(I) chloride (BDH, 1.0 g, 0.010 mol) was added. Diethylisopopylidene malonate **3.1** (100.0 g, 0.50 mol) dissolved in anhydrous diethyl ether (100 mL) were then added dropwise over 80-90 minutes at such a rate that the temperature did not rise above 0°C. On complete addition, the ice-bath was removed and stirring was continued for 30 minutes. The mixture was then poured onto a mixture of crushed ice (ca. 500-1000 g) and aqueous H_2SO_4 (10%, 400 mL). The ether layer was separated and the aqueous layer extracted with diethyl ether (3 X 200 mL). The combined ether extracts were washed with saturated sodium thiosulfate solution (100 mL), then dried with Na_2SO_4 and taken to dryness *in vacuo*. The residue was distilled to yield diethyl *t*-butyl malonate **3.2** (96.4 g, 0.45 mol, 89%) bp.45-55°C (0.1 mm Hg) lit.[61] 60-61°C (0.7 mm Hg). HMR: $\delta(CDCl_3)$ 4.18 (q, 4H, $-CH_2CH_3$), 3.22 (s, 1H, CH), 1.27 (t, 6H, $-CH_2CH3$), 1.13 (s, 9H, $-C(CH_3)_3$). IR: (CH_2Cl_2)

2965 (C-H), 1745 (C=O), 1718 (C=O) cm^{-1}.

Diethyl t-butylhydroxymethylmalonate 3.3

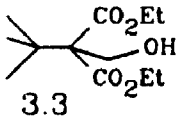

3.3

Diethyl *t*-butylhydroxymethylmalonate **3.3** was synthesized by the method of Ozoe and Eto[62]. Sodium hydroxide (BDH, 2.0 g, 0.05 mol) was ground in dry DMSO (20 mL) and added to a mixture of paraformaldehyde (12.8 g, 0.43 mol) and diethyl *t*-butylmalonate **3.2** (15.3 g, 0.071 mol) dissolved in dry DMSO (15 mL) and the mixture was stirred overnight. The mixture was then diluted with water (200 mL) and then extracted with chloroform (8 X 50 mL). The combined chloroform extracts were washed with water (3 X 50 mL) to remove the remaining DMSO. The combined chloroform layers were dried with Na_2SO_4 and taken to dryness *in vacuo*. The residue was distilled through a 20-cm Vigreux column to yield diethyl *t*-butylhydroxymethyl-malonate **2.2**, (10.1 g, 0.041 mol, 58%; b.p.80-90°C (0.4 mm Hg); lit.[62] 120-125°C (10 mm Hg). HMR: $\delta(CDCl_3)$ 4.25 (q, 4H, $-CH_2CH_3$), 4.04 (s, 2H, $-CH_2OH$), 3.50 (bs, 1H, $-CH_2OH$), 1.32 (t, 6H, $-CH_2CH_3$), 1.14 (s, 9H, $-C(CH_3)_3$). IR: (CH_2Cl_2) 3065 (C-H), 2980 (C-H), 1725 (C=O), 1708 (C=O) cm^{-1}, along with (1 g, 0.03 mol, 8%) of the starting material **3.2**.

2-t-Butyl-2-hydroxymethyl-1,3-propanediol 3.4

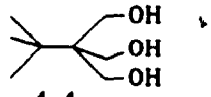

4.4

2-t-Butyl-2-hydroxymethyl-1,3-propanediol 3.4 was also made according to the method of Ozoe and Eto[62]. Diethyl *t*-butylhydroxymalonate (10.0 g, 0.06 mol) was dissolved in absolute diethyl ether (50 mL) and added dropwise to a stirred suspension of $LiAlH_4$ (BDH, 4.4 g, 0.12 mmol) in diethyl ether (100 mL). The mixture was allowed to stir in an argon atmosphere for four days at which time the excess $LiAlH_4$ was destroyed by the dropwise addition of a solution of potassium hydroxide (BDH, 19.0 g, 0.34 mol) in water (500 mL). A solution of potassium phosphate (BDH, dibasic, 14.0 g, 0.08 mol) and potassium phosphate (BDH, monobasic, 11.0 g, 0.08 mol) in water (50 mL) was then added and the mixture heated to 50°C to remove the remaining ether. The resulting slurry was neutralized with acetic acid, filtered and the filtrate taken to dryness *in vacuo* The resulting solid was extracted with acetone in a Soxhlet extractor for 3-4 hours. The acetone was then removed under vacuum to yield a viscous oil which solidified on standing. The solid was recrystallized from dichloromethane/ 60-80°C pet. ethers to yield 2-t-butyl-2-hydroxymethyl-1,3-propanediol 3.4 (4.2 g, 0.026 mol, 43%), m.p. 197-204°C, lit. 204-207°C[39]. HMR: $\delta(CDCl_3)$ 4.02 (bs, 3H, -OH), 3.87 (s, 6H, $-CH_2-$), 0.90 (s, 9H, $-C(CH_3)_3$). IR: (CH_2Cl_2)

3500 (C-H), 2965 (C-H), 2880 (C-H), 1040 (C-O) cm^{-1}.

3-t-Butyl-3-hydroxymethyl oxetane 3.5

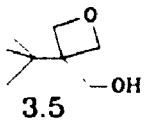

3.5

Following the procedure of Pattison[63], a solution of 2-t-butyl-2-hydroxymethyl-1,3-propanediol 3.5 (4.62 g, 0.029 mol) was prepared in diethyl carbonate (Aldrich, 3.04 g, 0.029 mol). A solution of potassium hydroxide in ethanol (150 μL, 40 μmol) was then added. The mixture was brought to reflux for one hour at which time the pressure was reduced and the residual ethanol distilled off. The temperature of the oil bath was increased until the evolution of CO_2 ceased. The solid residue was then sublimed to yield 3-t-butyl, 3-hydroxymethyl oxetane 4.5 (3.34 g, 0.023 mol, 80%), m.p. 171-174°C. lit.[39] 163-165°C. HMR: $\delta(CDCl_3)$ 4.38 (dd, 4H, J_{gem}=8.4 Hz, $J_{1,3}$=5.2 Hz, $-CH_2-O-CH_2-$), 3.82 (s, 2H, $-CH_2OH$), 0.99 (s, 9H, $-(CH_3)_3$). IR: (CH_2Cl_2) 3610 (O-H), 2950 (C-H), 2885 (C-H), 1135 (C-O) cm^{-1}.

3-t-Butyl-3-hydroxymethyl oxetane, 4'-iodobenzoate 3.6

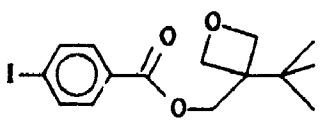

3.6

To triethylamine (BDH, 330 μL, 2.20 mmol) and 3-t-butyl-3-

hydroxymethyl oxetane **4.5** (172 mg, 1.15 mmol) in dry dichloromethane (5 mL) was added a solution of 4-iodobenzoyl chloride (Aldrich, 320 mg, 1.19 mmol) in dry dichloromethane (5 mL). The mixture was allowed to react for one hour at which time the dichloromethane solution was washed with water (2 X 2 mL). The dichloromethane layers were combined and dried with Na_2SO_4 and the dichloromethane removed *in vacuo*. The solid residue was recrystallized from hexanes to yield 3-*t*-butyl-3-hydroxymethyl oxetane 4'-iodobenzoate **4.6** (423 mg, 1.13 mmol, 96%), m.p. 94-96°C. HMR: $\delta(CDCl_3)$ 7.83 (s, 4H, H_{arom}), 4.61 (d, 4H, J_{gem}=0.57 Hz, $-CH_2O-CH_2$), 1.06 (s, 9H, $-(CH_3)_3$). IR: (CH_2Cl_2) 2970 (C-H), 2900 (C-H), 1725 (C=O), 1590 (C=C), 1485 (C=C), 1270 (C-O) cm^{-1}. HRMS: m/e calculated for $C_{15}H_{19}O_3I$: 374.0379 found: 374.0380.

3-t-Butyl-3-hydroxymethyl oxetane 4'-bromobenzoate **3.6**

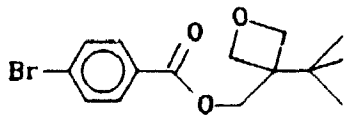

3.7

The corresponding 3-t-Butyl-3-hydroxymethyl oxetane 4'-bromobenzoate **3.7** was synthesized in the same manner as the iodinated analogue **3.6** from 4-bromobenzoyl chloride in 92% yield. The product was recrystallized from hexanes m.p. 60-61°C. HMR: $\delta(CDCl_3)$ 7.79 (dd, 4H, J_o=37 Hz, J_m=8.6 Hz, H_{arom}), 4.61 (s, 4H, $-OCH_2-$), 4.45 (s, 2H, $-OCH_2O$), 1.06 (s, 9H, $-(CH_3)_3$). IR: (CH_2Cl_2) 2960 (C-H), 2890 (C-H), 1715 (C=O), 1590

(C=C), 1205 (C-O) cm^{-1}.

4-t-butyl-1-(4'-iodophenyl)-2,6,7-trioxabicyclo [2.2.2] octane **3.8**

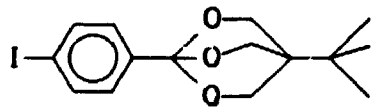

3.8

A solution of 2-*t*-butyl,2-hydroxymethyl oxetane, 4'-iodobenzoate **3.6** (100 mg, 0.267 mmol) was prepared in dry dichloromethane (2 mL) in a round-bottomed flask flushed with argon. The mixture was cooled in a dry-ice acetone bath and boron trifluoride etherate (10 μL, 0.08 μmol) was added via syringe. The mixture was monitored by TLC as it was slowly allowed to warm to room temperature. On complete consumption of starting materials the reaction was quenched with dry triethylamine (100 μL, 0.72 mmol). The mixture was washed with water, the combined dichloromethane layers dried with Na_2SO_4 and taken to dryness *in vacuo*. The resulting solid could be recrystallized from hexanes to yield 4-*t*-butyl-1-(4-iodophenyl)-2,6,7-trioxabicyclo[2.2.2] octane **3.8**, (53 mg, 0.14 mmol, 53%) m.p. 196-198°C; lit.[64] 202-204°C. HMR: $\delta(CDCl_3)$ 7.51, (dd, 4H, J_o=39.1 Hz, J_m=8.6 Hz H_{arom}), 4.17, (s, 6H, $-CH_2O-$), 0.91 (s, 9H, $-(CH_3)_3$). IR: (CH_2Cl_2) 2950 (C-H), 2885 (C-H), 1342 (C=C), 1120 (C-O), 1070 (C-O) cm^{-1}. HRMS: m/e calculated for $C_{15}H_{19}O_3I$: 374.0379 found: 374.0384.

4-t-Butyl-1-(4'-bromophenyl)-2,6,7-trioxabicyclo [2.2.2] octane 3.9

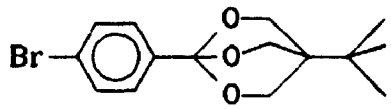

3.9

The corresponding bromo compound 3.9 was synthesized in the same manner as 3.8 from 2-*t*-butyl,2-hydroxymethyl oxetane, 4'-bromobenzoate 3.7 in 60% yield. Crystals were obtained from hexanes m.p. 170-174°C, lit[65] 176-178°C. HMR: $\delta(CDCl_3)$ 7.47, (s, 4H, H_{arom}), 4.17, (s, 6H, $-CH_2-$), 0.91 (s, 9H, $-(CH_3)_3$).

4-t-Butyl-1-(4'-trimethylstannylphenyl)-2,6,7-trioxabicyclo [2.2.2] octane 3.10

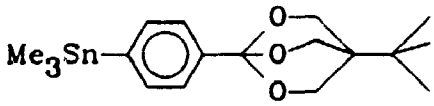

3.10

A solution of 4-*t*-butyl-1-(4-bromophenyl)-2,6,7-trioxabicyclo[2.2.2] octane (70 mg, 0.21 mmol) was prepared in freshly distilled THF (2 mL) in a flame-dried vial flushed with dry. The solution was cooled for 10 minutes in a dry-ice acetone bath at which time n-butyllithium (Aldrich, 2.5M, 150 μl, 1.8 eq) were added via syringe. The metallation reaction was allowed to proceed for 30 minutes at which point trimethyltin chloride (Aldrich, 80 mg, 0.40 mmol) dissolved in dry THF (500 μl) were added via syringe. The cold bath was then removed and the mixture was allowed to warm slowly to

room temperature and then stirred overnight. The solvent was then removed *in vacuo* and the residue was recrystallized from hexanes to yield 4-*t*-butyl-1-(4-trimethylstannylphenyl)-2,6,7-trioxabicyclo[2.2.2] octane **3.10** (84.4 mg, 0.21 mmol, 96%), m.p. 137-142°C. HMR: δ(CDCl3) 7.44 (dd, 4H, H_{arom}), 4.17, (s, 6H, $-CH_2O-$), 0.90 (s, 9H, $-(CH_3)_3$), 0.25 (s, 9H, SnMe3). IR: (CH_2Cl_2) 2970 (C-H), 2900 (C-H), 1340 (C=C), 1130 (C-O), 1060 (C-O) cm^{-1}. HRMS. m/e calculated for $C_{18}H_{28}O_3Sn$: 412.1060 found: 412.1061.

3.24 Radiolabelling

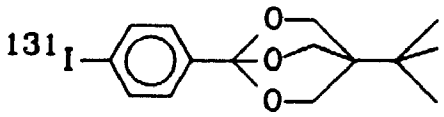

3.11

N-chlorosuccinimide (500 μg, 3.74 μmol) and 4-*t*-butyl-1-(4-trimethylstannylphenyl)-2,6,7-trioxabicyclo[2.2.2] octane **3.10** (300 μg, 0.73 μmol) were dissolved in freshly distilled chloroform (500 μL) and placed in a stoppered test-tube equipped with a 5 mm magnetic stirring flea. No-carrier-added $Na^{131}I$ solution (chemical grade, Frosst, 10 μL, 14 Mbq) was added via syringe and the mixture vigorously stirred for one hour. The reaction was quenched by addition of saturated sodium bisulphate solution (500 μL). The chloroform layer was drawn off by Pasteur pipette and the remaining aqueous solution was extracted with two additional 500 μL portions of chloroform. The combined chloroform layers were evaporated in

a stream of argon and redissolved for HPLC injection in 100 μL of methanol. The crude radioactive material was injected on to a LC-RP 18 column (Supelco) and eluted with an isocratic 1:4 mixture of water in methanol. A previously injected cold standard eluted at 8.9 minutes and the radioactive peak eluting at this time was collected. The fraction was found to contain 4-*t*-butyl-1-(4-[^{131}I]iodophenyl)-2,6,7-trioxabicyclo[2.2.2] octane **3.8** (12.3 Mbq, 88% radiochemical yield). 4-*t*-butyl-1-(4-[^{123}I]iodophenyl)-2,6,7-trioxabicyclo[2.2.2] octane **3.8** was prepared in an exactly analogous fashion starting with 46 MBq Na^{123}I (Nordion). After removal of the chloroform layers in a stream of Argon there remained 31 MBq of ^{123}I activity. The residue was dissolved in 100 μL of HPLC grade methanol and chromatographed to yield 22 MBq of activity at the correct retention time for the desired product. The overall radiochemical yield was 49%.

3.25 Determination of Partition Coefficient

Phosphate buffered saline (pH 7.4, 1 mL) and freshly distilled n-octanol (BDH, 1 mL) were placed in each of ten 15 mL plastic centrifuge tubes (Becton-Dickinson). (0.037 Mbq, 10 μL) 4-*t*-butyl-1-(4-[^{131}I]iodophenyl)-2,6,7-trioxabicyclo[2.2.2] octane **3.11** dissolved in n-butanol were then added, the tubes capped, and placed in a rotating mixer for one hour. The tubes were then centrifuged for one minute at 500 R.P.M. to obtain good separation of the layers. An

aliquot taken from each layer was weighed and then assayed for radioactivity in a well counter.

3.26 Biological Studies

Approximately 0.037 MBq of no-carrier-added [^{131}I] **3.9** dissolved in salt-balanced saline solution (pH 7.4) were injected via tail vein into female CD1 mice. Three mice per time point were sacrificed by cervical dislocation, dissected, and the organs of interest were assayed for radioactivity in a well-counter.

Table 3.7 Uptake of [^{131}I]-labelled **3.8** in female CD1 Mice. Uptake shown is % injected dose per gram except thyroid which is % injected dose.

	Time				
Organ	5 min	15 min	30 min	1 hr	2 hrs
Blood	12.9±3.4	1.7±0.8	1.1±0.4	0.2±0.0	0.1±0.0
Heart	4.4±1.0	0.6±0.3	0.4±0.1	0.1±0.0	0.1±0.0
Lung	6.5±1.4	1.1±0.5	0.8±0.3	0.1±0.0	0.1±0.0
Liver	11.2±1.8	1.3±0.5	0.9±0.4	0.3±0.1	0.2±0.2
Stomach	1.4±0.4	1.5±0.5	1.4±0.4	0.4±0.1	0.4±0.3
Intestine	2.5±0.6	1.0±0.4	1.3±0.3	0.8±0.1	0.3±0.1
Kidneys	33.7±9.0	2.9±1.3	1.8±1.1	0.2±0.0	0.4±0.5
Fat	3.2±0.5	2.3±2.6	2.1±1.2	0.0±0.2	0.2±0.1
Muscle	2.0±0.2	0.3±0.2	0.4±0.1	0.1±0.0	0.1±0.0
Brain	1.0±0.3	0.2±0.1	0.2±0.0	0.0±0.0	0.0±0.0
Thyroid	.42±0.0	0.2±0.1	0.2±0.1	0.1±0.0	0.0±0.0

3.27 References

1.Awapara, J., Landura, A.J., Fuerst, R., Seale, B., *J. Biol. Chem.*, **1950**, *187*, 35-39.

2.Roberts, E., Frankel, S., *J. Biol. Chem.*, **1950**, *187*, 55-64.

3.Udenfriend, S., *J. Biol. Chem.*, **1950**, *187*, 65-69.

4.Hayashi, T., Suhara, R., *20th Int. Physiol. Congr. Brussels, Abstracts of Reviews: Abstracts of Communications*, **1956**.

5.Enna, S.J., Karlsen, E.W., *GABA Receptors, An Overview;* in Olsen, R.W., Venter, J.C. (eds), *Benzodiazepine/GABA Receptors and Chloride Ion Channels*, **1986**, Alan R. Liss Inc., New York.

6.Taylor, P., Insel, P.A., *Molecular Basis of Pharmacological Selectivity*, in Pratt, W.B., Taylor, P., *Principles of Drug Action*, 3rd Edition, **1990**, Churchill Livingstone, New York.

7. Clark, A.J., *J. Physiol.* **1926**, *61*, **530**.

8.Scatchard, G.A.C., *Ann. N.Y.. Acad. Sci.*, **1949**, *51*, **660**.

9.Jensen, E.V., and Jacobsen, H.I., *Recent. Prog. Horm. Res.*, **1962**, *18*, **387**.

10.Hill, A.W., *J. Physiol.*, **1910**, *iv*, **40**.

11.Giambalvo, C.T., Rosenberg, P., *Biochim. Biophys. Acta.*, **1976**, *436*, **741-756**.

12.Roberts, E., in Olsen, R.W., Venter, J.C. (eds), *Benzodiazepine/GABA Receptors and Chloride Ion Channels*, **1986**, Alan R. Liss Inc., New York, p. 17.

13.Elliott, K.A.C., Florey, E., *J. Neurochem.*, **1956**, *1*, **181-191**.

14.Fischer, J.B., Olsen, R.W., *Biochemical Aspects of GABA/Benzodiazepine Receptor Function*, in Olsen, R.W., Venter, J.C., (eds), *Benzodiazepine/GABA Receptors and Chloride Channels*, Alan R. Liss, Inc. New York, **1986**.

15.Onda, M., Fukushima, H., Akagawa, M., *Chem. Pharm. Bull.*, **1964**, *12*, **751**.

16.Windholz, M., (ed) *The Merck Index, Ninth Ed.*, **1976**, Merck and Co. Inc., Rahway N.J., **1976**, p. *818*.

17.Wang, Y.J., Salvaterra, P., Roberts, E., *Biochem. Pharmac.*, 1979, *28*, 1123-1128.

18.Manske, R.H.F., *Can. J. Res.*, 1932, *7*, 265.

19.Manske, R.H.F., *Can. J. Res.*, 1933, *8*, 142.

20.Curtis, D.R., Duggan, A.W., Felix, D., Johnston, G.A.R., *Nature*, 1970, *226*, 1222.

21.Olsen, R.W., Ban,M., Miller, T., Johnston, G.A.R., *Brain Res.*, 1975, *98*, 383-387.

22.Mohler, H., Okada, T., *Mol. Pharmac.*, 1978, *14*, 256-265.

23.Enna, S.J., Snyder, S.H., *Brain Res.*, 1975, *100*, 81-97.

24.Hill, D.R., Bowery, N.G., *Nature*, 1981, *290*, 149-152.

25.Porter, L.A., *Chem. Rev.*, 1967, *67*, 441-464.

26.Van der Kloot, W.G., Robbins, J., Cooke, I.M., *Science*, 1958, *127*, 521.

27.Barth, L., Kretschy, M., *Monatsh.*, 1881, *1*, 99; 1881, *2*, 796; 1884, *5*, 65.

28.Olsen, R.W., Ticku, M.K., Van Ness, P.C., Greenlee, D., *Brain Res.*, 1978, *139*, 277-294.

29.Ticku, M.K., Olsen, R.W., *Neuropharmacology*, 1979, *18*, 315-318.

30.Casida, J.E.; Bellet, E.M.; *Science*, 1973, *182*, 1135.

31.Eto, M.; Ozoe, Y.; Fujita, T.; Casida, J.E.; *Agric. Biol. Chem.* 1976, *40*, 2113-2115.

32.Bowery, N.G.; Collins, J.F.; Hill, R.G.; *Nature*, 1976, *261*, 601-603.

33.Mattsson, H.; Brandt, K.; Heilbronn, E.; *Nature*, 1977, *268*, 52-53.

34.Ticku, M.J., *Convulsant Binding Sites on the Benzodiazepine/GABA Receptor*, in Olsen, R.W., Venter, J.C., (eds), *Benzodiazepine/GABA Receptors and Chloride Channels*, 1986, Alan R. Liss Inc., p. 195-207.

35.Milbrath, D.S.; Eto, M.; Casida, J.E.; *Toxicology and Applied Pharmacology*, 1978, *46*, 411-420.

36.Voronkov, M.; Platonova, A.; Kuznetsov, I.; Shevtchenko, S.; Maierova, E.; Suslova, S.; Emelianov, I.; Diakov, V.; *Latv. PSR Zinat. Akad. Vestis Kim. Ser. Riga*, **1977**, *2*, **204-208.**

37.Casida, J.E.; Eto, M.; Moscioni, A.D.; Eugel, J.L.; Milbrath, D.S.; Verkade, J.G.; *Toxicology and Applied Pharmacology*, **1976**, *36*, **261-279.**

38.Milbrath, D.S.; Engel, J.L.; Verkade, J.G.; Casida, J.E.; *Toxicology and Applied Pharmacology*, **1979**, *47*, 287-293.

39.Casida, J.E.; Palmer, C.J.; Cole, L.M.; *Molecular Pharmacology* **1985**, *28*, **246-253.**

40.Lawrence, L.J.; Palmer, C.J.; Gee, K.W.; Wang, X., Yamamura, H.I.; Casida, J.E.; *J. Neurochem.*, **1985**, *45*, **798-804.**

41.Mitchell, A.C.G., Juliano, J.O., Creager, C.B., Kocher, C.W., *Phys. Rev.*, **1959**, *113*, **628-633.**

42.Casida, J.E., personal communication.

43.Chugani, H.T., Olsen, R.W., Benzodiazepine/GABA Receptor Binding In Vitro and In Vivo in Analysis of Clinical Disorders, in Olsen, R.W., Venter, J.C., *Benzodiazepine/GABA Receptors and Chloride Channels*, **1986**, Alan R. Liss, Inc., New York, p. **315-335.**

44.Muhr, C., Bergstrom, M., Lundberg, P.O., Bergstrom, K., Hertsig, P., Lundquist, H., Antoni, G., Langstom, B., *J. Comput. Assist. Tomogr.*, **1986**, *10*, **175.** Hagglund, J., Aquilonius, S.-M., Eckernas, S.-A., Hartzig, P., Lundquist, H., Gullberg, P., Langstom, B., *Acta. Neurol. Scand.*, **1987**, *75*, **87.** Smith, M., Wolf, A.P., Brodie, J.D., Arnett, C.D., Barouche, F., Shino, G.-Y., Fowler, J.S., Russell, J.A.G., MacGregor, R.R., Wolken, A., Amgrist, B., Rotrosen, J., Peselow, E., *Biol. Psychiatry*, **1988**, *23*, **653.**

45.Walker, F.O., Young, A.B., Penney, J.B., Dovorini-Zis, K., Shoulson, I., *Neurology*, **1984**, *34*, **1237-1240.**

46.Kabalka, G.W., Varma, R.J., *Tetrahedron*, **1989**, *45*, **6601-6621.**

47.Corey, E.J.; Raju, N.; *Tetrahedron Letters*, **1983**, *24*, 5571-5574.

48.Eaborn, C.; Hornfeld, H.L.; Walton, D.R.M.; *J. Organomet. Chem.*, **1967**, *10*, **529-30.**

49.Pattison, D.B.; *J. Am. Chem. Soc.*, **1983, 79, 3455.**

50.Cooper, G.H.; Lawston, I. W.; Rickard, R.L.; Inch, T.D.; *Eur. J. Med. Chem. Chim. Ther.*, **1978, 13, 207-212.**

51.Chan, S.M.C., *HBSc Thesis*, **1989**, Department of Chemistry, University of Western Ontario.

52.Ozoe, Y., Eto, M., *Agric. Biol. Chem.*, **1982, 46, 411-418.**

53.Scott, J.G., Palmer, C.J., Casida, J.E., *Xenobiotica*, **1987, 17, 1085-1093.**

54.Wang, Y. (ed) *CRC Handbook of Radioactive Nuclides*, **1969**, The Chemical Rubber Company, Cleveland. p 47.

55.Loc'h, C., Maziere, B., *Seventh. Int. Symp. Radiopharm. Chem.*, **1988**, Gronigen, The Netherlands p. 100.
Mertens, J., Terriere, D., Bossuyt, A., Bossuyt-Piron, C., *ibid*, p. 135.

56.Wiebe, L.I., Jette, D.C., Chapman, J.D., *Nuklearmedizin*, **1984, 23, 62-67.**

57.Fujita, T., Iwasa, J., Hansch, C., *J. Amer. Chem. Soc.*, **1964, 86, 5175.**

58.McCall, J.M., *J. Med. Chem.*, **1975, 18, 549-552.**

59.L., Albert, Hansch, C., Elkins, D., *Chem. Rev.*, **1971, 71, 525-613.**

60.L., Albert, Hansch, C., Elkins, D., *Chem. Rev.*, **1971, 71, 525-613.**

61.Eliel, E.L.; Hutchins, R.O.; Knoeber, Sr. M.; *Organic Synthesis*, **1970**, *50*, 38-42.

62.Ozoe, Y. and Eto, M.; *Agric. Biol. Chem.*, **1982, 46, 411-418.**

63.Pattison, D.B.; *J. Am. Chem. Soc.* **1983, 79, 3455.**

64.Palmer, C.J.; Casida, J.E.; *J. Agric. Food Chem.*, **1989, 37, 213-216.**

65.Lawrence, L.J.; Palmer, C.J.; Gee, K.W.; Wang, X.; Yamamura, H.I.; Casida, J.E.; *Journal of Neurochemistry*, **1985, 45, 798- 804.**

Chapter 4: Radiopharmaceuticals via an Organotin Polymer

4.1 Introduction

Radiopharmaceuticals of iodine, especially those incorporating ^{123}I, continue to attract attention as radioactive probes for receptor systems in the human body. Iodine-123 has ideal characteristics for use in Single Photon Emission Computed Tomography (SPECT); its half-life and its γ-ray energy are ideal at 13.1 hours and 159 keV respectively. ^{123}I is a "pure" γ-emitter without β-decay and thus it delivers comparatively little radiation dose per Nuclear Medicine procedure.

Iodine is particularly important as a radionuclide for medical use since it can be covalently attached to organic molecules. Since a non-radioactive isotope of iodine (^{127}I) exists, potential radiopharmaceuticals bearing ^{127}I can be tested using standard chemical and biochemical techniques prior to testing the radioactive molecule.

Iodine radiopharmaceuticals are not without their drawbacks. ^{123}I is a neutron-deficient isotope and must therefore be produced in a cyclotron. Only a few centres exist in North America to produce the isotope and this coupled with the short half-life results in a need for an efficient delivery system for the isotope. Perhaps a more imposing problem faced by clinicians who wish to use ^{123}I radiopharmaceuticals in routine Nuclear Medicine is the complicated and often inconsistent chemistry associated with

the isotope. The following chapter will describe our attempts to simplify the radiochemistry of iodine radiopharmaceuticals.

The use of polymer-bound reagents in organic chemistry and biochemistry has enjoyed tremendous success for nearly half a century. Several books[1] and numerous reviews have dealt with the subject but the use of polymer-bound reagents in radiochemistry is relatively unknown[2].

We are aware of one system[3] (Scheme 4.1) in which the organomercury precursor to a radiopharmaceutical is covalently attached to a polymeric material bearing thiol functionality. Treatment of the resulting polymer with radioiodide and an oxidizing agent yields the radiopharmaceutical free of impurity. The mercury side-products which usually accompany the reaction remain bound to the polymer. An observed drawback of the system is the high absorption of the radiopharmaceutical by the lipophilic polymer particles. The result is a low overall yield of isolated radioactive material.

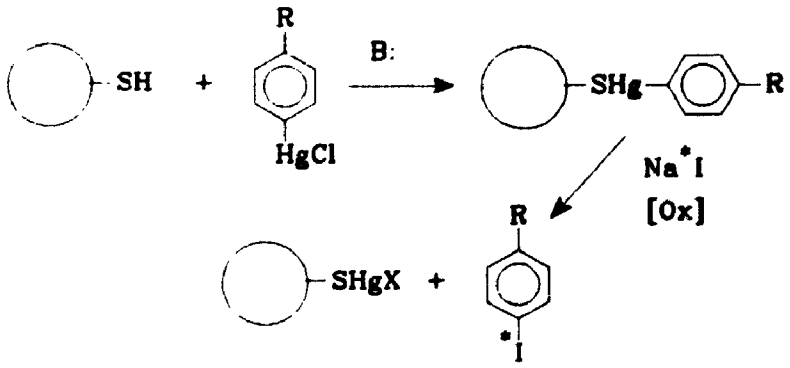

Scheme 4.1

A second approach which we have investigated uses the ionic interaction between an ion exchange resin and a diazonium salt to yield a polymeric material which, in principle, should yield radiopharmaceutical upon gentle heating with an aqueous solution of radioiodide (Scheme 4.2).

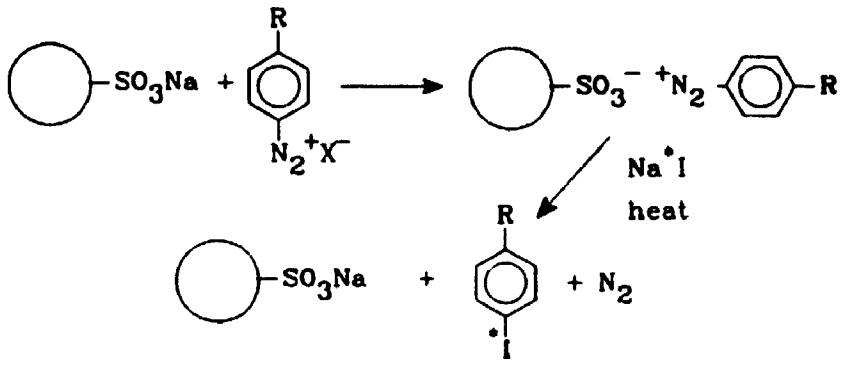

Scheme 4.2

Though this method provides acceptable yields of radiopharmaceutical, the presence of appreciable amounts of impurities necessitates purification by HPLC. The initial goal was to develop a labelling protocol which did not require HPLC purification. In this regard the method holds few advantages over traditional strategies.

4.2 A Kit Based on a Polymeric Organotin?

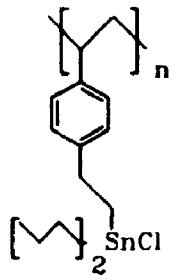

4.1

The organotin polymer **4.1** has recently been reported[4] as a precursor to a sequestered organotin hydride reducing agent. We recognized that such a polymer, if treated with the appropriate organolithium or Grignard reagent, might produce a polymer-bound precursor suitable for use in a radiopharmaceutical "kit" (Scheme 4.3).

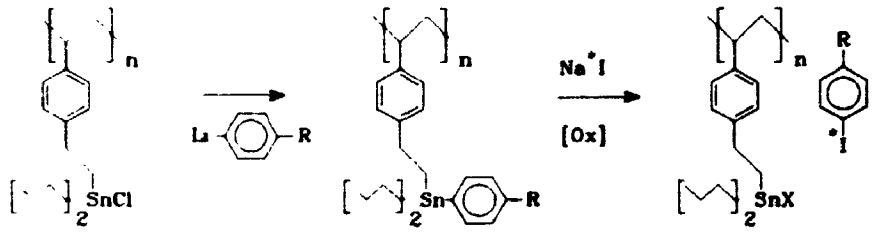

1 2

Scheme 4 3

The synthesis of the organotin polymer proved straightforward (Scheme 4.4).

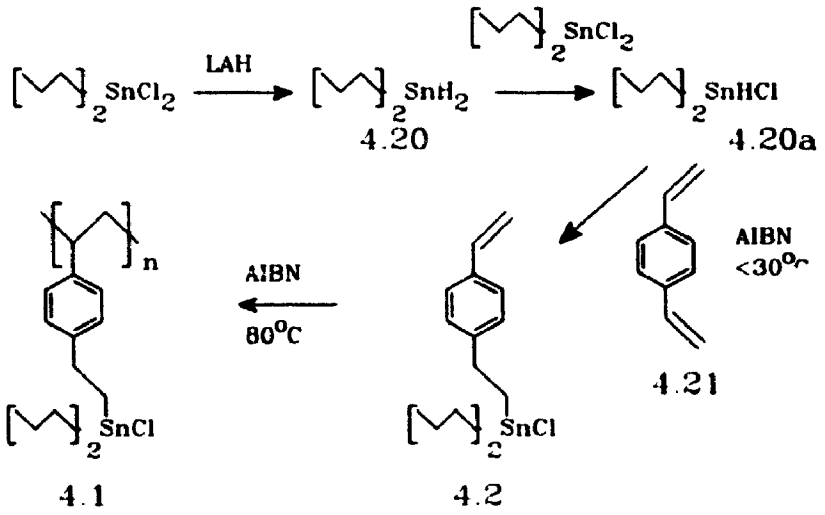

Scheme 4.4

Commercial divinylbenzene (DVB) **4.21** contains 45% by weight ethylvinylbenzene (EVB) as impurity. The pure divinylbenzene necessary for this preparation was obtained by the method of Leikin et al[5]. Carbon tetrachloride was added to a solution of commercial divinylbenzene to act as a chemisorption inhibitor. The divinylbenzene was then separated from the ethylvinyl benzene by complexation with copper(I) chloride. The copper complex of divinylbenzene is thermally stable to 70-75°C while the corresponding complex with ethylvinyl benzene decomposes at 35-40°C. The EVB complex does not form at room temperature in the presence of about 20 weight percent of CCl_4. This difference in stability allows the formation of the DVB complex while the residual EVB can simply be washed away. The divinylbenzene could be liberated from the copper complex with aqueous ammonia and distilled under reduced pressure.

The monomer for the polymerization reaction was obtained by treating the purified divinylbenzene **4.21*** with one equivalent of dibutyltin chloride hydride. The dibutyltin chloride hydride reagent was prepared *in situ* by the disproportionation reaction between dibutyltin dichloride and dibutyltin dihydride. The dibutyltin chloride hydride reagent hydrostannates one double bond of divinylbenzene when initiated by AIBN. Careful control of the temperature of the reaction results in a monomer which was shown by the original authors to be exclusively the mono-hydrostannation product **4.2**.

Additional divinylbenzene was then added to the reaction mixture to achieve about 7% cross-linking. n-Octanol was added as a diluent, additional AIBN added to initiate the reaction and the bath temperature was raised to 80°C to complete the polymerization. The polymeric material was obtained as beads with diameters of ca. 500 μm. The presence of tin and chlorine was confirmed by X-Ray Photoelectron Spectroscopy and elemental analysis.

With the organotin polymer **4.1** in hand, our attention turned to the functionalization of the polymer with the appropriate Grignard or organolithium reagent.

Though simple in principle, few radiopharmaceuticals can

---

*The polymer is synthesized from purified commercial divinylbenzene which is an approximately equimolar mixture of the meta and the para isomers. The polymer will be represented as the para isomer throughout for simplicity.

be directly metallated because of incompatible functional groups. Our initial approach was to prepare protected precursors, metallate these precursors, and then covalently attach them to the organotin polymer by substitution at the tin-chlorine bond.

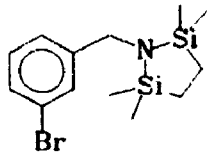

4.4

We began these studies with compound **4.4**, a protected 3-bromobenzylamine. The "stabase" adduct[6] has been shown to protect amines to conditions of strong base. Unfortunately, *meta* halogenated aromatic compounds are prone to elimination reactions yielding benzynes when subjected to lithiation conditions. When a lithiation reaction was attempted on compound **4.4** (Scheme 4.5) and quenched with chlorotrimethyltin only very polar material resulted.

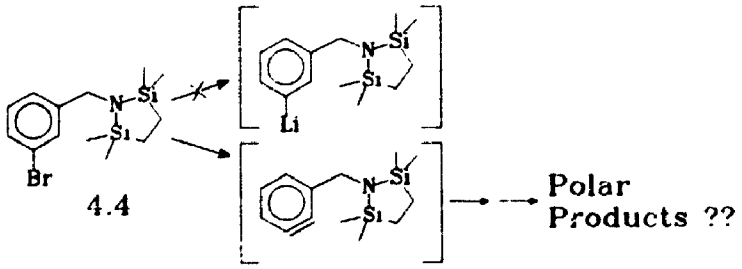

Scheme 4.5

It was apparent that if halogen-metal exchange had occurred other reactions had followed. Lowering the temperature of the reaction to -100°C did not seem to affect the course of the

reaction. The failure of this molecule to undergo simple metal-halogen exchange may be a result of the stabilization of the *ortho*-lithiated intermediate by the chelating effect of the lone pair electrons of the nitrogen[7]. The preparation of the Grignard reagent corresponding to compound **4.4** might have succeeded since Grignard reagents are less basic and less prone to formation of benzynes. Unfortunately, this was not realized until sometime after this approach had been abandoned.

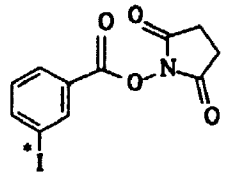

4.5

The activated benzoic acid ester **4.5** has been reported[8] as a protein labelling agent. We turned our attention to the protected benzoic acid derivative **4.6** (Scheme 4.6) as a possible means of coupling the benzoic acid moiety to the organotin polymer. The oxazoline functionality has been used extensively[9] to protect carboxylic acids under strongly basic conditions.

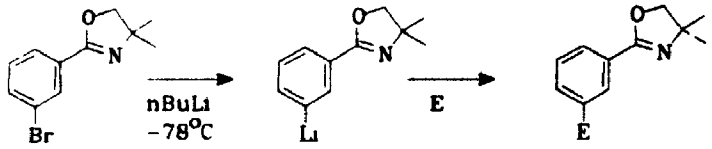

4.6

Scheme 4.6

The lithiation of the bromo oxazoline **4.6** once again did not provide any product arising from simple metal-halogen

exchange; instead only polar products were isolated from a quenching reaction with chlorotrimethyltin. A.I. Meyers has recently reported[10] a similar result for the corresponding chloro oxazoline **4.7** (Scheme 4.7).

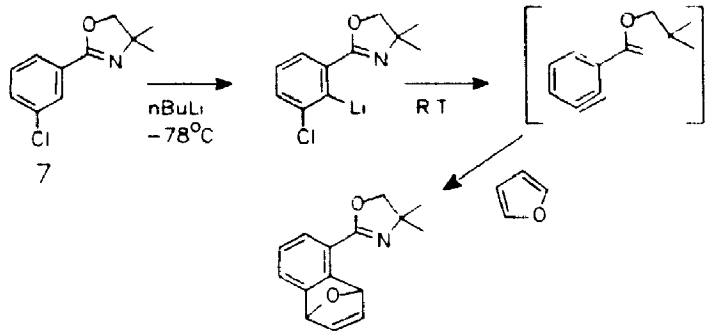

Scheme 4.7

Treatment of **4.7** with n-butyl lithium resulted in *ortho*-lithiation followed by elimination to the corresponding benzyne if the reaction mixture was allowed to warm to room temperature. Since the Grignard reagent of **4.6** had been reported we decided to attempt the coupling reaction via this reagent (Scheme 4.8).

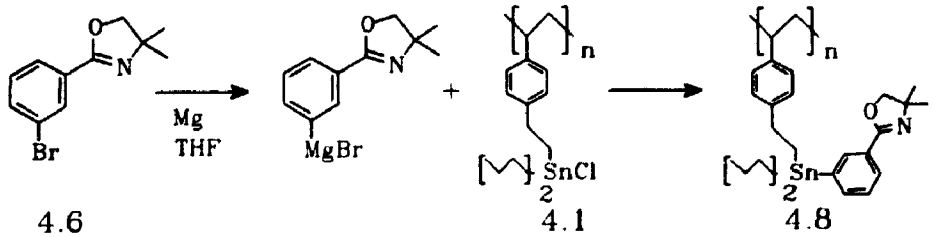

Scheme 4.8

We were able to prepare the Grignard reagent and reacted it with the organotin polymer **4.1**. On work-up of the resulting polymer **4.8** we obtained a material which decolorized a solution of iodine in chloroform resulting in a residue which

gave NMR and mass spectra consistent with 2-(3-iodophenyl)-4,4-dimethyloxazoline **4.9** (Scheme 4.9).

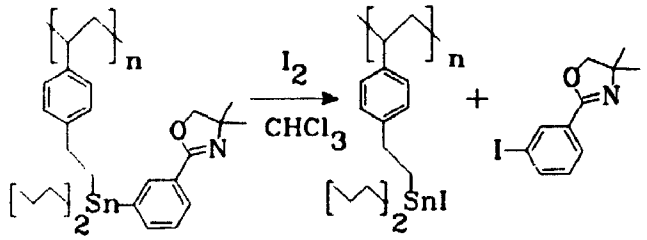

4.8 4.9

Scheme 4.9

Unfortunately, attempts to hydrolyse the polymer-bound oxazoline under basic or acidic conditions proved unsuccessful. It appears that the polymer-bound oxazoline is somehow shielded from the reagents used in the attempted hydrolysis. It is known that hydrophobic repulsions inhibit aqueous reactions on polymer surfaces. Phase transfer catalysis has been reported as a means of circumventing the problem but reactions of this type were not attempted.

Our frustration with the protection/deprotection route led us to reconsider the direct metallation of existing radiopharmaceuticals. We were able to show that *p*-dibromobenzene could be mono-lithiated and coupled to the organotin polymer (Scheme 4.10).

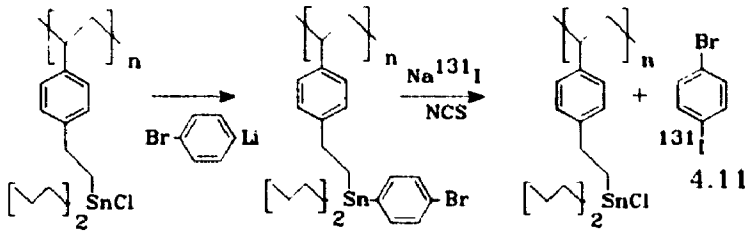

4.1 4.10 4.11

Scheme 4.10

The resulting polymer **4.10** was treated with $Na^{131}I$ and an oxidizing agent (NCS) in chloroform. After filtration of the polymer, 70% of the radioactivity was found in the filtrate. The filtrate was subjected to reversed-phase HPLC chromatography and showed three radioactive peaks. Radioactive material eluting at a time corresponding to a previously injected 4-iodobromobenzene **4.11** standard accounted for 67% of the total activity. A radioactive peak corresponding to the solvent front was not observed indicating that all radioiodide had been bound to organic residues. The appearance of two radioactive peaks in advance of the product peak was cause for concern. We believe that the monolithiation reaction may occur with some dilithiation. If this is the case then iodobenzene resulting from the protonation of the dilithiated species or iodophenol arising from the oxidation of the dilithiated species may account for the presence of additional radioactive peaks. We did not pursue the identity of the additional peaks.

Buoyed by this minor success we returned to a search for a radiopharmaceutical which could be subjected to direct

lithiation.

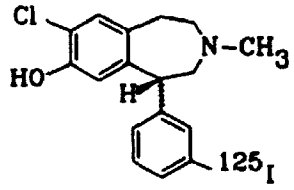

R-(+)-[^{125}I]TISCH

4.12

4.13

Potential candidates included compound **4.12** which has recently shown promise[11] as a high-affinity ligand for the D1-Dopamine receptor and iodobenzene **4.13** which has been reported[12] as an experimental myelin imaging agent. Unfortunately, neither of these compounds is clinically important as yet. In order for our procedure to gain attention, we felt that the pursuit of a radiopharmaceutical presently in clinical use was prudent.

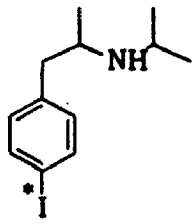

4.14

N-Isopropyl-*p*-iodoamphetamine **4.14**, a commercial radiopharmaceutical[13] used clinically to image brain perfusion, seemed to fit the bill. We anticipated that treatment of the brominated analogue **4.15** (Scheme 4.11) with two equivalents of n-butyllithium would lead to the dilithiated product **4.16**.

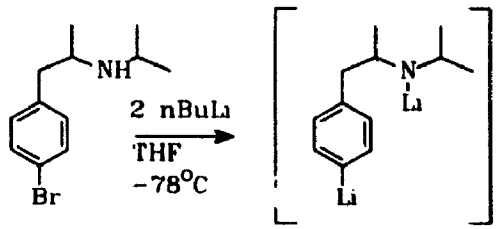

4.15 4.16

Scheme 4.11

We hoped that, of the two potential sites for reaction, the nitrogen anion would be less nucleophilic than the carbanion due to its higher electronegativity and greater degree of steric hindrance.

We tested our hypothesis using the following model reaction (Scheme 4.12):

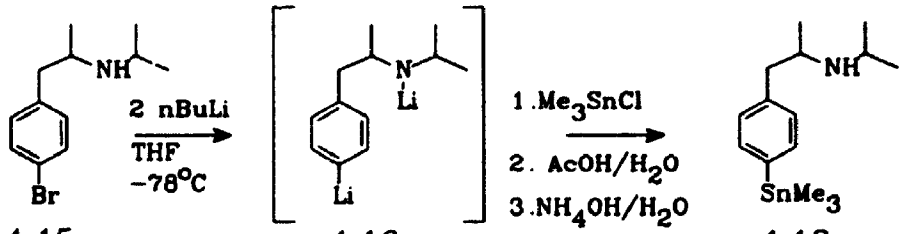

4.15 4.16 4.18

Scheme 4.12

The dianion was formed by addition of two equivalents of n-butyl lithium to the brominated analogue **4.15** followed by quenching with chlorotrimethyltin. We were encouraged by a 70% yield (by NMR) of the desired trimethylstannyl derivative **4.18**. We then reacted the organotin polymer with two equivalents of the dilithiated intermediate **4.16** (Scheme 4.13).

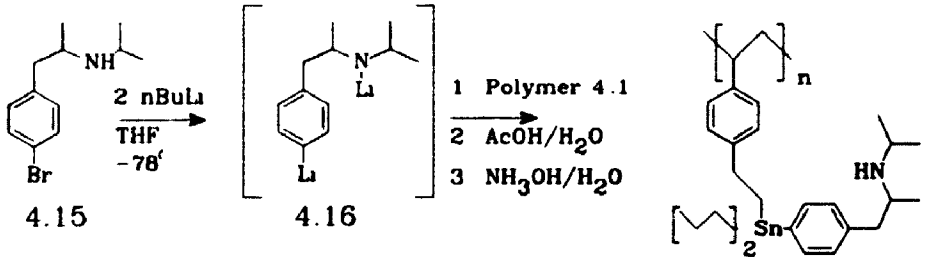

Scheme 4.13

The resulting polymer decolorized a solution of iodine in chloroform. The residue from the decolorization was subjected to TLC analysis and gave a single spot with an R_f consistent with the value expected for authentic N-isopropyl-p-iodoamphetamine. TLC did not adequately distinguish between the iodinated product and the brominated starting material which might reasonably be expected as a contaminant. The decolorization product was distinguished from the brominated starting material by HPLC analysis employing the system of Carlsen and Andresen[14]. Authentic N-isopropyl-p-bromoamphetamine was dissolved in 0.05 M phosphoric acid and applied to a RP-18 (250mm X 4.6mm i.d.) analytical column (Supelco) and eluted with a 95:5 ratio of solvent A (4:1 MeOH:H_2O; 0.45M in tetramethyl ammonium chloride) to solvent B (water) at a flow rate of 1.5 mL/min. The brominated standard had a reduced retention time of 1.19 minutes while the decolorization product had a reduced retention time of 1.36 minutes. Co-injection of the decolorization product and authentic N-isopropyl-p-bromoamphetamine gave rise to two distinct peaks in the chromatogram.

Treatment of (64 mg, 0.15 meq) of the polymer **4.19** with excess iodine in chloroform followed by filtration and isolation of the chloroform-soluble residue yielded (11 mg, 0.036 mmol) of material whose ^1H NMR and mass spectra were consistent with the literature data for N-isopropyl-*p*-iodoamphetamine. We were concerned that this analysis might be prone to large errors due to the uncertainty introduced when weighing small liquid samples in tared glassware. As an independent check, a sample of polymer **4.19** was treated with excess iodine solution to liberate all the available N-isopropyl-p-iodoamphetamine from the polymer. An internal standard (p-dinitrobenzene) was added at the beginning of the reaction. The N-isopropyl-p-iodoamphetamine was isolated and analyzed by proton NMR. The integrals from the aromatic protons of the internal standard and the product N-isopropyl-p-iodoamphetamine were compared. The ratio of the two integrals, when related back to the original concentration of internal standard, gave rise to a value of 0.43 for the number of milliequivalents of N-isopropyl-p-iodoamphetamine per gram of polymer **4.19**. The theoretical maximum was calculated to be 2.3 milliequivalents of N-isopropyl-p-iodoamphetamine per gram of polymer if every tin-chlorine bond had undergone substitution. The degree of functionalization of the polymer was thus 18.3%.

Confident that we had indeed prepared a polymer at least partially functionalized to the desired polymer **4.19** we turned

our attention to the radiolabelling reaction. One milligram of the polymer was treated with $Na^{131}I$ solution using two "Iodobeads"** as oxidant in acetonitrile. The mixture was allowed to react for four hours at which point the polymer was separated from the solvent by filtration. The solvent was evaporated, the residue dissolved in 0.05 M phosphoric acid and analyzed by HPLC with UV and radioactivity detection (Figure 4.1, following page). Radioactive product was isolated at the elution time corresponding to a previously injected non-radioactive standard. The bottom trace in Figure 4.1 is the UV absorbance arising from the injection of a non-radioactive standard. A large peak was observed at the solvent front due to the phosphate buffer present in the injection solvent. The peak eluting at 4.8 minutes corresponds to the standard. The middle trace in Figure 4.1 is the UV absorbance arising from the injection of the radioactive preparation. It can be seen that no peak is observed for non-radioactive **4.14**. There is a slight impurity at 6.0 minutes. The upper trace is the readout from the γ-ray detector. The peak at 5 minutes corresponds to ^{131}I-**4.14** which is accompanied by radioactive impurities at the origin which may correspond to iodide or iodate. The radiochemical yield of the reaction was determined to be 44%.

**"Iodobeads are a polymer supported form of Chloramine-T an oxidizing agent similar to N-chlorosuccinimide.

Figure 4.1: HPLC analysis of [^{131}I] N-isopropyl-p-iodo-amphetamine **4.14**.

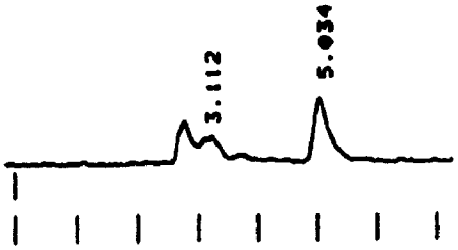

Top Trace: γ-Ray detector trace from injection of [^{131}I]- N-isopropyl-p-iodoamphetamine **4.14**. Peak at 5.03 minutes corresponds to product **4.14**.

Middle Trace: UV detector trace corresponding to upper trace.

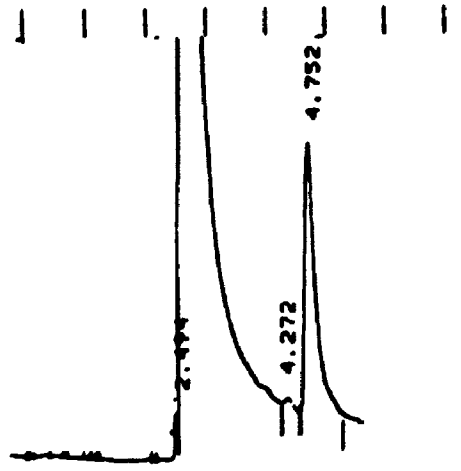

Bottom Trace: UV detector trace from previouly injected N-isopropyl-p-iodoamphetamine standard. The peak at 4.75 minutes is due to the standard.

Figure 4.1

4.3 X-Ray Photoelectron Spectroscopy as an Analytical Tool in Polymer Chemistry

X-Ray Photoelectron Spectroscopy (XPS) also known as Electron Spectroscopy for Chemical Analysis (ESCA) has been described[15] as a spectroscopic tool *par excellence* for the study of polymer surface features. XPS is not a common analytical tool in organic chemistry, and as such, the technique will be briefly outlined.

The XPS experiment is quite simple in principle. A solid sample is irradiated with a monoenergetic beam of x-rays and the kinetic energy of the electrons ejected from the constituent atoms is analyzed (fig. 4.2).

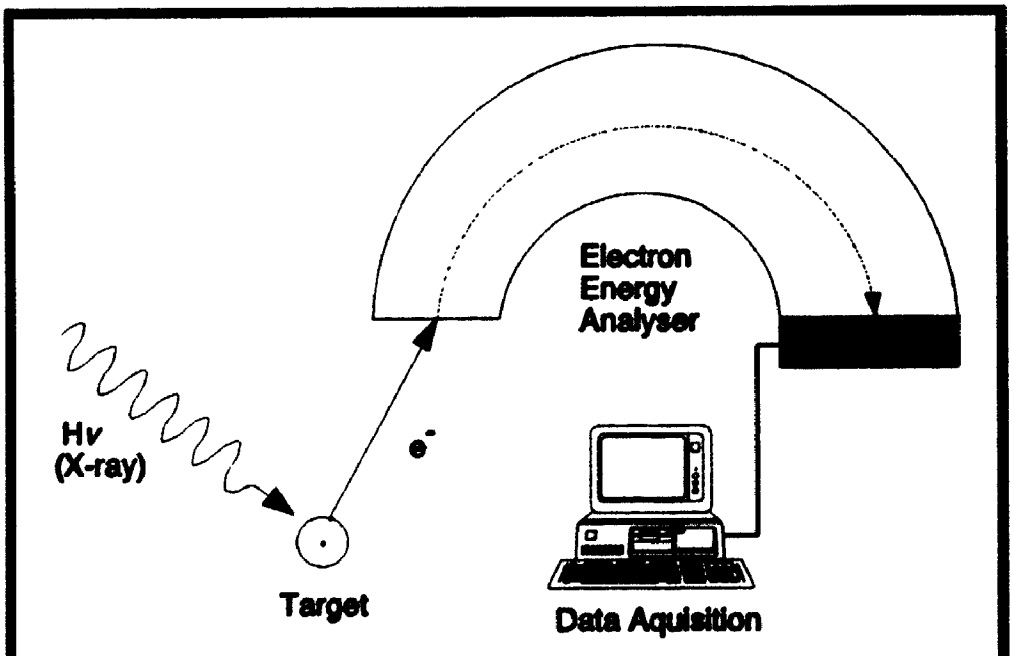

Figure 4.2: Schematic of the XPS Experiment

With the appropriate X-ray source the electrons from the core to the valence levels can be studied. The technique is sufficiently sensitive to detect all the elements from lithium through to uranium.

XPS is predominantly concerned with the study of core levels since these electrons are essentially localised on the atom and the binding energy will be characteristic of the particular element. While XPS is extremely useful for the qualitative identification of the constituent elements of a sample there are large errors associated with quantitative applications. XPS signal intensities depend on a number of factors: the mean-free-path of electrons in the material, the efficiency of absorption of the exciting x-rays by the sample, and various matrix effects. The most important of these factors in terms of quantitative polymer analysis is the x-ray absorption efficiency[16]. The sensitivity of XPS to a particular element is directly proportional to the cross-section for x-ray absorption of that particular element. A great deal of empirical data has been compiled which shows a periodic relationship between the cross-section for x-ray absorption for a particular subshell and the atomic number of the element being observed[17]. The photoelectric cross-sections for the elements of interest in our research are compiled in Table 4.1. The values are normalized to carbon which is assigned the value of 1.00.

Table 4.1: Photoelectric cross-sections for various elements normalized to carbon (1.00).

	Orbital													
	1s	2s	2p	2p	3s	3p	3p	3d	3d	4s	4p	4p	4d	4d
C	1.0													
N	1.78													
O	2.85													
Cl		1.5	0.81	1.6	0.16	0.05	0.10							
Br					1.3	1.5	2.9	1.2	1.8	0.16	0.10	0.19		
Sn					2.5	3.6	7.6	10	15	0.65	0.74	1.5	1.1	1.5

Figure 4.3 shows the XPS data for the organotin polymer 4.1.

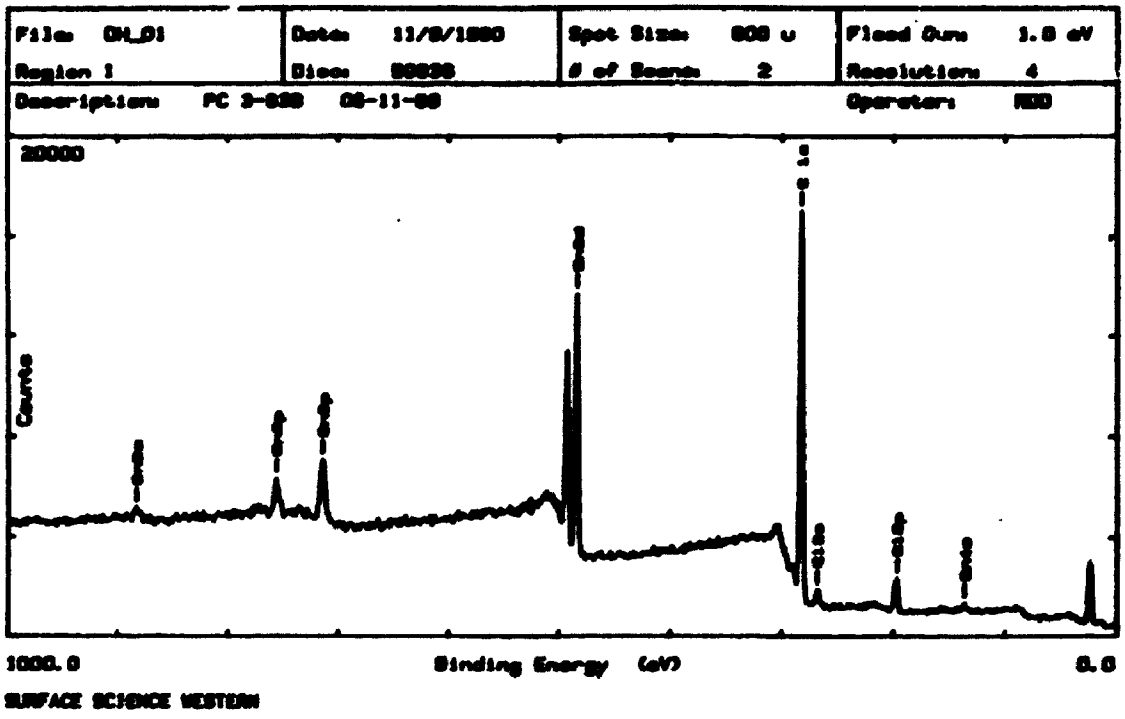

Figure 4.3

The spectra shows peaks for each of the elements expected. The dominant peaks are due to the carbon 1s electrons (283.2 eV) and the tin 3d electrons ($3d_{5/2}$ 484.4 eV, $3d_{3/2}$ 492.4 eV).

The weaker peaks due to chlorine (2s 268.6 eV, 2p 197.3 eV) and tin (3s 883.8 eV, $3p_{1/2}$ 756.9 eV, $3p_{3/2}$ 714.9 eV, 4s 136.7 eV) are also clearly visible.

An analysis of the number of electrons detected for the Sn_{3d}, C_{1s}, and the Cl_{2p} levels followed by a correction for the relative cross-sections of each element gives the relative composition (in atom %) of ea ı element (Table 4.2).

Table 4.2 Calculated and observed elemental compositions expressed as atom % in Polymer 4.1. ND: element not detected. EA: composition as determined by combustion analysis.

Element	Atom% (Calc'd)	Atom% (XPS)	Atom% (EA)
Carbon	91.09	91.21	93.10
Nitrogen	4.45	4.55	3.40
Tin	4.45	4.23	3.40

The good agreement between the calculated and the observed values indicates that XPS should be a useful tool to aid in the characterization of further functionalized polymers. A second important conclusion may also be drawn, that is, the good agreement between the calculated and observed elemental composition implies that the surface of the polymer reflects the composition of the bulk sample and thus, the functional groups can be assumed to be evenly distributed throughout the resin. It is important to note that combustion analysis gave results which are not consistent with the data obtained by XPS. The importance of this observation will be discussed later in the chapter.

Two other polymer samples were analyzed in the same manner.

Figure 4.4 shows the XPS data for polymer **4.8**.

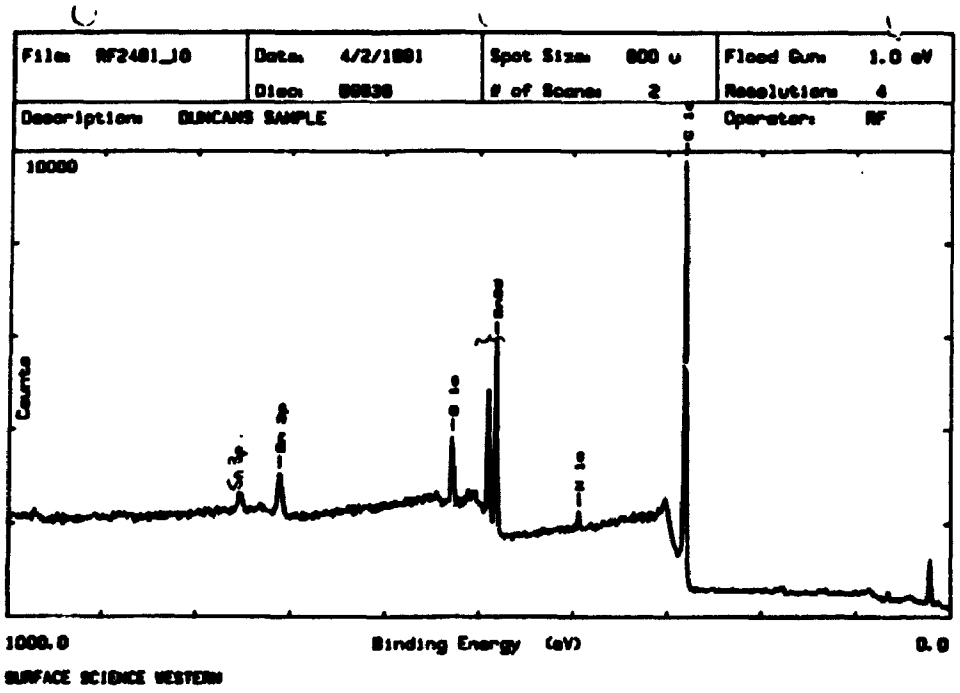

Figure 4.4

Table 4.3 lists the calculated elemental composition of polymer **4.8** along with the experimental values from XPS and elemental analysis (EA).

Table 4.3 Calculated and observed elemental compositions expressed as atom % in Polymer **4.8**. ND: element not detected.

Element	Atom% (Calc'd)	Atom% (XPS)	Atom% (EA)
Carbon	91.3	88.61	92.50
Nitrogen	2.90	2.91	1.80
Chlorine	0.00	ND	0.83
Tin	2.90	1.84	3.24
Oxygen	2.90	6.64	1.63

Figure 4.5 shows the XPS data for polymer 4.19.

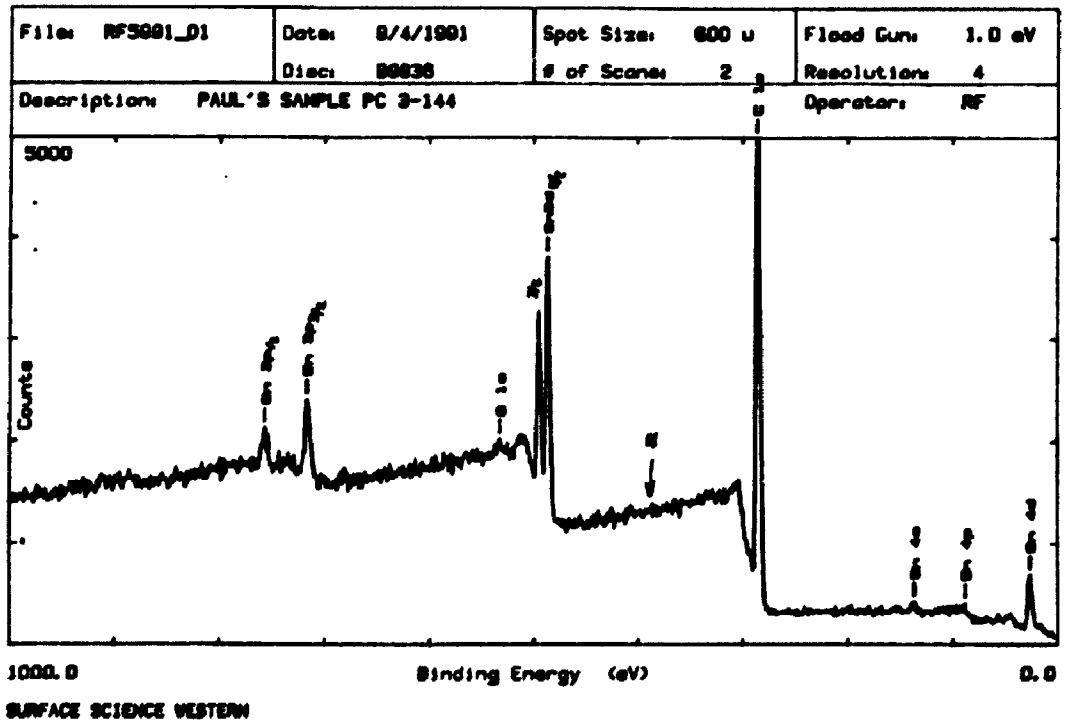

Figure 4.5

Table 4.4 lists the calculated elemental composition of

polymer 4.8 along with the experimental values from XPS and elemental analysis (EA).

Table 4.4 Calculated and observed elemental compositions expressed as atom % in Polymer 4.19. ND: element not detected.

Element	Atom% (Calc'd)	Atom% (XPS)	Atom% (EA)
Carbon	94.2	95.27	95.42
Nitrogen	2.85	ND	0.70
Tin	2.85	3.81	3.78

4.4 Discussion

The quantitative analysis of highly cross-linked polymers is complicated by the low solubility and the low chemical reactivity of the material. We were initially encouraged by the excellent agreement between the calculated elemental composition for polymer **2.1** and the experimentally observed elemental composition found using x-ray photoelectron spectroscopy (XPS). The generation of XPS data for polymers **4.8** and **4.19** convinced us that our initial results were serendipitous. When polymer **4.1** was subjected to combustion analysis the values for elemental composition were quite different from those found using XPS. The ratio of chlorine to tin in polymer **2.1** must be 1:1. The combustion analysis of polymer **4.1** resulted in a chlorine to tin ratio of 1.00. The good agreement between the theoretical and observed ratios suggests that combustion analysis may be the more reliable of the two analysis techniques. One more piece of evidence supports this conclusion. The ratio of nitrogen to tin found by combustion analysis for polymer **4.19** was 18.5%. In the absence of impurities, this ratio should also furnish the degree of functionalization of the polymer. The degree of functionalization calculated using an internal standard and NMR spectroscopy was 18 ±1%. The good agreement between the two values found for degree of functionalization once again suggests that combustion analysis may be the more reliable technique.

Despite some uncertainty in the exact composition of the functionalized organotin polymers we believe that we have demonstrated the utility of this technique for the radioiodination of N-isopropyl-p-iodoamphetamine. [^{123}I]-N-isopropyl-p-iodoamphetamine is currently synthesized via a halogen exchange reaction. Exchange-labelling implies that non-radioactive [^{127}I]-N-isopropyl-p-iodoamphetamine is heated with Na^{123}I and the radioactive iodine atoms exchange with the non-radioactive iodine atoms. Exchange-labelling necessarily results in low-specific activity radiopharmaceutical. The production of high-specivic activity material is desirable since it eliminates the possibility of a pharmacological response occuring as a result of the administration of the radiopharmaceutical. The product of the exchange-labelling reaction must be purified by HPLC to remove impurities arising from thermal decomposition of the starting material. The use of polymer **4.19** for the labelling of N-isopropyl-p-iodoamphetamine would result in high-specific activity material and would not require HPLC purification. The organotin polymer method should be directly applicable to the production of existing radiopharmaceuticals which are stable to metallation conditions. With the appropriate chemistry the technique should be suitable for base-sensitive substrates. A particularly appealing application would be the production of radiolabelled peptides via this method; this may be the goal of future members of the radiopharmaceutical development

group.

4.5 Experimental

Di-n-butyltin Dihydride 4.20

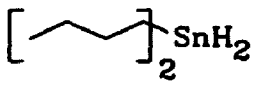

4.20

Di-n-butyltin dihydride **4.20** was synthesized according to the general procedure of Van der Kerk *et al*[18]. $LiAlH_4$ (BDH, 3.75 g, 0.099 mol) was suspended in 200 mL of freshly distilled diethyl ether. Dibutyltin dichloride (Aldrich, 30.0 g, 0.099 mol) was dissolved in ether (75 mL) and added dropwise to the $LiAlH_4$ suspension over ca. 10 minutes. The mixture was brought to reflux for seven hours at which point hydroquinone (Kodak, 200 mg, 1.8 mmol) were added as antioxidant. The excess $LiAlH_4$ was destroyed by the *careful* addition of water (10 mL). An aqueous solution of sodium potassium tartrate (20%, 200 mL) was then added to assist in the dissolution of the aluminum salts. The ether layer was collected and the aqueous layer was washed with ether (2 X 50 mL). The organic layers were combined, dried with Na_2SO_4, and the ether stripped *in vacuo*. The residue was vacuum distilled to yield di-n-butyltin dihydride **4.20** (17.9 g; 0.076 mmol; 76%; bp. 32°C, 0.8 mm Hg, (lit[18] 75-76°C, 12 mm Hg) . HMR: $\delta(C_6D_6)$ 4.80 (m, 2H, $-SnH_2$), 1.55 (m, 2H, $-CH_2-$), 1.35 (m, 2H, $-CH_2-$), 0.98 (m, 2H, $-CH_2-$), 0.91 (t, 3H, $-CH_3$). CMR: $\delta(C_6D_6)$ 30.4, 26.9, 13.5, 6.8.

Purification of Divinylbenzene 21

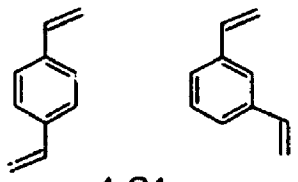

4.21

Commercial divinylbenzene 4.21 was purified according to the method of Leikin *et al*[19]. Technical divinylbenzene (Aldrich, 55% DVB, 21.93 g, 12.06 g DVB, 0.093 mol) containing 16 weight percent CCl_4 was mixed with copper(I)chloride (BDH, 93%, ca. 20g) in a porcelain crucible. The resulting paste was stirred occasionally over approximately three hours until the mixture solidified. The solid was powdered then washed with cold (ca.-10°C) heptane (100 mL) to wash away the unbound ethylvinyl benzene. The solid was then vacuum dried (0.5 mm Hg) overnight in the presence of paraffin wax. The resulting powder was then treated with aqueous ammonia (BDH, 28%, 100 mL) until a dark blue solution was obtained. Treatment with ultrasound proved useful in the dissolution/ dissociation of the copper-divinylbenzene complex. The solution was then extracted with ether (3 X 100 mL), the ether layers combined and dried (Na_2SO_4), and the ether stripped *in vacuo*. The residue was distilled under reduced pressure to yield *m* and *p*-divinylbenzene free of contaminants (9.4 g; 0.072 mol; 78%; bp. 48°C, 2.0 mm Hg). HMR δ ($CDCl_3$) 7.41 (s, 1H, H_{arom}(*meta*)), 7.35 (s, 4H, H_{arom}(*para*)), 7.29 (s, 3H, H_{arom}(*meta*)), 6.75 (dd, 2H, -CH).

Poly-β-(Chlorodibutylstannyl)-4-ethyl styrene 1

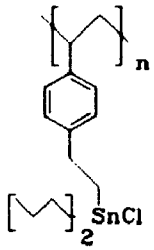

4.1

The organotin polymer 4.1 was prepared according to the method of Gerigk *et al*[4]. Purified divinylbenzene 4.21 (9.0 g, 0.069 mol) and dibutyltin dichloride (Aldrich, 10.5g, 0.035 mol) were dissolved together with azobisisobutyronitrile (Kodak, 215 mg, 1.3 mmol) under an Argon atmosphere. Dibutyltin dihydride 4.20 (8.29 g, 0.35 mmol) was added dropwise at such a rate that the temperature of the mixture did not rise above 30°C. The mixture was stirred overnight in a water bath such that the temperature remained at 20°C. The following morning additional divinylbenzene (1.96 g, 0.015 mol) and AIBN (377 mg, 2.3 mmol) were added to the hydrostannation mixture along with n-octanol (BDH, 25.8g) methyl cellulose (118 mg) and deionized, degassed (Argon) water (75 mL). The magnetic stirrer was replaced with a mechanical stirrer and the speed was adjusted to 250 r.p.m. The reaction mixture was heated to 80°C with an oil bath and allowed to react for 24 hours. The solid product was isolated by filtration. The solid was washed by Soxhlet extraction with methanol, acetone and finally toluene each for ca. 90 minutes. The product consisted of off-white beads (15.8 g, 53%). A melting point was

attempted with only a slight discoloration occurring at up to 230°C. The polymer was insoluble in all solvents tested. IR (KBr) 3019 (C-H), 2922 (C-H), 2853 (C-H), 1603 (C=C), 1446 (C=C) cm^{-1}.

N-(3-bromobenzyl) 1,1,4,4,-tetramethyl-1,4-disilylazacyclopentane 4.4

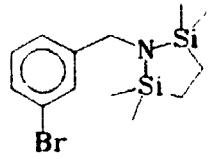

4.4

N-(3-bromobenzyl) 1,1,4,4,-tetramethyl-1,4-disilylazacyclpentane 4.4 was prepared according to the general procedure of Djuric *et al*[20] In a solution of concentrated ammonium hydroxide solution (BDH, 28%, 10 mL, .15 mol) was dissolved 3-bromobenzylamine hydrochloride (Aldrich, 2.0 g, 9.0 mmol) . The mixture was then extracted with ether (3 x 25 mL), the ether layers combined and dried (Na_2SO_4) and the ether stripped *in vacuo*. The residue was dissolved in dry CH_2Cl_2 (25 mL) and 1.2-bis(chlorodimethylsilyl) ethane (Lancaster Synthesis, 1.93 g, 9.0 mmol) and triethylamine (BDH, 2.5 mL, 18.0 mmol) were then added. The mixture was brought to reflux overnight under a blanket of dry Argon. The volatiles were stripped *in vacuo* to yield a semi-solid residue which was triturated with 30-60° petroleum ether. The petroleum ether fractions were then evaporated *in vacuo*. The resulting viscous liquid was

distilled at reduced pressure through a short Vigreux column to yield N-(3-bromobenzyl) 1,1,4,4,-tetramethyl-1,4-disilylazacyclpentane **4.4** (2.23 g; 6.7 mmol; 75%; bp. 112°C, 1.3 mm Hg). H.M.R. δ (acetone d_6): 7.2-7.55 (m, 4H, H_{AR}), 4.06 (s, 2H, N-CH_2), .78 (s, 4H, -CH_2CH_2-), 0.00 (s, 6H, -CH_3). C.M.R. 147.3, 131.4, 130.8, 130.1, 127.3, 122.5, 45.8, 8.1, -0.6. MS. m/e calculated for $C_{13}H_{22}BrNSi_2$: 327.0474, observed 327.0477.

Attempted Lithiation of 4.4.

N-(3-bromobenzyl) 1,1,4,4,-tetramethyl-1,4-disilyl-azacyclopentane **4.4** (72 mg, 0.22 mmol) was dissolved in freshly distilled THF (10 mL) in a flame-dried round-bottomed flask under an Argon atmosphere. n-Butyl lithium in hexanes (Aldrich, 2.32 M, 95 μL, 0.22 mmol) was then added dropwise via syringe. The metal halogen exchange was allowed to proceed for 30 minutes at which point the reaction was quenched with chlorotrimethyltin (Aldrich, 43.4 mg, 0.22 mmol) dissolved in THF (1 mL). The mixture was allowed to slowly warm to room temperature and was stirred overnight. The crude reaction mixture was subjected to TLC analysis (alumina, 20% EtOAc/Hexanes). The R_f of the starting material was 0.88. The reaction mixture contained only polar products which could not be eluted with the solvent system described.

2-(3-Bromophenyl)-4,4-dimethyloxazoline 4.6

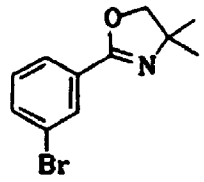

4.6

The procedure of Meyers et *al*[21] was used to prepare 2-(3-Bromophenyl)-4,4-dimethyloxazoline 4.6. To a solution of 2-amino, 2-methyl propanol (Aldrich, 9.4 g, 0.11 mol) in dry CH_2Cl_2 (100 mL) was added dropwise 3-bromobenzoyl chloride (Aldrich, 11.03 g, 0.05 mol) . The mixture was stirred for four hours at which time water (100 mL) was added. The methylene chloride layer was collected and the water layer was washed with additional portions of CH_2Cl_2 (3 x 50 mL). The methylene chloride layers were combined, dried with Na_2SO_4, and the methylene chloride was stripped *in vacuo*. Thionyl chloride (12.02 mL, 0.17 mmol) was added dropwise to the solid residue and the mixture was stirred as a vigorous reaction ensued. The reaction mixture was stirred for an additional hour at which point the excess thionyl chloride was destroyed by the careful addition of a saturated solution of sodium bicarbonate. The solution was made basic then extracted with CH_2Cl_2 (3 x 50 mL). The organic layers were combined, dried with Na_2SO_4 and the CH_2Cl_2 was stripped *in vacuo*. The residue was distilled under reduced pressure to give 2-(3-Bromophenyl)-4,4-dimethyloxazoline 4.6 (10.73 g; 0.042 mol; 85%; bp. 90-100°C, 0.03 mm Hg, (lit[21]. 105-108°C, 0.05 mm Hg)).

H.M.R. δ ($CDCl_3$): 8.09 (s, 1H, H_{AR}), 8.72 (d, 1H, H_{AR}), 7.65 (d, 1H, H_{AR}), 7.25 (t, 1H, H_{AR}), 4.09 (s, 2H, $-CH_2-$), 1.36 (s, 6H, $-CH_3$). IR: (CH_2Cl_2) 2964 (C-H), 2930 (C-H), 2895 (C-H), 1638 (C=N). HRMS: m/e calculated for $C_{11}H_{12}BrNO$: 253.0102, observed: 253.0097.

Poly-(β-(3-(4',4'-dimethyl-2'-oxazolinyl)phenyl)-4-ethylstyrene 4.8

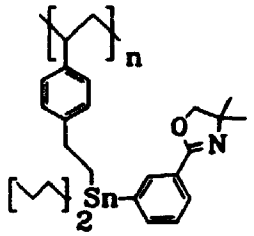

4.8

Freshly milled, triply sublimed magnesium (257 mg, 10.6 mmol) was placed in a 50 mL 2-necked round-bottomed flask equipped with magnetic stirrer, reflux condenser and argon inlet. A gentle flow of Argon was passed through the apparatus and it was flame-dried. A solution of 1,2-dibromoethane (200 μl, 2.26 mmol) in dry THF (1 mL) was added dropwise to the vigorously stirred magnesium filings. When initiation occurred 2-(3-Bromophenyl)-4,4-dimethyloxazoline 6 (2.0 g, 7.9 mmol) dissolved in THF (5 mL) was added dropwise at such a rate that gentle reflux was maintained. On complete addition of the oxazoline solution the reaction was allowed to proceed until the mixture returned to room temperature. The Grignard solution was then added via an Argon frit to the vacuum dried

(80°C, 1 mm Hg) organotin polymer **4.1** (2.0 g, 4.68 meq) suspended in dry THF (10 mL). On complete addition the Argon frit was replaced with the reflux condenser and the mixture was brought to reflux overnight. The polymer was then isolated by filtration. The polymer **4.8** was washed with a 10% solution of acetic acid in THF followed by twelve hours of soxhlet extraction with each of THF and toluene.

2-(3-Iodophenyl)-4,4-dimethyloxazoline 9

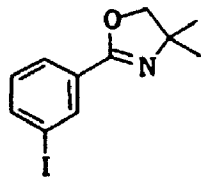

4.9

A solution of 3-iodobenzoic acid (Aldrich, 1.0 g, 4.0 mmol) and dicyclohexylcarbodiimide (Aldrich, 832 mg, 4.0 mmol) was prepared in dry CH_2Cl_2 (25 mL) followed by the dropwise addition of 2-amino-2-methyl propanol (Aldrich, 359 mg, 4.03, mmol) the stirred solution. The mixture was stirred overnight and then filtered to remove the dicyclohexylurea. The methylene chloride was stripped then stripped *in vacuo*. The residue was treated with excess thionyl chloride (5 mL, 0.07 mol) and stirred for one hour at which time the thionyl chloride was removed *in vacuo*. The residue was taken up in diethyl ether (50 mL) and extracted with saturated sodium bicarbonate solution. The aqueous layers were washed with ether (3 x 25 mL), the ether layers combined and dried

(Na_2SO_4), and then the ether was stripped *in vacuo*. The residue was purified by Kugelrohr distillation to yield 2-(3-Iodophenyl)-4,4-dimethyloxazoline **4.9** (640 mg; 2.12 mmol; 53%; bp. 95°C, 0.1 mm Hg). H.M.R. δ ($CDCl_3$): 8.32 (s, 1H, H_{AR}), 7.95 (d, 1H, H_{AR}), 7.80 (d, 1H, H_{AR}), 7.14 (t, 1H, H_{AR}), 4.13 (s, 2H, $-CH_2-$), 1.39 (s, 6H, $-CH_3$). HRMS: m/e calculated for $C_{11}H_{12}INO$: 300.9964, observed: 300.9966.

Poly-(β-(4-bromophenyl-dibutyl-stannyl)-4-ethylstyrene 4.10

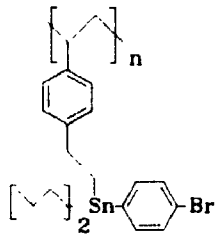

4.10

p-Dibromobenzene (Eastman, 0.55 g, 2.3 mmol) was dissolved in freshly distilled THF (100 mL) and the mixture was cooled (-78°C) under an atmosphere of dry Argon. n-Butyl lithium (Aldrich, 2.3 M, 1.0 mL, 2.3 mmol) in hexanes was then added via syringe. The halogen-metal exchange reaction was allowed to proceed for 30 minutes at which point the vacuum dried (0.1 mm, 80°C) organotin polymer **4.1** (1.0 g, 2.34 meq) were added in one portion. The mixture was stirred for four hours at -78°C then allowed to slowly warm to room temperature overnight. The reaction mixture was then washed with a 10% solution of acetic acid in THF. The solid polymer was collected by filtration then washed by Soxhlet extraction for

nine hours with each of THF and toluene.

Analysis of Poly-(β-(4-bromophenyl-dibutylstannyl)-4-ethylstyrene **4.10**

Poly-(β-(4-bromophenyl-dibutylstannyl)-4-ethylstyrene **4.10** (0.0122 g, 0.029 meq) was suspended in freshly distilled chloroform (1 mL) and treated with excess iodine dissolved in chloroform until the iodine colour persisted. The solution was filtered and collected in a volumetric flask (2.00 mL). The beads were washed with chloroform and the wash was collected in the same volumetric flask. The volume was adjusted to the meniscus and the flask was shaken. The resulting solution served as the stock. A sample of the stock solution (25 μl) was diluted to 1.5 mL with $CHCl_3$ and a U.V. spectra was obtained with $CHCl_3$ in the reference beam. The absorbance at 245.5 nM was compared to a Beer-Lambert plot of absorbance versus concentration obtained for authentic 4-iodobromobenzene. The concentration was found to be 17.2 μM. The concentration of the stock solution was calculated to be 1.03 mM. The number of μmoles of 4-iodobromobenzene obtained from the original 12.2 mg of resin **4.10** was determined to be 2.1. The theoretical maximum was 29 μmoles at 100% functionalization. The conversion in the lithiation reaction was calculated to be 7.2%.

4-[^{131}I] Iodobenzene **4.11**

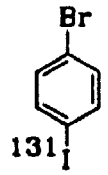

4.11

Organotin resin **4.10** (500 μg, 0.086μ eq) and N-chlorosuccinimide (500 μg, 3.74 μmol) were taken up in $CHCl_3$ (1 mL) with a 5 mm magnetic stirring bar in a 10 mL Vacutainer (Becton-Dickinson). $Na^{131}I$ (Frosst, 8.39 MBq) in distilled water (10 μL) was then added and the mixture vigorously stirred for one hour. The polymer was filtered and the filtrate collected. The polymer was washed once with $CHCl_3$ (500 μL). The filtrate was assayed in a dose calibrator and contained 5.62 MBq while the filter contained 2.55 MBq. A portion (ca 0.96 MBq) of the crude filtrate was applied directly to a RP-18 HPLC column (Supelco) and eluted with an isocratic mixture of 90% MeOH and 10% water. The radioactive HPLC trace showed three peaks, none corresponding to the solvent front. The peak eluting at a time corresponding to that of a previously injected non-radioactive standard contained (0.64 MBq, 67%) of the target molecule 4-[^{131}I]-iodobromobenzene **4.11**. The overall radiochemical yield was 47%.

1-(p-Bromophenyl)-1-cyano-2-propanone **4.15a**

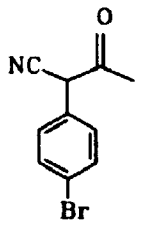

4.15a

The method of Benkeser and Johnson[22] was used to prepare 1-(p-Bromophenyl)-1-cyano-2-propanone **4.15a**. p-Bromophenylacetonitrile (Aldrich, 10.0 g, 0.051 mol), ethyl acetate (BDH, 7.81 mL, 0.080 mol) and sodium ethoxide (3.04 g, 0.066 mol) were taken up in absolute ethanol (18 mL). The mixture was heated for two hours on a steam bath and then stirred overnight. The following day the ethanol and other volatiles were stripped on the rotary evaporator. The residue was dissolved in water (40 mL) then cooled (-10°C) in an ice-salt bath. Glacial acetic acid (2.5 mL, 0.04 mol) was then added with vigorous stirring. The solid produced was filtered, air dried , then recrystallized from methanol to yield 1-(p-Bromophenyl)-1-cyano-2-propanone **4.15a** (3.9 g, 0.02 mol, 32%) mp 138-143°C, (lit[22] 136-137°C). HMR: δ(acetone-d_6): 7.45 (q, 4H, H_{AR}), 2.28 (s, 3H, $-CH_3$), 2.12 (s, 1H, -OH). IR: (CH_2Cl_2) 3090 (C-H), 2810 (C-H), 2670 (C-H), 2210 (CN), 1620 (C=O), 1466 (C=C), 1320 (C=C) cm^{-1}.

1-(4-Bromophenyl)-2-propanone 4.15b

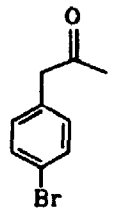

4.15b

The procedure of Benkeser and Johnson[22] was also used to prepare 1-(4-Bromophenyl)-2-propanone **4.15b**. Recrystallized 1-(p-bromophenyl)-1-cyano-2-propanone **4.15a** (3.8 g, 0.016 mol) was dissolved in concentrated H_2SO_4 by heating on a steam bath. On complete dissolution the mixture was heated an additional five minutes at which point it was cooled to 0°C in an ice bath and water (80 mL) were added. The mixture was then refluxed for two hours. The mixture was cooled, then extracted with diethyl ether (3 x 50 mL). The ether layers were combined, dried with Na_2SO_4 and the ether was stripped *in vacuo*. The residue was distilled at reduced pressure to yield 1-(4-Bromophenyl)-2-propanone **4.15b** (1.9 g; 8.9 mmol; 54%; bp. 88°C, .15 mm Hg (lit[22] 74°C, 0.15 mm Hg). HMR: $\delta(CDCl_3)$ 7.25 (q, 4H, H_{AR}), 3.65 (s, 2H, $-CH_2-$), 2.15 (s, 3H, $-CH_3$). IR: (neat) 3040 (C-H), 2900 (C-H), 1707 (C=O), 1484 (C=C), 1355 (C=C) cm^{-1}. HRMS: m/e calculated for C_9H_9BrO: 211.9836, observed: 211.9830.

N-Isopropyl-p-bromoamphetamine **4.15**

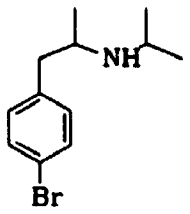

4.15

N-isopropyl-p-bromoamphetamine **4.15** was prepared by the general procedure of Borch *et al*[23]. A solution of 1-(4-Bromophenyl)-2-propanone (500 mg, 2.35 mmol) and 6.5 N methanolic HCl (722 μl, 4.69 mmol) was prepared in dry methanol (6.0 mL). Isopropyl amine (Eastman, 832 mg, 14.0 mmol), $NaBH_3CN$ (Aldrich, 103 mg, 1.64 mmol) and activated 3A molecular sieves (1.0 g) were added and the mixture stirred for 78 hours. Concentrated HCl was then added until the pH of the solution was less than 2 (pH paper) and the methanol was stripped *in vacuo*. The residue was extracted with ether (3 x 50 mL) and the aqueous portion was made basic with careful addition of solid KOH. The resulting solution was repeatedly extracted with ether (5 x 50 mL), the combined ether extracts dried with Na_2SO_4 and the ether was then stripped *in vacuo*. The residue was Kugelrohr distilled to yield N-isopropyl-p-bromoamphetamine **4.15** (412 mg; 1.61 mmol; 69%; bp. 62-65 °C, .03 mm Hg). HMR: δ(CDCl3) 7.17 (q, 4H, H_{AR}), 2.9 (m, 2H, 2(-CH-)), 2.55 (qd, 2H, $-CH_2-$), 0.95 (m, 9H, 3($-CH_3$). IR: (neat) 3055 (C-H), 2985 (C-H), 2950 (C-H), 2890 (C-H), 1489 (C=C), 1382 (C=C) cm^{-1}. HRMS: m/e calculated for $C_{12}H_{18}BrN$: 256.0622

observed: 256.0621.

N-Isopropyl-p-trimethylstannylamphetamine 4.18

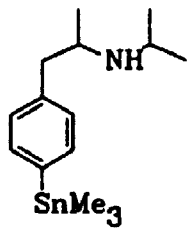

4.18

N-Isopropyl-p-bromoamphetamine 4.15 (100 mg, 0.39 mmol) was dissolved in freshly distilled THF (10 mL) and cooled to -78 C under an atmosphere of dry Argon. A solution of n-butyl lithium (Aldrich, 2.3 M, 340 μL, 0.780 mmol) was then added via syringe. The metal halogen exchange reaction was allowed to proceed for thirty minutes at which point chloro-trimethyltin (78 mg, 0.39 mmol) dissolved in dry THF (2 mL) was added dropwise via syringe. The mixture was allowed to stir overnight as it slowly warmed to room temperature. The reaction was then quenched with water. Sufficient ethyl acetate (1 mL) was added to obtain two phases. The organic layer was isolated, washed with water (1 mL) and dried with Na_2SO_4. The aqueous portion of the reaction mixture was extracted with ethyl acetate (2 x 2 mL) and the ethyl acetate layers were combined with the original. The volatiles were then stripped *in vacuo*. TLC (20% Et_2O: 80% hexanes, silica gel) showed two spots: one remaining at the origin and a second with an R_f of 0.93. The second spot remained white when

exposed briefly to an iodine chamber (a characteristic of aromatic organotin compounds). The ^1H spectrum was consistent with the expected product N-isopropyl-p-trimethylstannylamphetamine **4.18**. HMR: δ(acetone-d_6) 7.15 (q, 4H, H_{AR}), 2.82 (m, 2H, 2(-CH-)), 2.45 (dq, 2H, $-CH_2-$), .84 (d, 3H, $-CH_3$), .77 (d, 6H, $-CH_3$), 0.11 (s, 9H, $Sn(CH_3)_3$).

Poly-(β-(4'-(N-isopropyl-2''-aminopropyl)phenyl)-4-ethylstyrene 4.19

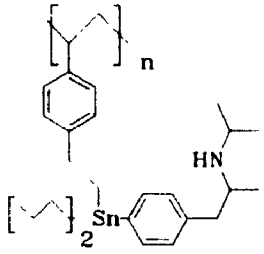

4.19

N-isopropyl-p-bromoamphetamine **4.15** (600 mg, 2.34 mmol), was dissolved in freshly distilled THF (10 mL) and cooled to -78 C under an atmosphere of argon. n-Butyl lithium (Aldrich, 2.3 M, 2.03 mL, 4.68 mol) was added dropwise via syringe and the metal-halogen exchange was allowed to proceed for one hour. Organotin polymer **4.1** (500 mg, 1.17 meq) was then added in one portion. The suspension was stirred at -78 C for 4 hours then allowed to warm to room temperature over 2 hours. The reaction was quenched with acetic acid (356 μL, 6.2 mmol) dissolved in THF (5 mL). Aqueous ethanol (50%, 10 mL) was then added and the mixture was stirred overnight. The polymer was isolated by filtration and soxhlet extracted with acetone for

6 hours.

N-isopropyl-p-iodoamphetamine 4.14

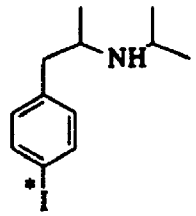

4.14

Organotin resin 4.19 (63.9 mg, 0.15 meq) was suspended in chloroform (1 mL). Excess iodine in chloroform was added dropwise until the iodine colour persisted. The polymer was filtered and washed with chloroform (2 x 1 mL). The combined chloroform filtrates were treated with 0.1N aqueous HCl (2 mL), the chloroform layer was separated and the aqueous layer washed with chloroform (2 x 1 mL). The aqueous layer was made basic with saturated sodium bicarbonate and was extracted with chloroform (4 x 1 mL) until the cloudiness was discharged. The organic layers were combined and dried (Na_2SO_4) and the chloroform was stripped *in vacuo*. The result was a film of oil whose HMR spectrum was consistent with the literature values for the desired N-isopropyl-p-iodoamphetamine 4.14. The yield (11.0 mg, 0.036 mmol) corresponds to a degree of functionalization of 0.24. HMR: δ(CDCl3) 7.27 (q, 4H, H_{AR}), 2.95 (m, 2H, 2(-CH-)), 2.63 (qd, 2H, $-CH_2-$), 1.073 (d, 3H, $-CH_3$), 1.015 (dd, 6H, 2($-CH_3$)). HRMS: (M+1)/e calculated for $C_{12}H_{19}IN$: 304.0562, observed: 304.0560.

N-isopropyl-p-[^{131}I]iodoamphetamine **4.14**

Organotin polymer **4.19** (1 mg, 0.6 μmol) and 2 "Iodobeads" (Pierce) were suspended in HPLC-grade acetonitrile (500 μL) in a 10 mL "Vacutainer" (Becton Dickinson) containing a 5 mm magnetic stirring bar. Na^{131}I (Frosst, 9.3 MBq) in distilled water (10 μL) was then added via syringe. The mixture was stirred for four hours at which point the polymer was filtered and washed with acetonitrile (500 μL). The filtrate and the filter were assayed for radioactivity. The filtrate contained 58% (4.8 MBq) of the remaining radioactivity and the filter contained 42% (3.4 MBq). A portion of the radioactivity was subjected to HPLC analysis. The sample was applied to a RP-18 column (Supelco, 4.6 x 250 mm) eluted with a 9:1 mixture of solvent A (4:1 Methanol:Water, 0.45 M in tetramethyl ammonium chloride) to water. The radioactive trace contained three peaks, two at the solvent front corresponding to 24.6% of the injected activity and a second eluting at the time expected for the desired product contained 75.4% of the injected activity. The overall radiochemical yield was 44%.

4.6 References

1.Takemoto, K., Inaki, Y., Ottenbrite, R. (eds); *Functional Monomers and Polymers*, 1987, *Marcel Dekker, New York.* Sherrington, D.C., Hodge, P. (eds); *Synthesis and Separations Using Functional Polymers*, 1988, *Wiley, New York.*

2.Kabalka, G.W., Green, J.F., McCollum, G., *Seventh Int. Symp. Radiopharm. Chem.*, 1988, Gronigen, The Netherlands, pp. 76,90.

3.Flanagan, R. personal communication.

4.Gerigk, U.; Gerlach, M.; Neumann, P.; Veiler, R.; Weintritt, V.; *Synthesis*, 1990, *448-452.* Gerlach, M., Jordens, F., Kuhn, H., Neumann, W.P., Peterseim, *J. Org. Chem.*, 1991, *56*, 5971-5972.

5.Leikin, J.A.; Davankov, A.B.; Krivova, T.I.; *J. Appl. Chem. USSR*, 1967, *40*, 1729.

6.Djuric, S., Venit, J., Magnus, P., *Tetrahedron Lett.*,1981, *22*, 1787.

7.Snieckus, V., *Chem. Rev.*, 1990, *90*, 879-933.

8.Zalutsky, M.R.; Narula, A.S.; *Appl. Radiat. Isot. Int. J. Radiat. Appl. Instrum. Part A.*, 1987, *38*, 1051-1055.

9.Meyers, A.I.; Temple, D.L.; Haidukewych, D.; Mihelich, E.D.; *J. Org. Chem.*, 1974, *39*, 2787-2793.

10.Pansegrau, P.D.; Rieker, W.F.; Meyers, A.I.; *J. Am. Chem. Soc.*, 1988, *110*, 7178-7184.

11.Chumpradit, S., Kung, M-P., Billings, J.J., Kung, H.F., *J. Med. Chem.*, 1991, *34*, 877-883.

12.Frey, K.A.; Wieland, D.M.; Brown, L.E.; Rogers, W.L.; Agranoff, B.W.; *Ann. Neurol.*, 1981, *10*, 214-221.

13.Windrell, H.S.; Horst, W.D.; Braun, L.; Oldendorf, W.H.; Hattner, R.; Parker, H.; *J. Nucl. Med.*, 1980, *21*, 947-952.

14.Carlsen, L.; Andresen, K.; *Eur. J. Nucl. Med.*, 1982, *7*, 280-281.

15.Clark, D.T. (ed); *Polymer Surfaces*, 1978, Wiley Interscience. Chap 16.

16.Czanderna, A.W. (ed); *Methods of Surface Analysis*, 1975, Elsevier Scientific Publishing.

17.Wagner, C.D.; *Anal. Chem.*, 1972, *44*, 1050.

18.Van der Kerk, G.J.M.; Noltes, J.G.; Luitjen, J.G.A.; *J. Appl. Chem.*, 1957, *366*.

19.Leikin, J.A.; Davankov, A.B.; Krivova, T.I.; *J. Appl. Chem. USSR*, 1967, *40*, 1729.

20.Djuric, S., Venit, J., Magnus, P., *Tetrahedron Lett.*,1981, *22*, 1787.

21.Meyers, A.I., Temple, D.I., Haidukewych, D., Mihelich, E.D.; *J. Org. Chem.*, 1974, *39*, 2787-2793.

22.Benkeser, R.A., Johnson, T.E., *J. Amer. Chem. Soc.*, 1966, *88*, 2220-2225.

23.Borch, R.F., Bernstein, M.D., Durst, H.D., *J. Amer. Chem. Soc.*, 1971, *93*, 2897-2904.

Appendix I

The Calculation of Partition Coefficients

In 1964, Hansch proposed[1] that a new substituent constant π could be derived from experimental partition coefficients. The substituent constant π is defined by the following expression (1):

$$\pi_x = \log P_X - \log P_H \qquad 1)$$

In expression 1, $\log P_H$ refers to the partition coefficient of a parent molecule while $\log P_X$ refers to the partition coefficient of a derivative of the parent molecule. Since liquid-liquid partitioning is an equilibrium process, the substituent constant π is exactly analogous to the Hammett constant σ.

Hansch has compiled an extensive list of π-values; some of which are reproduced in table A1.

Table A1: The substituent constant π for a number of functional groups.

Substituent	π^2	Substituent	π
-F	0.14±0.02	$-NH_2$	-1.23±0.02
-Cl	0.17±0.03	$-CONH_2$	-1.49±0.02
-Br	0.86±0.02	$-NO_2$	-0.28±0.02
-I	1.11±0.05	$-CH_2OH$	-1.03±0.02
$-CH_3$	0.56±0.02	-OH	-0.67±0.01

In the simplest case, the change in log P for a poly-functional aromatic compound is just the sum of the individual π-values for the individual substituents (2).

$$\Delta\log P_{XYZ} = \pi_X + \pi_Y + \pi_Z \qquad 2)$$

In expression 2 $\Delta\log P_{XYZ}$ is just the change in the log of the

partition coefficient that is expected when the parent molecule is functionalized with the substituents X, Y, and Z and π_X π_Y and π_Z are the substituent constants for groups X,Y, and Z respectively. Not every π-value has been determined and it is often necessary to estimate a value based on the best available information. We used this approach for the calculation of the putative hypoxia markers **2.7**, **2.15**, and **2.23**. The extensive list of experimental log P values compiled by Leo, Hansch and Elkins[2] did not contain values for any N-methyl, O-benzyl carbamates. The compilation did include a value of 1.20 for the log P value of N-methyl, O-phenyl carbamate. From this value, and the value for phenol (1.47) we estimated the π-value of the N-methyl carbamoyl substituent to be -0.27 (1.20-1.47). Starting with the experimental value of 1.10 for the log P of benzyl alcohol and the π-values for the nitro group and iodine (-0.28 and 1.11 respectively) the log P value for compounds **2.7** and **2.15** were calculated according to equation 3:

$$\log P = 1.10 - 0.27 + 1.11 - 0.28 \quad 3)$$
$$= 1.66 \pm 0.15$$

The log P value for compound **2.23** was calculated by including the value for one additional nitro group:

$$\log P = 1.10 - 0.27 + 1.11 - (2 \times 0.28) \quad 4)$$
$$= 1.38 \pm 0.17$$

The log P value calculation for compound **3.8** was somewhat more difficult owing to its unique structure.

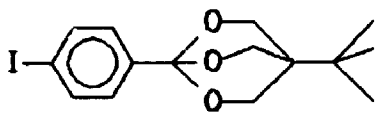

3.8

We estimated the log P for **3.8** by considering it to be constructed from 4-tertiary butyl, iodobenzene and 1.5 molecules of dioxane. The π-values for iodine and the t-butyl group are 1.11 and 1.68 respectively and the log P for 1,4 dioxane is -0.42. Thus:

$$\log P = 2.14 + 1.5(-0.42) + 1.11 + 1.97$$

$$= 4.59$$

Since molecule **3.8** is really made up of 1.5 molecules of 1,3 dioxane it would be more accurate to use the log P for 1,3 dioxane. Unfortunately this value is not included in Hansch's compilation. The value of 4.59 may be high since 1,3 dioxane would be expected to be more water soluble (lower log P) due to the presence of a permanent dipole moment.

1.Fujita, T., Iwasa, J., Hansch, C., *J. Amer. Chem. Soc.*, 1964, *86*, 5175-5180.

2.Leo, A., Hansch, C., Elkins, D., *Chem. Rev.*, 1971, *71*, 525-613.

Appendix II

Equipment

Nuclear Magnetic Resonance spectra were run on Varian spectrometers models XL-200, XL-300 or Gemini. Infrared spectra were run on a Beckman Acculab 4 spectrometer in a 1 mm solution cell. High performance liquid chromatography was performed on a Varian Vista 5500 chromatograph equipped with a Harshaw NaI(Tl) flow scintillation detector. The output from the UV detector and the scintillation detector were linked to a Varian Vista 402 Data system. Mass spectra were performed on a Varian MAT model 8230 spectrometer. Melting points were determined with a Gallenkamp melting point apparatus or a Fischer Johns stage melting point apparatus. The melting points are reported uncorrected. The X-ray photoelectron spectra were obtained on a custom-designed SSL-SSX-100 spectrometer using Al K_{α} monochromatized exciting radiation. The samples were analyzed using a neutralizing grid to reduce differential charging. Biological samples were analyzed for radioactivity using a Packard Minaxi-γ Auto Gamma 500 series well counter. The polarography was performed using a Sargeant-Welch polarograph.